Electronic Supplementary Material (ESI) for ChemComm.

Supporting Information

Quantum Dot Gels as Efficient and Unique Photocatalysts for Organic Synthesis

Daohua Liu,[a] James Nyakuchena,[b] Rajendra Maity,[a] Xin Geng,[a] Jyoti P. Mahajan,[a] Chathurange C. Hewa-Rahinduwage,[a] Yi Peng,[a] Jier Huang,*[b] and Long Luo*[a]

a. Department of Chemistry, Wayne State University, Detroit, Michigan 48202, USA.

b. Department of Chemistry, Marquette University, Milwaukee, Wisconsin, 53201, USA.

Table of Contents

Experimental Methods

Chemicals and Materials: Cadmium oxide (CdO, 99.99%), trioctylphosphine oxide (TOPO, 90%), 1-tetradecylphosphonic acid (TDPA), hexamethyldisilathiane, tetramethylammonium hydroxide (TMAH), thioglycolic acid (TGA), tetrabutylammonium hexafluorophosphate ($TBAPF_6$), methyl 4-bromobenzoate (99%), tributylamine (99%), pyridine (anhydrous, 99.8%), 1,4-dicynobenzene (1,4-DCB, 98%), 1,2-dicynobenzene (98%), ethyl 4-cyanobenzoate (99%), 4-pyridinecarbonitrile (98%), potassium carbonate (K_2CO_3, 99%), *p*-anisidine (99%), 5-aminoindan (95%), 1,4-dibromobutane (99%), ethyl 4-aminobenzoate (98%), 3,4-(methylenedioxy)aniline (97%), 4-aminobiphenyl (98%), 4-bromo-fluorobenzene (99%), piperazine (99%), 1,4-dioxane (99%), Di-*tert*-butyl decarbonate (Boc anhydride, 99%) (97%), triethylamine (99%), 4-dimethylaminopyridine (DMAP, 99%), dichloromethane (DCM, anhydrous, 99.8%), dimethylformamide (DMF, anhydrous, 99.8%), N,N-dimethylacetamide (DMA, anhydrous, 99.8%), acetonitrile (ACN, anhydrous, 99.8%), tris(dibenzylideneacetone)dipalladium(0) ($Pd_2(dba)_3$, 97%), Sphos (98%), 4-bromoanisole (99%), tetrahydroisoquinoline (95%), Sodium tert-butoxide (NaOtBu, 97%) 2-dicyclohexylohosphino-2',6'-diisopropoxybiphenyl (RuPhos, 98%), anhydrous toluene (99.8%), nitric acid (HNO_3, aqueous OminTrace, 67-71%), and Cadmium ICP/DCP standard solution (Supelco, 10,000 μg/mL Cd^{+2} in 2% HNO_3)was purchased from Millipore Sigma.

Synthesis of CdS QDs: CdS QDs were synthesized following the literature procedure.[1] Briefly, a mixture of 0.47 mmol CdO, 0.83 mmol TDPA, and 7.8 mmol TOPO was placed in a 100 mL Schlenk flask under an active vacuum at 150 ^oC for 20 min. Then, a low and continuous flow of Ar went through the system at 350 ^oC for around 1 hour until the solution became colorless. Next, 2 mL of TOP was injected at 320 ^oC, and the temperature was increased to 370 ^oC. A mixture of 2.4 mL TOP and 90 μL TMS was injected, and the system temperature was maintained at 370 ^oC for 15 min. Then, the temperature was reduced to 75 ^oC for 18 hours under argon. The QDs were washed by adding toluene and centrifugation. The red/brown precipitate was discarded, and methanol was added to the supernatant, followed by centrifuge to precipitate the QDs. The supernatant was removed, and toluene was introduced to redisperse the QDs. Repeat the washing procedure two times. The purified TOPO-capped CdS was stored in a sealed vial in the dark. A TGA solution in 10 mL methanol was prepared according to the molar ratio of TGA: Cd = 4: 1.

TMAH was used to adjust the pH of the TGA solution to 10. The TGA solution was introduced to TOPO-capped CdS solution in toluene and sonicated for 1 hour. Then, the CdS QDs were purified using ethyl acetate to precipitate and methanol to disperse. The resulting TGA-capped CdS QDs were stored in a sealed vial in the dark.

Electrogelation: Pt wires were used as the working electrode and counter electrode. An Ag/AgCl electrode in saturated KCl was used as the reference electrode. The electrodes were polished electrochemically in 0.5 M H_2SO_4 before use. TGA-capped QDs were dispersed in methanol with $TBAPF_6$ as an electrolyte. CHI 650E workstation was used to apply the potential of 2.0 V. After 1 hour, the supernatant was removed. The vial was filled with acetone and shaken for 5 seconds. After the gel settled down on the bottom, the supernatant was removed, and acetone was filled again. Repeat the solvent exchange five times. The resulting wet gel was stored in a sealed vial in the dark.

Characterization: Scanning Transmission electron microscopy (STEM) images were taken using a JEOL 3100R05 TEM operated at 300 kV, whereas TEM images were taken using a JEOL 2010 electron microscope. TEM samples were prepared by drop-casting the samples onto carbon-coated 200-mesh Cu grids. Powder X-ray diffraction (PXRD) spectra were taken using a Bruker D2 Phaser diffractometer. XRD patterns were identified using the powder diffraction file database of the International Center for Diffraction Data. Optical absorption measurements were carried out using a Thermo Scientific Genesys 50 UV-Vis spectrophotometer. Inductively coupled plasma mass spectrometry (ICP-MS) was performed using an Agilent 7700x. Photoluminescence (PL) was measured using a Jasco FP-6500 spectrofluorometer. Fourier-transform infrared spectroscopy (FT-IR) was performed using a Jasco FT/IR-6600 spectrometer. Gas chromatography (GC) analysis was performed on Shimadzu GC-2010 pro with a pulsed discharge ionization detector using helium as an ionization source. Nuclear magnetic resonance spectrometer (NMR) DirectDrive System with dual RF channels Agilent premium shielded 400 and 600 MHz Magnet. All ^{1}H NMR and ^{13}C NMR spectra are reported to be parts per million (ppm) downfield of TMS and were calibrated using the signal of $CDCl_3$ (7.26 ppm and 77.23 ppm, respectively). High-resolution mass spectrometry (HRMS) was performed using Thermo Orbitrap Exploris 120 mass

spectrometers in the ESI Positive Mode. Ultraviolet photoelectron spectroscopy (UPS) was measured using a Nexsa G2 X-Ray Photoelectron Spectrometer.

Femtosecond transient absorption (TA) spectroscopy: A regenerative amplified Ti-Sapphire laser (Solstice, 1KHz repetition rate, 800 nm, <100 fs FWHM, 3.5mJ/pulse) provides the pump and probe pulses for femtosecond TA measurements. The tunable (235-1100 nm) pump is generated by TOPAS from 75% of the Solstice output and is chopped at 500 Hz. The remaining 25% of Solstice output is used to generate white light in a sapphire crystal (420-750 nm) in a Helios ultrafast spectrometer (Ultrafast Systems LLC). Sample solutions (30 μL QDs solution in 1 mL acetonitrile) were purged with N_2 for 5 minutes and a 380 nm excitation pump pulse (0.1 Mw). The same sample was spiked with NBu_3 and purged with N_2 before repeating the measurement at the same conditions.

Substrate synthesis

N-aryl pyrrolidines were synthesized using the following procedure according to the literature[2]:

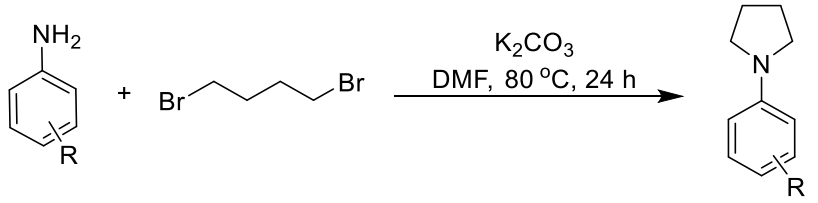

A mixture of aniline (25 mmol, 1 equiv.), K_2CO_3 (30 mmol, 1.2 equiv.), 1, 4- dibromobutane (30 mmol, 1.2 equiv.), and anhydrous DMF (30 mL) were placed into a 100 mL two-neck round bottom flask under argon. The reaction mixture was heated to 80 °C and stirred for 24 hours. Then, 100 mL of water was added to the flask when the reaction mixture was cooled to room temperature. The aqueous layer was extracted with 100 mL ethyl acetate twice, and the separated organic layer was washed with brine (50 mL) and dried through sodium sulfate. The organic layer was concentrated in vacuo and purified using flash silica gel column chromatography.

tert-butyl-4-(4-fluorophenyl)piperazine-1-carboxylate was synthesized in two steps following the literature procedures[3-4]:

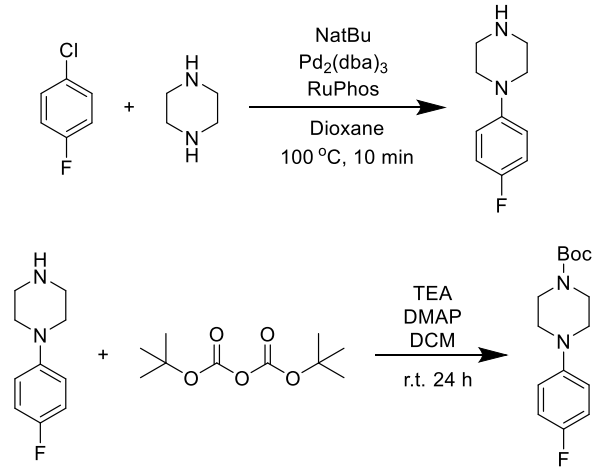

First, a mixture of 4-bromo-fluorobenzene (2 mmol, 1 equiv.), piperazine (8 mmol, 4 equiv.), NaOtBu (3 mmol, 1.5 equiv.), $Pd_2(dba)_3$ (1 mol%), RuPhos (2 mol%), and dioxane (7 mL) was placed into an oven-dried pressure vial equipped with a stir bar and sealed. The reaction mixture was heated to 100 °C and stirred for 10 min. Then, 5 mL of water was added to the flask when the reaction mixture was cooled to room temperature. The aqueous layer was extracted with 5 mL DCM twice. The organic layer was washed with brine (5 mL) and dried through sodium sulfate. The organic layer was concentrated under a vacuum to obtain the crude product. The obtained crude product was purified using flash silica gel column chromatography to obtain 1-(4-fluorophenyl)piperazine.

Second, a mixture of 1-(4-fluorophenyl) piperazine (4.5 mmol, 1 equiv.), Boc anhydride (6 mmol, 1.3 equiv.), triethylamine (4.5 mmol, 1 equiv.), DMAP (0.92 mmol, 0.2 equiv.) and DCM (20 mL) were placed into an oven-dried pressure vial equipped with a stir bar and sealed. The reaction mixture was stirred for 24 h. Then, 20 mL of water was added to the flask when the reaction mixture was cooled to room temperature. The aqueous layer was extracted with 20 mL DCM twice. The organic layer was washed with brine (20 mL) and dried through sodium sulfate. The organic layer was concentrated under a vacuum to obtain the crude product. The obtained crude product was purified using flash silica gel column chromatography to *tert*-butyl-4-(4-fluorophenyl)piperazine-1-carboxylate.

N-aryl tetrahydroisoquinoline was synthesized using the following procedure according to the literature[5]:

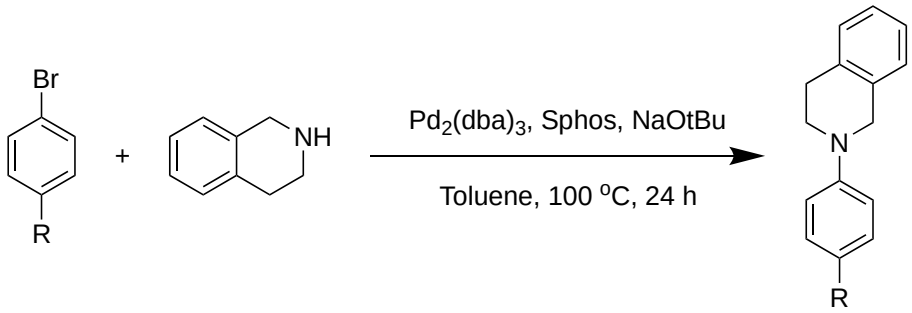

A mixture of $Pd_2(dba)_3$ (3 mol %), Sphos (8 mol%), bromoarene (2.5 mmol, 1 equiv.), tetrahydroisoquinoline (3 mmol, 1.2 equiv.), and NaOtBu (3.5 mmol, 1.4 equiv.) and anhydrous toluene (5 mL) was placed into an oven-dried pressure tube equipped with a stir bar under argon atmosphere. The pressure tube was sealed under the stream of argon. The reaction mixture was heated to 100 °C and stirred for 24 h. Then, 20 mL of water was added to the flask when the reaction mixture was cooled to room temperature. The aqueous layer was extracted with 20 mL ethyl acetate twice. The organic layer was washed with brine (50 mL) and dried through sodium sulfate. The organic layer was concentrated under a vacuum to obtain the crude product. The obtained crude product was purified using flash silica gel column chromatography to obtain the N-aryl tetrahydroisoquinolines.

General procedures for photocatalytic reactions: All reactions were carried out in an oven-dried 10 mL Schlenk vial under a positive pressure of argon using a Kessil PR160 Rig w/Fan Kit setup. The photographs of the reaction setup are shown below. After the reaction, all the isolation was performed using Teledyne Isco Combi Flash R_f flash chromatography with silica gel columns. Ethyl acetate: Hexane: NEt_3 (v/v/v) indicated gradients were used in purification.

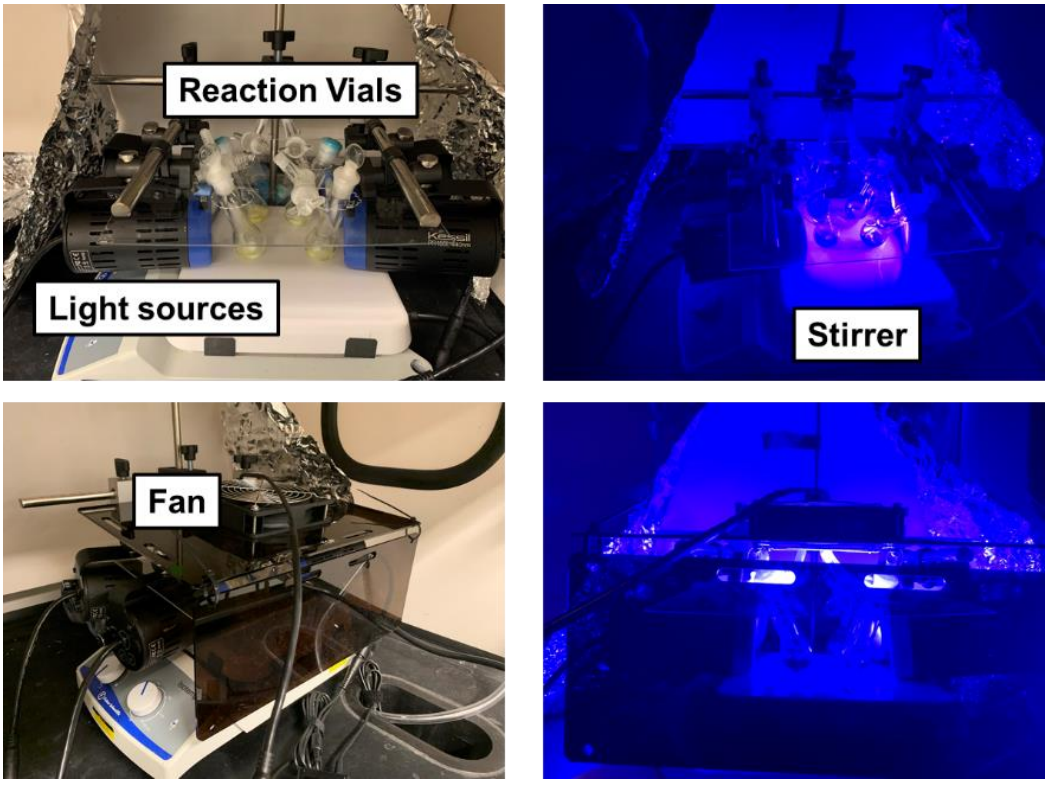

(a) Dehalogenation reaction: The reaction followed the procedures reported by Stephenson and coworkers.[6] Methyl 4-bromobenzoate (0.250 mmol, 1.00 equiv.), acetonitrile (2.50 mL), decane (15.0 µL), tributylamine (1.25 mmol, 3.00 equiv.), formic acid (1.25 mmol, 5.00 equiv.), and CdS QDs or gel (2 x 10^{-6} mmol QDs, 8 x 10^{-6} equiv.) were added to a 10 mL argon-filled Schlenk vial equipped with an oven-dried magnetic stir bar. The reaction mixture was irradiated with blue light while stirring at 400 rpm for 5 h. After the reaction, 5 µL of the reaction mixture was diluted with 2.0 mL of diethyl ether before GC analysis. A typical GC chromatogram for dehalogenation of methyl 4-bromobenzoate is shown below.

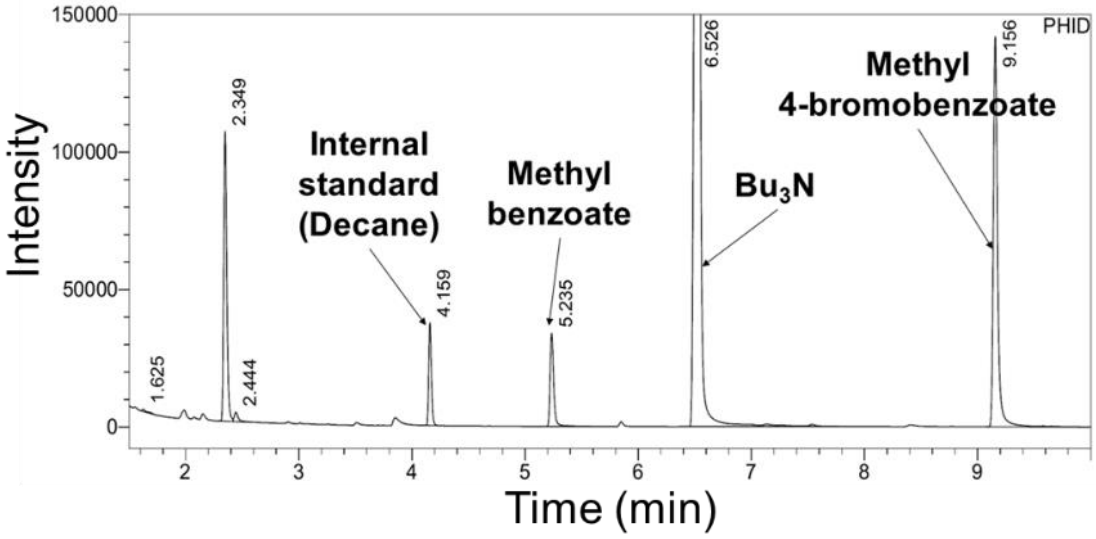

GC yields were calculated using decane as an internal standard. The correction factor, which accounts for the different sensitivities of the GC detector towards the internal standard (i.e., decane) and the reaction product (i.e., methyl benzoate), was calculated from the slope of the plot of their GC peak area ratio vs. concentration ratio (see below). The correction factor was found to be 0.797.

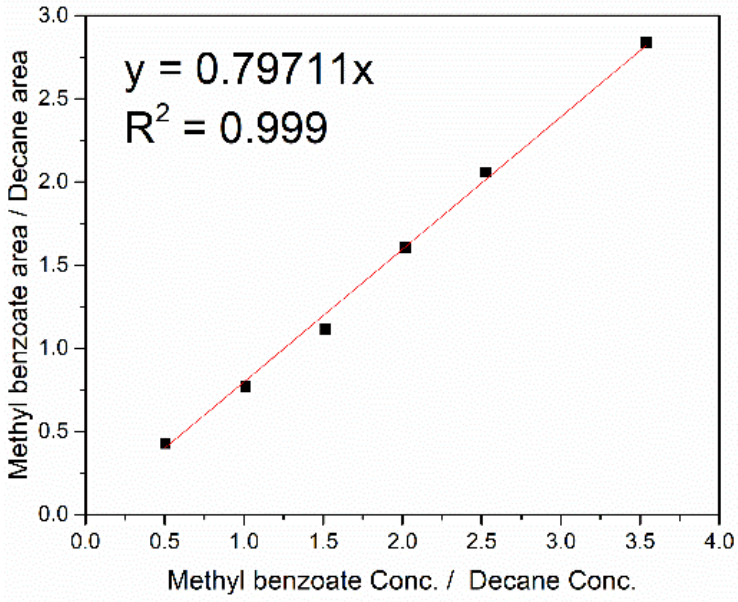

(b) α-amino arylation reaction: The reaction followed the procedures reported by MacMillan and coworkers.[7] Tertiary amine (0.625 mmol, 1.25 equiv.), NaOAc (1.0 mmol, 2.0 equiv.), 1,4-dicyanobenzene (0.5 mmol, 1.0 equiv.), and anhydrous DMA (2.0 mL) were added to a 10 mL argon-filled Schlenk vial equipped with an oven-dried magnetic stir bar. The reaction mixture was

irradiated with blue light while stirring at 400 rpm for 5-33 h until the limiting reagent, 1,4-dicyanobenzene, was completely consumed (monitored by ^{1}H NMR). Then, the reaction mixture was diluted with 10 mL ethyl acetate. The organic layer was washed with 15 mL saturated sodium bicarbonate solution twice and then washed with 15 mL brine. The separated organic layer was dried over sodium sulfate and concentrated under a vacuum. The crude product was purified using flash silica gel chromatography using Ethyl acetate: Hexane: NEt_3 (v/v/v) indicated gradient to obtain the desired products.

Quantification of catalyst loading:

(a) UV-Vis analysis: CdS QD concentration and size can be estimated from the UV-Vis data using the following equations developed by Peng and coworkers:[8]

Size of CdS (D) = $(-6.6521 \times 10^{-8})\lambda^3 + (1.9557 \times 10^{-4})\lambda^2 - (9.2352 \times 10^{-2})\lambda + 13.29$,

Extinction coefficient of CdS (ε) = $21536\ (D)^{2.3}$,

Calibrated absorbance value (A) = $A_m\ (HWHM)_{UV}$ /11,

Concentration of CdS (C) = $A/\varepsilon L$,

where λ (nm) is the wavelength of the first excitonic absorption peak of the CdS QDs, A_m is measured absorbance, $(HWHM)_{UV}$ is the half-width at the half-maximum on the long-wavelength side of the first excitonic UV-Vis absorption peak, and L is the light path length.

(b) ICP-MS analysis: The UV-Vis analysis discussed above does not apply to CdS QD gels because gels do not form a uniform solution. Therefore, we used ICP-MS to determine the concentration of QD gel. Here, the concentration of QD gel was defined as the molar concentration of QD building blocks in the wet gel sample—for easy comparison with the colloidal QD samples. Experimentally, 50 μL CdS QD wet gel samples were digested by sonication in concentrated HNO_3 for 6 hours, followed by dilution with 2% HNO_3 to achieve a concentration within the calibration range of 0-200 ppb Cd^{2+}. The calibration curve was established using standard Cd^{2+} solutions with concentrations of 0, 1, 5, 10, 25, 50, 100, 150, and 200 ppb. The calibration curve shows perfect linearity with an R-value of 1.0000 (see below).

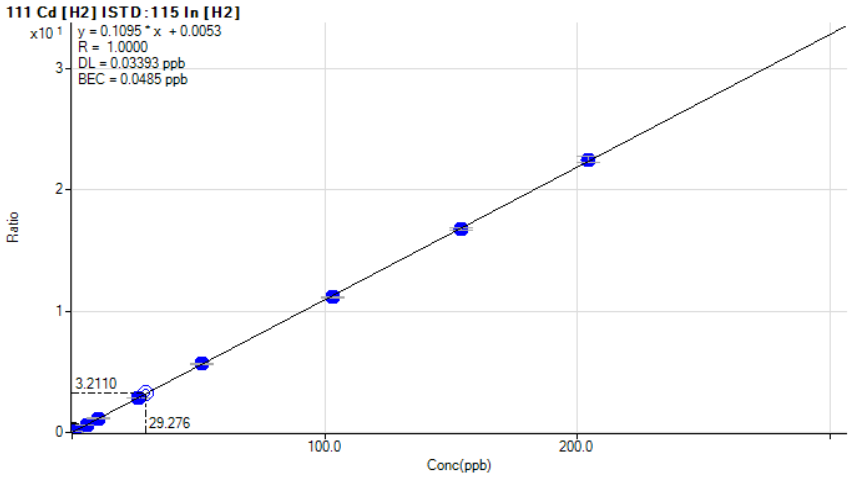

The QD gel concentration was calculated using the following equation:

$$the\ molar\ concentration\ of\ QDs\ in\ the\ gel = \frac{the\ mass\ concentration\ of\ Cd^{2+}\ in\ the\ gel\ from\ ICP-MS}{the\ atomic\ mass\ of\ Cd * the\ number\ of\ Cd\ in\ one\ QD\ particle}$$

The number of Cd in one QD particle is estimated to be 343 from the QD size (r = 1.6 nm), CdS density (4.826 g/cm^3) and molar mass (144.47 g/mol, assuming the stoichiometric ratio of Cd to S is 1:1).

Comparison between the catalyst loadings obtained from UV-Vis and ICP-MS analysis:

The catalyst loading is defined as below:

$$Catalyst\ loading = \frac{the\ molar\ amount\ of\ QDs}{the\ molar\ amount\ of\ substrate}$$

The catalyst loading for QD samples can be calculated from the UV-Vis and ICP-MS analysis, so it is ideal for cross-validating the two analytical methods. The table below shows that the TGA/CdS catalyst loadings for the dehalogenation reaction estimated using the UV-Vis and ICP-MS analysis are very close (3.47×10^{-3} mol % vs. 3.30 ± 0.02 mol%), confirming that both methods are reliable. The catalyst loading of 50 μL wet gel was determined to be 0.82×10^{-3} mol % using the ICP-MS method.

Methods / QDs type	UV-Vis ($\times 10^{-3}$ mol %)	ICP-MS ($\times 10^{-3}$ mol %)
TGA/CdS	3.47	3.30 ± 0.02
Gel (50 μL)	-	0.82 ± 0.04

Supplemental Tables and Figures

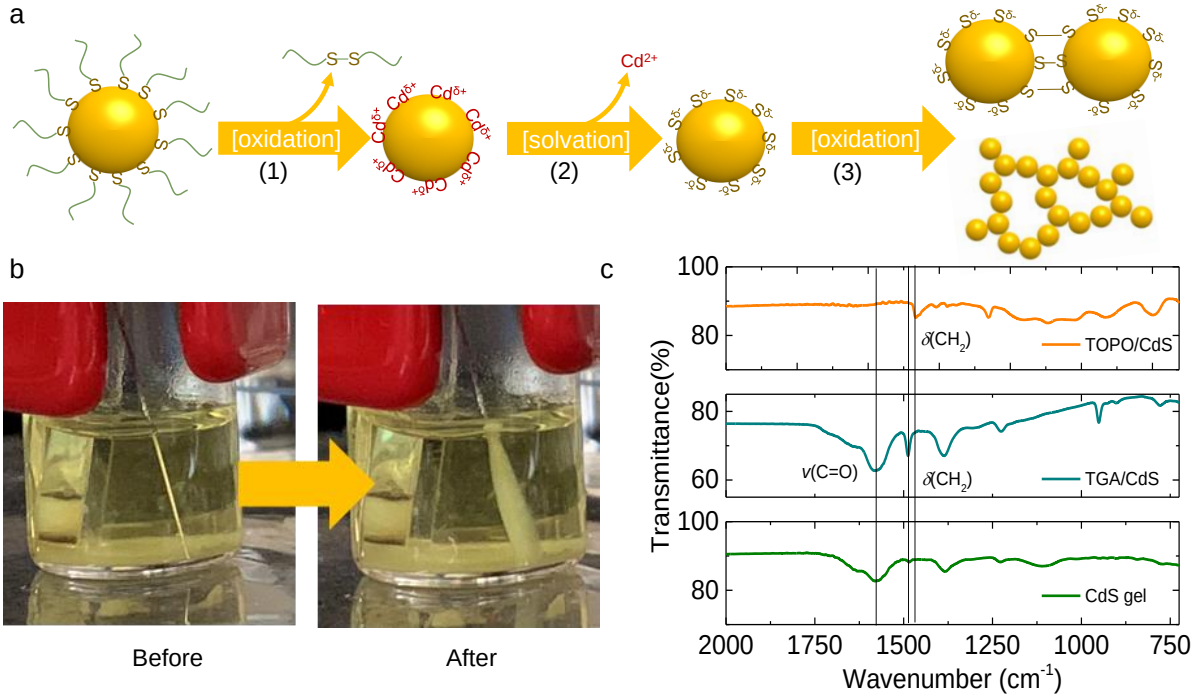

Figure S1. (a) Schematic illustration of CdS QD gelation mechanism. (b) Photographs of the CdS QD solution before and after electrogelation and (c) FTIR spectra of TOPO/CdS, TGA/CdS, and CdS gel under the same loading. The scissoring peaks of CH_2 at ~1500 cm^{-1} in the FTIR spectra of TOPO/CdS and TGA/CdS disappear in the spectrum of CdS gel, indicating the removal of the thioglycolate ligands during electrogelation.

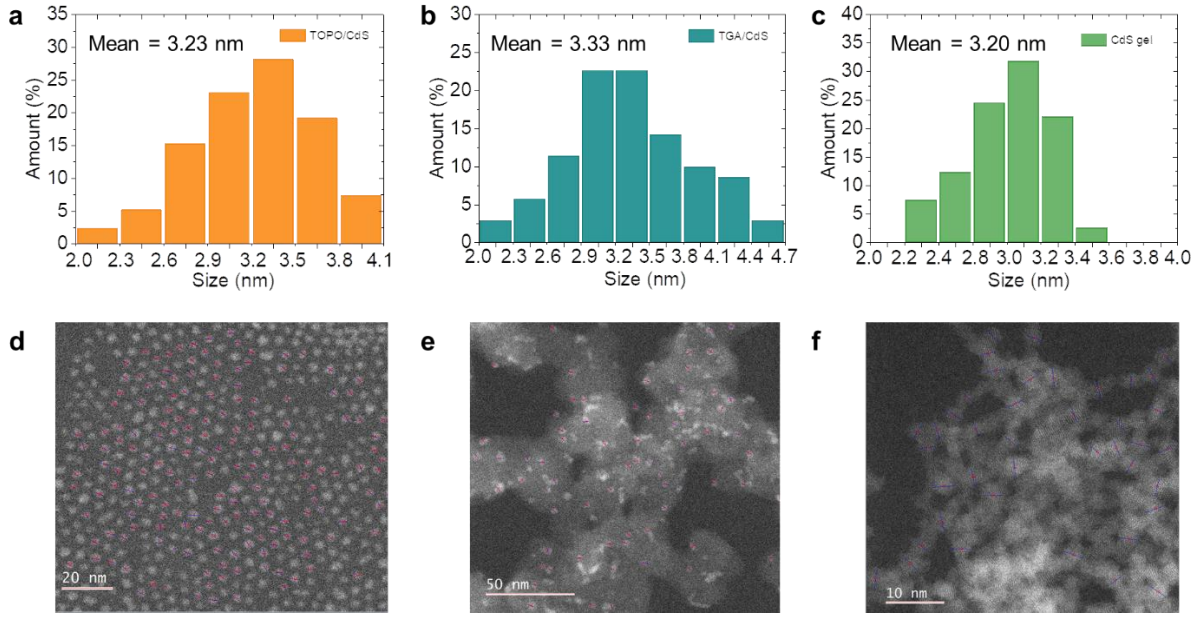

Figure S2. Size distributions of (a) TOPO/CdS, (b) TGA/CdS QDs, and (c) CdS gel, measured using Nano Measurer. Representative images in panels (d - f) showing how the size was measured for (d) TOPO/CdS, (e) TGA/CdS QDs, and (f) CdS gel, respectively. The size of CdS gel is defined as the crystallite size of the CdS QD building blocks in the gel network.

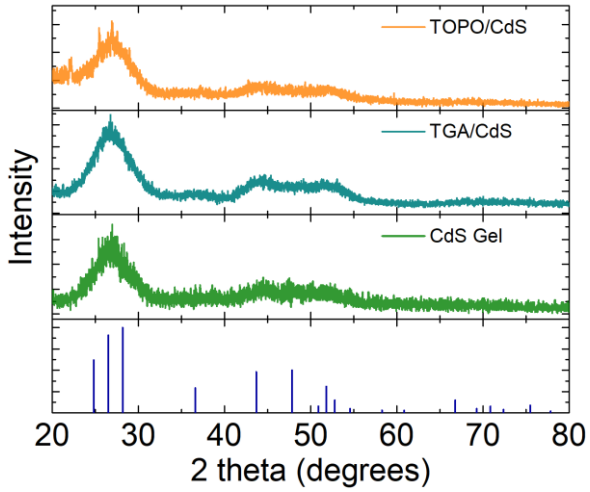

Figure S3. Powder X-ray diffraction (PXRD) patterns of TOPO/CdS, TGA/CdS QDs, and CdS gel. The stick diagram shows the PXRD pattern of hexagonal CdS (wurtzite, PDF 00-001-0780) as a reference. The peak widths at half height were similar for TOPO/CdS, TGA/CdS QDs, and CdS gel, suggesting the average crystallite size did not significantly change during the ligand exchange and electrogelation.

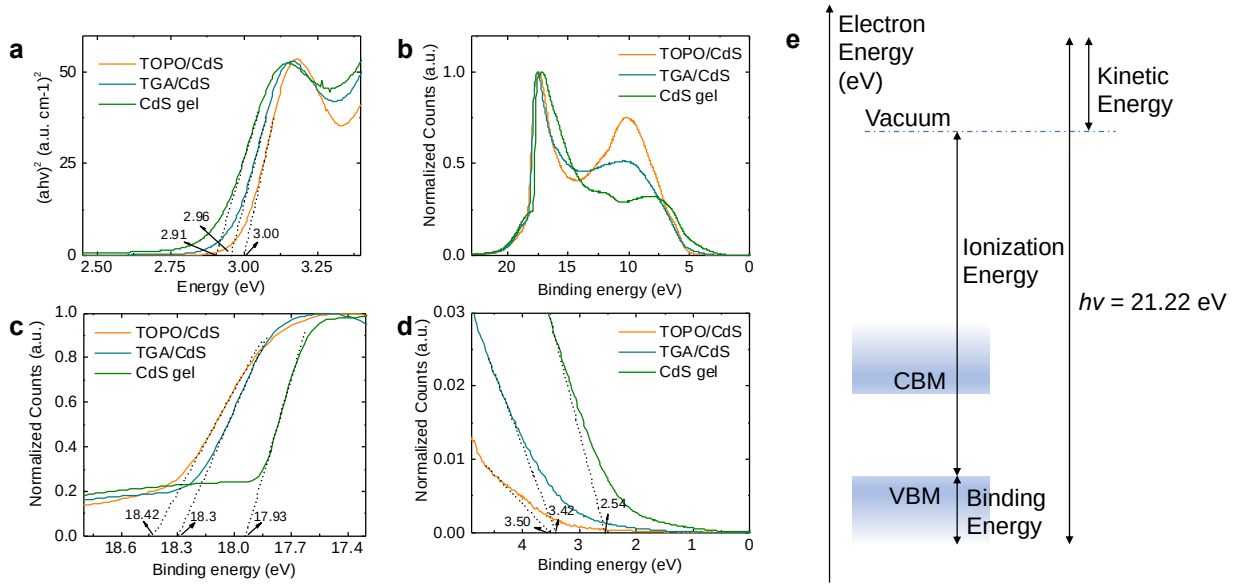

Figure S4. (a) Tauc plots and (b) the full-range ultraviolet photoelectron spectra (UPS) of TOPO/CdS, TGA/CdS, and CdS gel and their expanded views at (c) the secondary electron cutoff region and (d) the fermi edge region. The cutoff and onset energies are labeled in panels (c) and (d), respectively. (e) Energy diagram of a semiconductor, showing the conduction band minimum (CBM), valence band maximum (VBM), vacuum level, binding energy, and kinetic energy. Helium I ($h\nu$ = 21.22 eV) was used as the ionization source, so the sum of binding energy, ionization energy, and kinetic energy should be equal to 21.22 eV. The VBM energy can be calculated using the following equation: VBM = 21.22 eV− (cutoff energy − onset energy). For example, the VBM of TOPO/CdS = 21.22 eV – (18.42 eV – 3.50 eV) = 6.30 eV vs vacuum or 1.86 V vs. NHE (NHE = – 4.44 vs vacuum). The CBM energy is then calculated from the bandgap in panel (a) and the measured VBM energy from UPS using the following equation: CBM = VBM – band gap. For example, the band gap and VBM energy of TOPO/CdS are 3.0 eV and 1.86 V vs. NHE, so its CBM is 1.86 – 3.00 = –1.14 V vs. NHE.

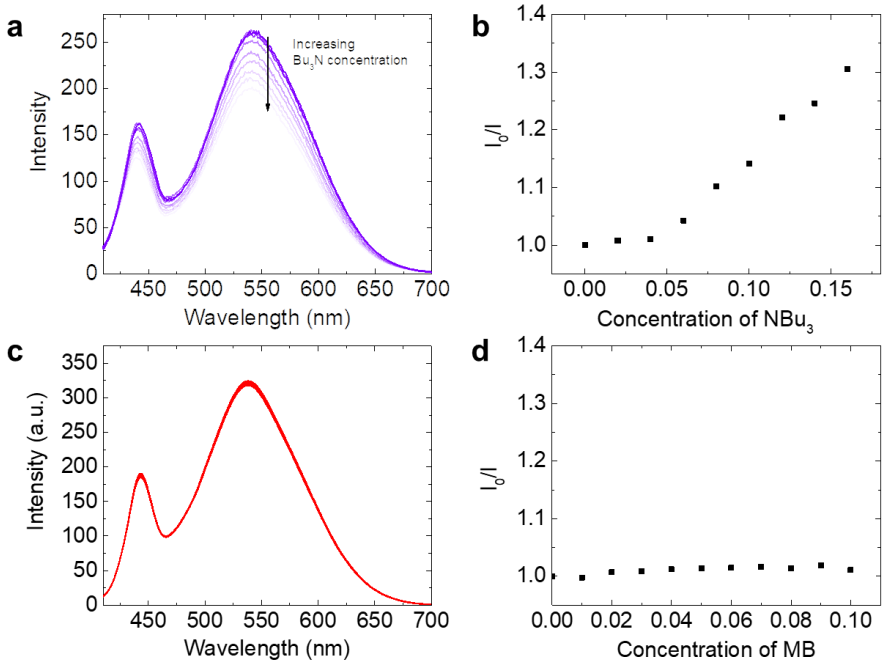

Figure S5. Photoluminescence (PL) spectra and Stern-Volmer plots for TOPO/CdS in acetonitrile after adding (a)-(b) tributylamine (NBu_3) and (c)-(d) methyl 4-bromobenzoate (MB), showing the PL quenching of TOPO/CdS by NBu_3, not by MB.

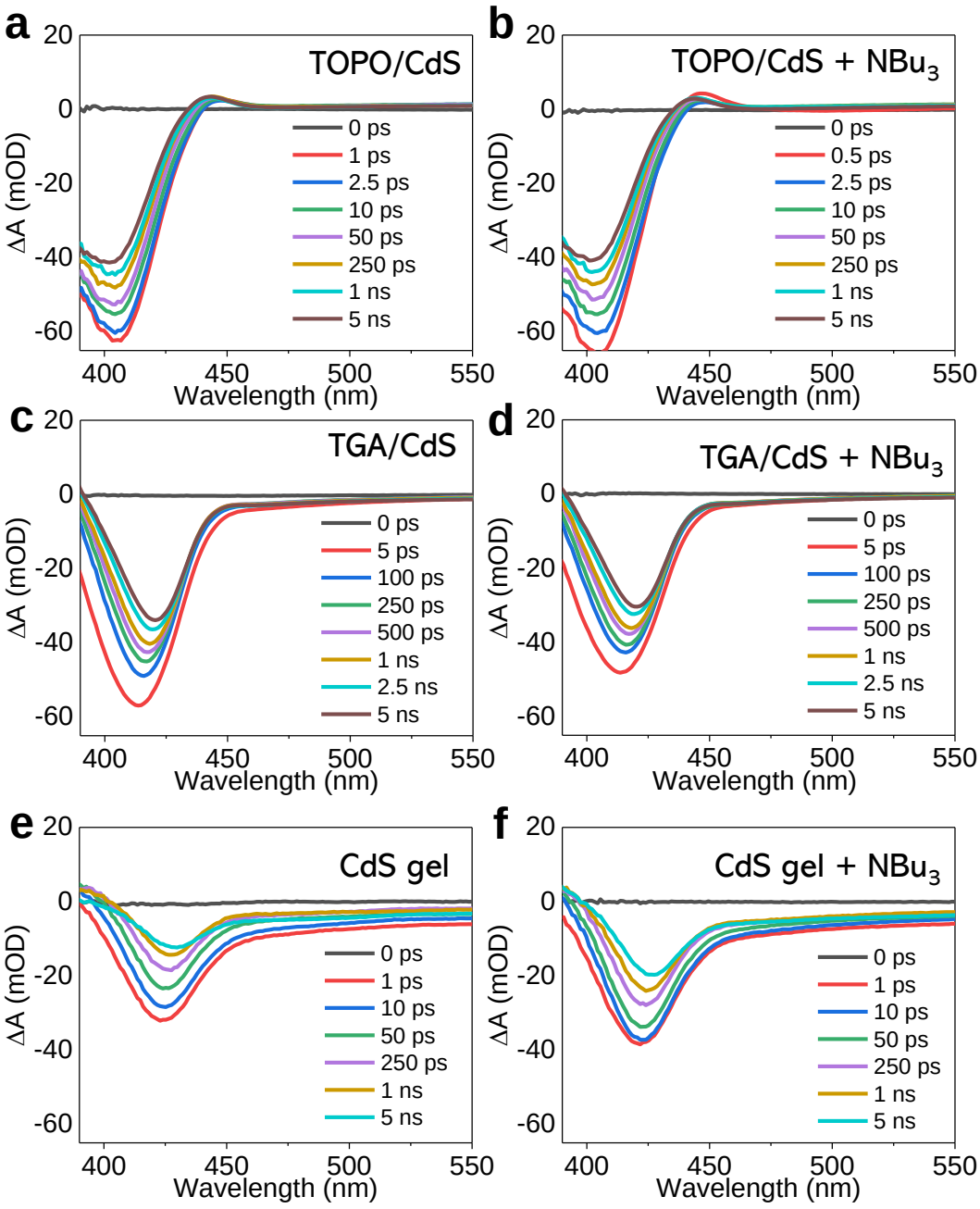

Figure S6. Transient absorption spectroscopy spectra for TOPO/CdS, TGA/CdS QDs, and CdS gel (a, c, e) in the absence and (b, d, f) presence of NBu_3 following a 380 nm excitation.

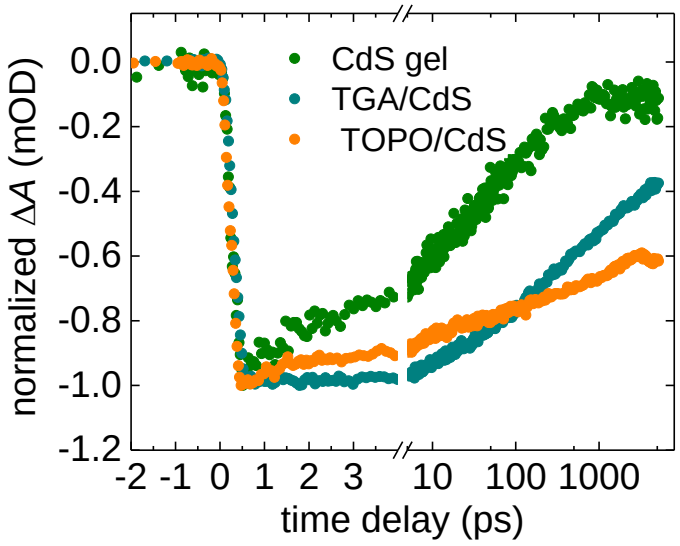

Figure S7. The bleach recovery kinetics for CdS gel, TGA/CdS, and TOPO/CdS in acetonitrile after a 380 nm excitation.

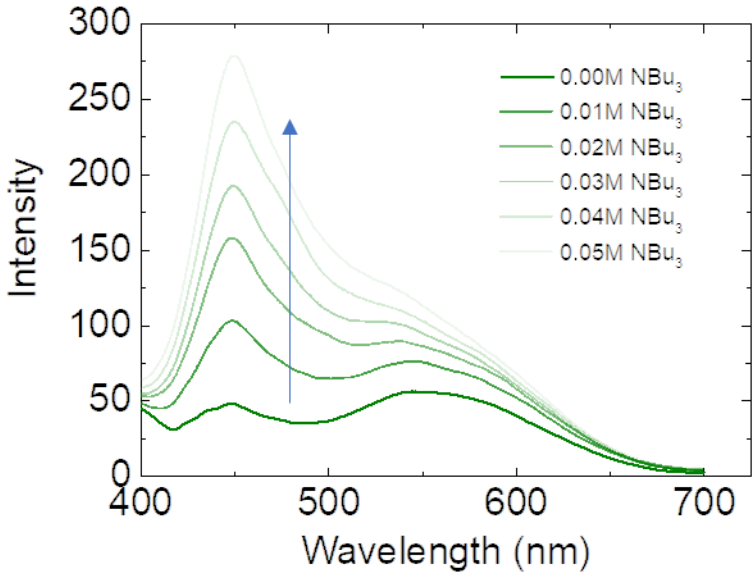

Figure S8. PL intensity of CdS gel after adding NBu_3, showing the PL intensity increase of the band edge emission at ~450 nm due to the passivation of surface trap sites of gel by NBu_3.[9]

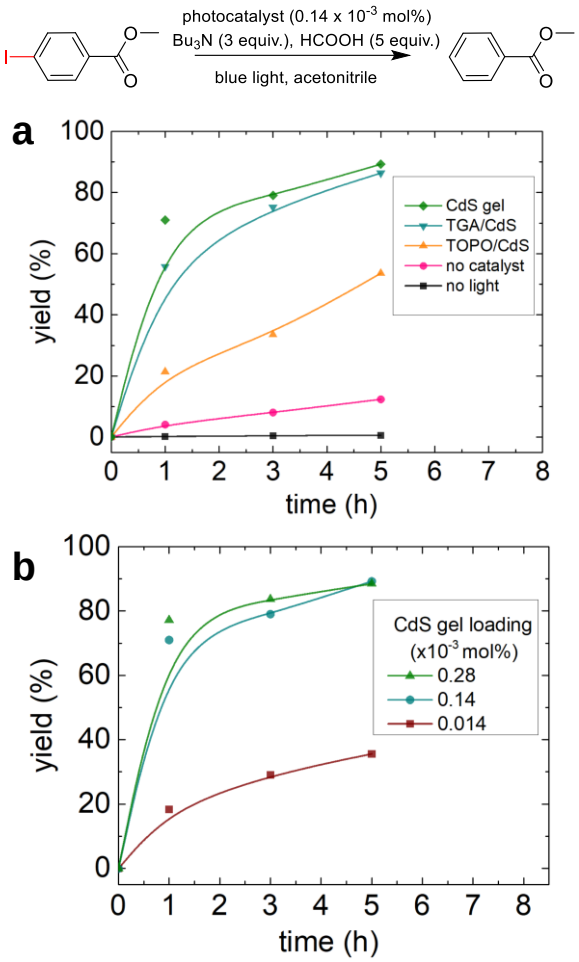

Figure S9. The time-dependent yield during dehalogenation of methyl 4-iodobenzoate (a) for various reaction conditions, including under no light with gel (black), and under blue light with no catalyst (pink), TOPO- and TGA-capped CdS (orange and cyan), and gel (green) at a catalyst loading of 0.14 x 10^{-3} mol%, and (b) for different CdS gel loadings from 0.014 x 10^{-3} mol% to 0.28 x 10^{-3} mol%. The reaction kinetics is no longer limited by the CdS gel catalyst loading at a loading of ≥0.14 x10^{-3} mol%.

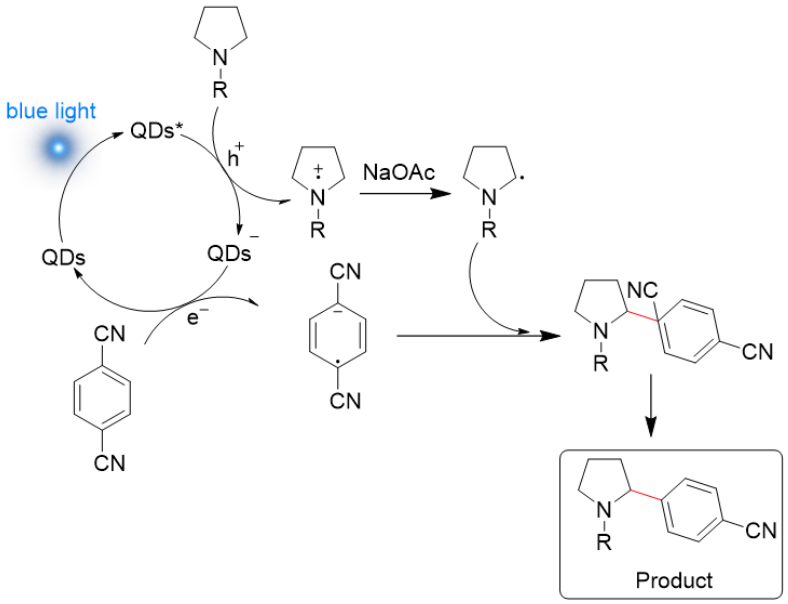

Figure S10. A plausible mechanism of α-amine arylation reaction using QDs and QD gel as the photocatalyst based on the literature.[10]

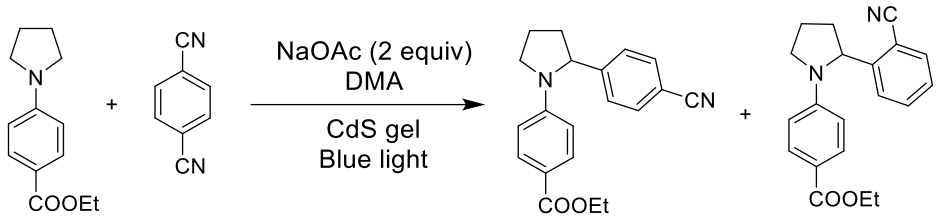

6 h	**3d** 67%	**4d** 0%
9 h	**3d** 51%	**4d** 11%
18 h	**3d** 33%	**4d** 5%

Figure S11. Time-dependent yields for the cyano dance reaction.

Table S1 Dehalogenation yield of methyl 4-bromobenzoate using CdS gel as a photocatalyst after adding TGA or pyridine.

Time (h)	0.2 equiv TGA yield (%)	0.6 equiv TGA yield (%)	0.2 equiv pyridine yield (%)
1	1.2	0.5	11.2
3	2.4	1.8	20.5
5	3.0	2.5	31.2

X-ray crystallography results

Experimental details

A colorless crystal (0.02 x 0.20 x 0.60) mm^3 was mounted on a MicroMount (MiTeGen) with paratone oil (Parabar 10312, Hampton Research) on a Bruker D8 Venture diffractometer with kappa geometry, an Incoatec IμS micro-focus source X-ray tube (Cu K_α radiation) and a multilayer mirror for monochromatization. The X-ray diffraction intensities were measured using a Photon III CPAD area detector at a distance of 38 mm and 0.3° image width. Data were acquired at 100 K with an Oxford 800 Cryostream low-temperature apparatus. Using APEX4 v2021.4-0, the intensities were integrated using SAINT V8.38a, and a multiscan absorption correction was applied using SADABS v2016/2. The crystal structure was solved using a dual-space approach as implemented in SHELXT[11] and difference Fourier (ΔF) maps during least-squares refinement, as embedded in SHELXL-2018[12] running under Olex2[13]. All non-hydrogen atoms were refined anisotropically. The hydrogen atoms were positioned with idealized geometry and refined isotropically using a riding model. At 100 K, **4i** was refined in the centrosymmetric space group $P2_1/c$ with one molecule in the asymmetric unit and Z=4.

Crystal data

$C_{23}H_{22}N_2O$ (*M* =342.42 g/mol): monoclinic, space group $P2_1/c$ (no. 14), *a* = 9.7900(3) Å, *b* = 16.4804(5) Å, *c* = 11.3323(3) Å, *β* = 101.5570(10)°, *V* = 1791.32(9) $Å^3$, *Z* = 4, *T* = 100 K, μ(Cu Kα) = 0.610 mm^{-1}, *Dcalc* = 1.270 g/cm^3, 36428 reflections measured (9.22° ≤ 2Θ ≤ 144.488°), 3517 unique (R_{int} = 0.0279, R_{sigma} = 0.0142) which were used in all calculations. The final R_1 was 0.0338 (I > 2σ(I)) and wR_2 was 0.0873 (all data).

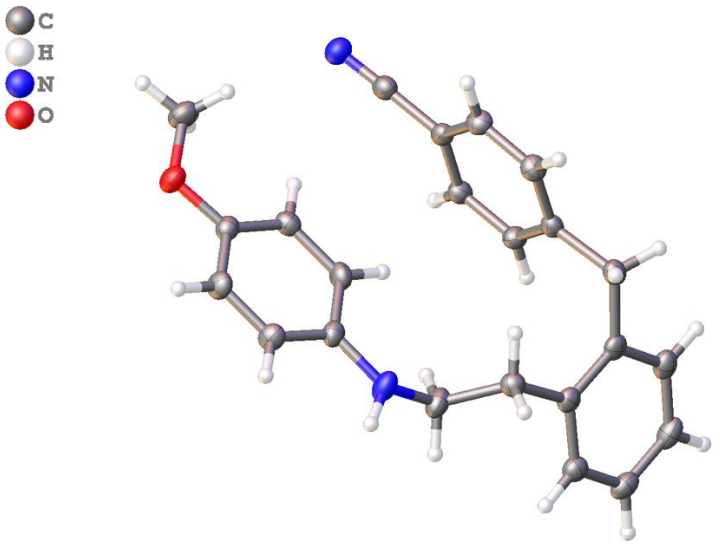

Image of the asymmetric unit of **4i**.

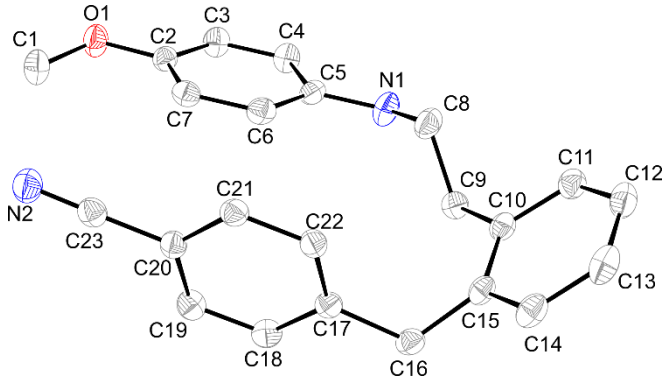

ORTEP image of **4i** with displacement ellipsoids at 50% and hydrogen atoms omitted for clarity.

c/Å	11.3323(3)
α/°	90
β/°	101.5570(10)
γ/°	90
Volume/Å^3	1791.32(9)
Z	4
ρ_{calc}g/cm^3	1.270
μ/mm^{-1}	0.610
F(000)	728.0
Crystal size/mm^3	0.6 × 0.2 × 0.02

Radiation	Cu Kα (λ = 1.54178)
2Θ range for data collection/°	9.22 to 144.488
Index ranges	$-12 \leq h \leq 12$, $-20 \leq k \leq 20$, $-13 \leq l \leq 12$
Reflections collected	36428
Independent reflections	3517 [R_{int} = 0.0279, R_{sigma} = 0.0142]
Data/restraints/parameters	3517/0/239
Goodness-of-fit on F^2	1.025
Final R indexes [I>=2σ (I)]	R_1 = 0.0338, wR_2 = 0.0858
Final R indexes [all data]	R_1 = 0.0354, wR_2 = 0.0873
Largest diff. peak/hole / e $Å^{-3}$	0.20/-0.16

Experimental and characterization data

The high-resolution mass spectrometry (HRMS) data are only provided for the compounds that have not been previously reported in the literature.

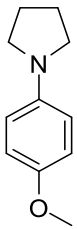

Starting material of 3: ^{1}H NMR (600 MHz, $CDCl_3$) δ 6.87 – 6.84 (m, 2H), 6.54 (d, *J* = 8.4 Hz, 2H), 3.76 (s, 3H), 3.25 – 3.23 (m, 4H), 2.00 – 1.98 (m, 4H).

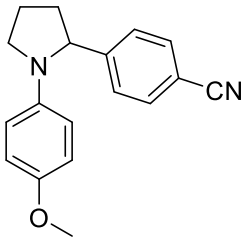

Reaction condition of 3: CdS gel (2 x 10^{-3} mol %): 15 h, 95 mg, 68% yield. The crude product was purified using flash silica-gel column chromatography (Ethyl acetate : Hexane : NEt_3 = 12:88:1 v/v/v) to afford **3** as yellow oil. **^{1}H NMR** (400 MHz, $CDCl_3$) δ 7.59 (d, *J* = 8.4 Hz, 2H), 7.37 (d, *J* = 8.4 Hz, 2H), 6.77 (d, *J* = 6.6 Hz, 2H), 6.39 (d, *J* = 9.2 Hz, 2H), 4.66 (d, *J* = 8.7 Hz, 1H), 3.72 (bs, 4H), 3.38 (q, *J* = 8.7 Hz, 1H), 2.44 (p, *J* = 9.7, 9.2 Hz, 1H), 2.07 – 1.83 (m, 3H). **^{13}C NMR** (151 MHz, $CDCl_3$) δ 151.5, 151.2, 141.8, 132.6, 127.0, 119.2, 115.1, 113.4, 110.7, 63.4, 56.0, 50.0, 36.2, 23.5.

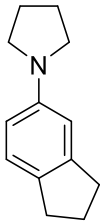

Starting material of 3a: ^{1}H NMR (400 MHz, $CDCl_3$) δ 7.11 (d, J = 8.1 Hz, 1H), 6.52 (s, 1H), 6.42 (d, J = 8.2 Hz, 1H), 3.31 – 3.27 (m, 4H), 2.92 – 2.83 (m, 4H), 2.08 (q, J = 7.3 Hz, 2H), 2.04 – 2.00 (m, 4H).

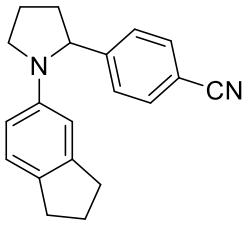

Reaction condition of 3a: CdS gel (2 x 10^{-3} mol %): 5 h, 92 mg, 64% yield. The crude product was purified using flash silica-gel column chromatography (Ethyl acetate : Hexane : NEt_3 = 10:89:1 v/v/v) to afford **3a** as yellow oil. **^{1}H NMR** (400 MHz, $CDCl_3$) δ 7.61 (d, *J* = 8.2 Hz, 2H), 7.39 (d, *J* = 8.1 Hz, 2H), 7.04 (d, *J* = 8.1 Hz, 1H), 6.41 (d, *J* = 2.4 Hz, 1H), 6.27 (dd, *J* = 8.2, 2.4 Hz, 1H), 4.73 (dd, *J* = 8.6, 2.3 Hz, 1H), 3.79 – 3.74 (m, 1H), 3.46 – 3.40 (m, 1H), 2.85 – 2.80 (m, 4H), 2.49 – 2.40 (m, 1H), 2.09 – 1.99 (m, 4H), 1.97 – 1.90 (m, 1H). **^{13}C NMR**

(101 MHz, $CDCl_3$) δ 151.05, 145.93, 145.53, 132.55, 132.26, 126.95, 124.82, 119.19, 110.82, 110.59, 108.65, 63.21, 49.77, 36.04, 33.44, 31.97, 25.84, 23.32.

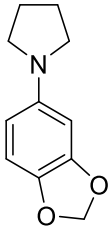

Starting material of 3b: ^{1}H NMR (400 MHz, $CDCl_3$) δ 6.73 (d, J = 8.4 Hz, 1H), 6.23 (d, J = 2.4 Hz, 1H), 5.97 (dd, J = 8.4, 2.4 Hz, 1H), 5.85 (s, 2H), 3.24 – 3.20 (m, 4H), 2.01 – 1.97 (m, 4H).

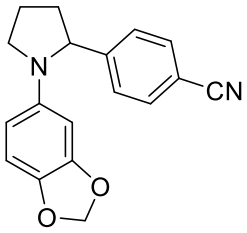

Reaction condition of 3b: CdS gel (2 x 10^{-3} mol %): 11 h, 106 mg, 73% yield. The crude product was purified using flash silica-gel column chromatography (Ethyl acetate : Hexane : NEt_3 = 10:89:1 v/v/v) to afford **3b** as brown oil. **^{1}H NMR** (400 MHz, $CDCl_3$) δ 7.59 (d, *J* = 8.3 Hz, 2H), 7.34 (d, *J* = 8.3 Hz, 2H), 6.63 (d, *J* = 8.4 Hz, 1H), 6.07 (d, *J* = 2.5 Hz, 1H), 5.84 – 5.80 (m, 3H), 4.64 (dd, *J* = 8.5, 2.7 Hz, 1H), 3.71 – 3.66 (m, 1H), 3.39 – 3.33 (m, 1H), 2.49 – 2.39 (m, 1H), 2.02 – 1.96 (m, 2H), 1.91 – 1.85 (m, 1H). **^{13}C NMR** (101 MHz, $CDCl_3$) δ 150.8, 148.5, 143.2, 139.0, 132.7, 126.9, 119.1, 110.8, 108.8, 104.1, 100.7, 95.3, 63.6, 50.2, 36.2, 23.4.

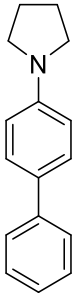

Starting material of 3c: ^{1}H NMR (400 MHz, $CDCl_3$) δ 7.58 (d, J = 7.8 Hz, 2H), 7.53 (d, J = 8.9 Hz, 2H), 7.41 (t, J = 7.8 Hz, 2H), 7.26 (d, J = 14.7 Hz, 1H), 6.66 (d, J = 8.8 Hz, 2H), 3.37 – 3.34 (m, 4H), 2.06 – 2.03 (m, 4H).

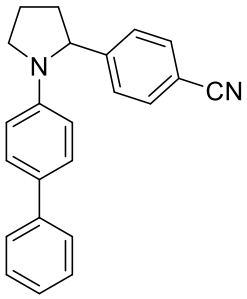

Reaction condition of 3c: CdS gel (2 x 10^{-3} mol %): 22 h, 84 mg, 73% yield. The crude product was purified using flash silica-gel column chromatography (Ethyl acetate : Hexane : NEt_3 = 10:89:1 v/v/v) to afford **3c** as white solid. **^{1}H NMR** (600 MHz, $CDCl_3$) δ 7.62 – 7.60 (m, 2H), 7.53 – 7.51 (m, 2H), 7.45 – 7.36 (m, 2H), 7.39 – 7.36 (m, 4H), 7.27 – 7.24 (m, 1H), 6.54 – 6.52 (m, 2H), 4.80 (dd, *J* = 8.4, 2.6 Hz, 1H), 3.80 – 3.77 (m, 1H), 3.51 – 3.47 (m, 1H), 2.50 – 2.44 (m, 1H), 2.08 – 1.98 (m, 2H), 1.96 – 1.92 (m, 1H). **^{13}C NMR** (101

MHz, $CDCl_3$) δ 150.4, 146.3, 141.2, 132.6, 129.5, 128.8, 127.9, 126.9, 126.4, 126.2, 119.1, 113.0, 110.8, 63.0, 49.5, 36.0, 23.3.

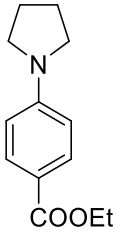

Starting material of 3d: ^{1}H NMR (600 MHz, $CDCl_3$) δ 7.91 (d, J = 9.1 Hz, 2H), 6.52 (d, J = 9.0 Hz, 2H), 4.33 (q, J = 7.1 Hz, 2H), 3.42 – 3.29 (m, 4H), 2.09 – 1.95 (m, 4H), 1.37 (t, J = 7.1 Hz, 3H).

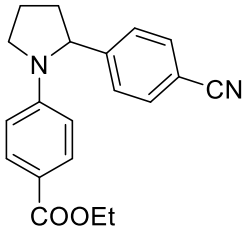

Reaction condition of 3d: TOPO/CdS (2 x 10^{-3} mol %): 9 h, 61 mg, 39% yield. **TGA/CdS (2 x 10^{-3} mol %):** 9 h, 71 mg, 45% yield. **CdS gel (2 x 10^{-3} mol %):** 6 h, 108 mg, 67% yield. The crude product was purified using flash silica-gel column chromatography (Ethyl acetate : Hexane : NEt_3 = 18:81:1 v/v/v) to afford **3d** as white solid. **^{1}H NMR** (600 MHz, $CDCl_3$) δ 7.83 (d, *J* = 9.1 Hz, 2H), 7.59 (d, *J* = 8.4 Hz, 2H), 7.28 (d, *J* = 8.2 Hz, 2H), 6.40 (d, *J* = 9.1 Hz, 2H), 4.85 (dd, *J* = 8.4, 2.4 Hz, 1H), 4.31 – 4.25 (m, 2H), 3.78 – 3.75 (m, 1H), 3.53 – 3.49 (m, 1H), 2.51 – 2.45 (m, 1H), 2.08 – 1.94 (m, 3H), 1.33 (t, *J* = 7.1 Hz, 3H). **^{13}C NMR** (151 MHz, $CDCl_3$) δ 167.0, 149.9, 149.3, 132.8, 131.5, 126.9, 119.0, 118.4, 111.9, 111.2, 62.8, 60.4, 49.4, 35.9, 23.2, 14.7. HRMS: *m/z* calculated for $C_{20}H_{20}N_2O_2$ $[M+H]^+$: 320.1598, found 321.1595.

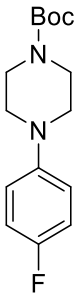

Starting material of 3e: ^{1}H NMR (400 MHz, $CDCl_3$) δ 6.98 – 6.92 (m, 2H), 6.89 – 6.84 (m, 2H), 3.56 (t, J = 5.2 Hz, 4H), 3.02 (t, J = 5.2 Hz, 4H), 1.47 (s, 9H).

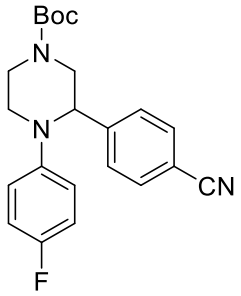

Reaction condition of 3e: CdS gel (2 x 10^{-3} mol %): 15 h, 166 mg, 87% yield. The crude product was purified using flash silica-gel column chromatography (Ethyl acetate : Hexane : NEt_3 = 18:81:1 v/v/v) to afford **3e** as white solid. **^{1}H NMR** (600 MHz, $CDCl_3$) δ 7.50 (d, *J* = 8.2 Hz, 2H), 7.41 (d, *J* = 8.4 Hz, 2H), 6.83 (d, *J* = 6.5 Hz, 4H), 4.24 (dd, *J* = 8.5, 3.7 Hz, 1H), 4.07 – 3.92 (m, 2H), 3.38 – 3.31 (m, 2H), 3.18 – 3.00 (m, 1H), 3.02 (t, *J* = 12.0 Hz, 1H), 1.44 (s, 9H). **^{13}C NMR** (151 MHz, $CDCl_3$) δ 159.4 (d, *J* = 242.1 Hz), 154.6, 146.8, 146.0, 132.5, 128.6, 123.0, 118.9, 116.0, 115.8, 111.4, 80.5, 62.8, 29.9, 28.5. **^{19}F NMR** (376 MHz, $CDCl_3$) δ -120.45. **HRMS** (TOF CI^+): *m/z* calculated for $C_{22}H_{24}FN_3O_2$ $[M+H]^+$: 382.1925, found: 382.1922.

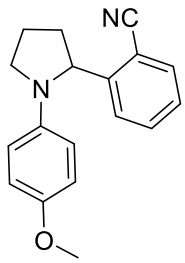

Reaction condition of 3f: CdS gel (2 x 10^{-3} mol %): 17 h, 62 mg, 42% yield. The crude product was purified using flash silica-gel column chromatography (Ethyl acetate : Hexane : NEt_3 = 10:89:1 v/v/v) to afford **3f** as white solid. **^{1}H NMR** (600 MHz, $CDCl_3$) δ 7.66 (dd, *J* = 7.6, 1.6 Hz, 1H), 7.46 – 7.43 (m, 1H), 7.33 – 7.28 (m, 2H), 6.75 – 6.73 (m, 2H), 6.38 – 6.35 (m, 2H), 4.95 (dd, *J* = 8.5, 2.9 Hz, 1H), 3.76 – 3.73 (m, 1H), 3.69 (s, 3H), 3.37 (q, *J* = 8.0, 7.5 Hz, 1H), 2.58 – 2.52 (m, 1H), 2.04 – 1.98 (m, 2H), 1.96 – 1.93 (m, 1H). **^{13}C NMR** (151 MHz, $CDCl_3$) δ 151.5, 149.7, 141.5, 133.7, 133.1, 127.4, 127.1, 117.9, 115.0, 113.4, 110.2, 62.1, 56.0, 50.1, 35.6, 23.7.

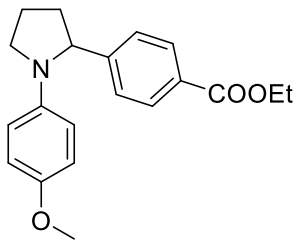

Reaction condition of 3g: CdS gel (2 x 10^{-3} mol %): 17 h, 46 mg, 30% yield. The crude product was purified using flash silica-gel column chromatography (Ethyl acetate : Hexane : NEt_3 = 10:89:1 v/v/v) to afford **3g** as colorless oil. **^{1}H NMR** (600 MHz, $CDCl_3$) δ 8.00 – 7.98 (m, 2H), 7.33 – 7.31 (m, 2H), 6.77 – 6.74 (m, 2H), 6.43 – 6.40 (m, 2H), 4.67 (dd, *J* = 8.5, 2.9 Hz, 1H), 4.37 (q, *J* = 7.1 Hz, 2H), 3.74 – 3.71 (m, 1H), 3.71 (s, 3H), 3.40 – 3.36 (m, 1H), 2.46 – 2.39 (m, 1H), 2.04 – 1.97 (m, 2H), 1.93 – 1.89 (m, 1H), 1.38 (t, *J* = 7.2 Hz, 3H). **^{13}C NMR** (151 MHz, $CDCl_3$) δ 166.7, 151.2, 150.8, 142.1, 130.1, 129.2, 126.1, 115.0, 113.3, 63.5, 61.0, 56.1, 50.0, 36.3, 23.6, 14.6.

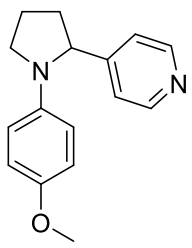

Reaction condition of 3h: CdS gel (2 x 10^{-3} mol %): 9 h, 43 mg, 35% yield. The crude product was purified using flash silica-gel column chromatography (Ethyl acetate : Hexane : NEt_3 = 20:79:1 v/v/v) to afford **3h** as yellow solid. **^{1}H NMR** (600 MHz, $CDCl_3$) δ 8.52 (d, *J* = 6.2 Hz, 2H), 7.22 (d, *J* = 6.3 Hz, 2H), 6.78 – 6.75 (m, 2H), 6.40 – 6.37 (m, 2H), 4.60 (dd, *J* = 8.7, 2.7 Hz, 1H), 3.72 (s, 4H), 3.39 – 3.35 (m, 1H), 2.47 – 2.41 (m, 1H), 2.03– 1.96 (m, 2H), 1.93 – 1.89 (m, 1H). **^{13}C NMR** (151 MHz, $CDCl_3$) δ 154.6, 151.5, 150.1, 141.8, 121.6, 115.1, 113.3, 62.8, 56.1, 50.0, 35.9, 23.6. **HRMS** (TOF Cl^+): *m/z* calculated for $C_{16}H_{18}N_2O$ $[M+H]^+$: 255.1492, found 255.1486.

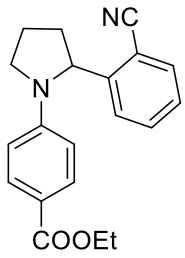

Reaction condition of 4d: TOPO/CdS (2 x 10^{-3} mol %): 9 h, 10 mg, 6% yield. **TGA/CdS (2 x 10^{-3} mol %):** 9 h, 8 mg, 8% yield. **CdS gel (2 x 10^{-3} mol %):** 9 h, 18 mg, 11% yield. The crude product was purified using flash silica-gel column chromatography (Ethyl acetate : Hexane : NEt_3 = 12:87:1 v/v/v) to afford **4d** as white solid. **^{1}H NMR** (600 MHz, $CDCl_3$) δ 7.85 – 7.82 (m, 2H), 7.71 – 7.69 (m, 1H), 7.49 – 7.45 (m, 1H), 7.36 – 7.32 (m, 1H), 7.19 – 7.17 (m, 1H), 6.42 – 6.39 (m, 2H), 5.16 – 5.13 (m, 1H), 4.28 (q, J = 7.1 Hz, 2H), 3.84 – 3.79 (m, 1H), 3.58 – 3.53 (m, 1H), 2.66 – 2.56 (m, 1H), 2.12 – 1.99 (m, 3H), 1.33 (t, J = 7.1 Hz, 3H). **^{13}C NMR** (101 MHz, $CDCl_3$) δ 166.07, 148.76, 146.92, 133.00, 132.24, 130.45, 126.83, 125.80, 117.53, 116.67, 111.01, 109.38, 60.68, 59.37, 48.57, 34.41, 22.34, 13.64.

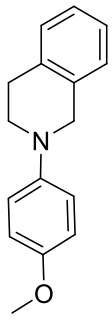

Starting material of 3i: ^{1}H NMR (400 MHz, $CDCl_3$) δ 7.20 – 7.13(m, 4H), 7.00 (d, J = 9.0 Hz, 2H), 6.88 (d, J = 9.0 Hz, 2H), 4.31 (s, 2H), 3.79 (s, 3H), 3.46 (t, J = 5.8 Hz, 2H), 3.00 (t, J = 5.9 Hz, 2H).

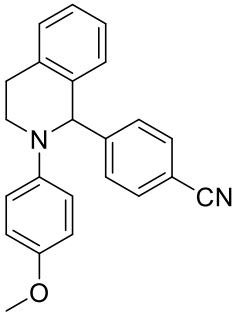

Reaction condition of 3i: TOPO/CdS (2 x 10^{-3} mol %): 5 h, 99 mg, 62% yield. **TGA/CdS (2 x 10^{-3} mol %):** 5 h, 149 mg, 92 % yield. The crude product was purified using flash silica-gel column chromatography (Ethyl acetate : Hexane : NEt_3 = 12:87:1 v/v/v) to afford **3i** as white solid. **^{1}H NMR** (400 MHz, CDCl3) δ 7.50 – 7.49 (m, 2H), 7.29 – 7.28 (m, 2H), 7.25 – 7.18 (m, 3H), 7.10 – 7.09 (m, 1H), 6.80 (s, 4H), 5.66 (s, 1H), 3.75 (s, 3H), 3.54 – 3.50 (m, 1H), 3.42 – 3.38 (m, 1H), 3.01 – 2.91 (m, 2H). **^{13}C NMR** (151 MHz, CDCl3) δ 153.67, 148.99, 144.04, 136.49, 135.60, 132.05, 128.98, 128.81, 128.14, 127.39, 126.43, 119.03, 118.54, 114.72, 110.85, 55.72, 45.32, 28.48.

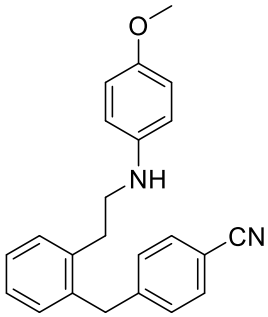

Reaction condition of 4i: CdS gel (2 x 10^{-3} mol %): 5 h, 80 mg, 47% yield. The crude product was purified using flash silica-gel column chromatography (Ethyl acetate : Hexane : NEt_3 = 50:49:1 v/v/v) to afford **4i** as white solid. **^{1}H NMR** (400 MHz, CDCl3) δ 7.56 – 7.53 (m, 2H), 7.29 – 7.23 (m, 3H), 7.19 – 7.17 (m, 2H), 7.13 (d, *J* = 7.6 Hz, 1H), 6.81 – 6.78 (m, 2H), 6.54 – 6.51 (m, 2H), 4.09 (s, 2H), 3.77 (s, 3H), 3.27 (td, *J* = 7.4, 2.6 Hz, 2H), 2.84 (td, *J* = 7.4, 2.7 Hz, 2H). **^{13}C NMR** (151 MHz, CDCl3) δ 152.4, 146.6, 142.2, 138.0, 137.3, 132.4, 131.0, 130.2, 129.5, 127.6, 127.1, 119.1, 115.1, 114.4, 110.2, 56.0, 45.6, 39.2, 32.7. **HRMS** (TOF CI$^+$): *m/z* calculated for $C_{23}H_{22}N_2O$ $[M+H]^+$: 343.1805, found 343.179.

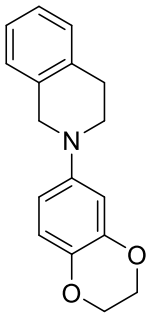

Starting material of 3j: ^{1}H NMR (400 MHz, $CDCl_3$) δ 7.16 (tt, J = 9.2, 4.6 Hz, 4H), 6.83 – 6.80 (m, 1H), 6.57 – 6.54 (m, 2H), 4.30 (s, 2H), 4.27 – 4.22 (m, 4H), 3.45 (t, J = 5.9 Hz, 2H), 2.98 (t, J = 5.9 Hz, 2H).

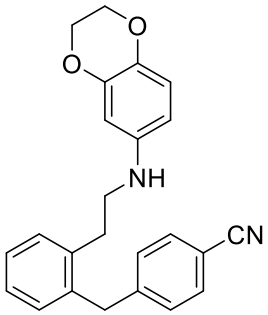

Reaction condition of 4j: CdS gel (2 x 10^{-3} mol %): 5 h, 25 mg, 14% yield. The crude product was purified using flash silica-gel column chromatography (Ethyl acetate : Hexane : NEt_3 = 50:49:1 v/v/v) to afford **4l** as white solid. **^{1}H NMR** (400 MHz, $CDCl_3$) δ 7.53 (d, *J* = 8.2 Hz, 2H), 7.26 – 7.19 (m, 3H), 7.17 (d, *J* = 8.1 Hz, 2H), 7.11 (d, *J* = 7.1 Hz, 1H), 6.69 (d, *J* = 8.3 Hz, 1H), 6.12 – 6.06 (m, 2H), 4.25 – 4.22 (m, 2H), 4.20 – 4.16 (m, 2H), 4.07 (s, 2H), 3.21 (t, *J* = 7.2 Hz, 2H), 2.81 (t, *J* = 7.2 Hz, 2H). **^{13}C NMR** (100 MHz, $CDCl_3$) δ 146.65, 144.34, 142.82, 138.00, 137.37, 136.12, 132.49, 131.06, 130.24, 129.51, 127.60, 127.14, 119.14, 117.93, 110.28, 107.19, 101.98, 77.55, 77.23, 76.91, 64.97, 64.42, 45.48, 39.24, 32.68. **HRMS** (TOF CI^+): *m/z* calculated for $C_{24}H_{22}N_2O_2$ $[M+H]^+$: 371.1754, found 371.1743.

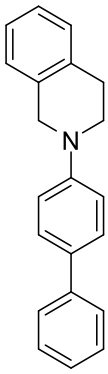

Starting material of 3k: ^{1}H NMR (400 MHz, $CDCl_3$) δ 7.61 – 7.57 (m, 4H), 7.44 (t, J = 7.7 Hz, 2H), 7.32 – 7.29 (m, 1H), 7.23 (d, J = 5.6 Hz, 4H), 7.07 (d, J = 8.8 Hz, 2H), 4.50 (s, 2H), 3.64 (t, J = 5.8 Hz, 2H), 3.04 (t, J = 5.9 Hz, 2H).

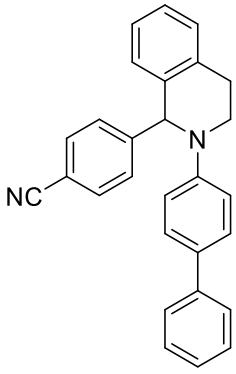

Reaction condition of 3k: CdS gel (2 x 10^{-3} mol %): 5 h, 42 mg, 21% yield. The crude product was purified using flash silica-gel column chromatography (Ethyl acetate : Hexane : NEt_3 = 12:87:1 v/v/v) to afford **3k** as yellow oil. **^{1}H NMR** (400 MHz, $CDCl_3$) δ 7.63 – 7.49 (m, 6H), 7.44 – 7.37 (m, 4H), 7.35 – 7.26 (m, 4H), 7.22 (q, *J* = 4.1 Hz, 1H), 6.89 (d, *J* = 8.9 Hz, 2H), 5.87 (s, 1H), 3.80 – 3.74 (m, 1H), 3.59 – 3.51 (m, 1H), 3.04 – 2.97 (m, 1H), 2.92 – 2.84 (m, 1H). **^{13}C NMR (100 MHz, $CDCl_3$)** δ 148.88, 148.61, 141.03, 136.67, 135.90, 132.43, 128.98, 128.91, 128.58, 128.42, 128.20, 128.15, 127.92, 126.80, 126.57, 119.01, 117.81, 114.31, 111.10, 77.55, 77.23, 76.91, 62.99, 53.15, 44.43.

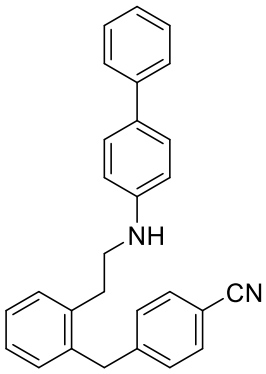

Reaction condition of 4k: CdS gel (2 x 10^{-3} mol %): 5 h, 43 mg, 21% yield. The crude product was purified using flash silica-gel column chromatography (Ethyl acetate : Hexane : NEt_3 = 50:49:1 v/v/v) to afford **4k** as white solid. **^{1}H NMR** (400 MHz, $CDCl_3$) δ 7.57 – 7.51 (m, 4H), 7.45 (d, *J* = 8.4 Hz, 2H), 7.40 (t, *J* = 7.6 Hz, 2H), 7.28 (d, *J* = 6.5 Hz, 2H), 7.23 (dd, *J* = 8.3, 4.5 Hz, 2H), 7.18 (d, *J* = 8.0 Hz, 2H), 7.13 (d, *J* = 7.2 Hz, 1H), 6.66 (d, *J* = 8.1 Hz, 2H), 4.09 (s, 2H), 3.34 (t, *J* = 7.2 Hz, 2H), 2.88 (t, *J* = 7.2 Hz, 2H). **^{13}C NMR (100 MHz, $CDCl_3$)** δ 147.33, 146.59, 141.28, 137.87, 137.36, 132.46, 131.06, 130.72, 130.22, 129.49, 128.86, 128.17, 127.62, 127.19, 126.44, 126.32, 119.08, 113.33, 110.25, 77.55, 77.23, 76.91, 44.65, 39.20, 32.61. **HRMS** (TOF CI$^+$): *m/z* calculated for $C_{28}H_{24}N_2$ $[M+H]^+$: 389.2012, found 389.1999.

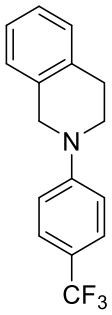

Starting material of 3l: ^{1}H NMR (400 MHz, $CDCl_3$) δ 7.52 (d, J = 8.6 Hz, 2H), 7.22 (q, J = 5.1 Hz, 4H), 6.95 (d, J = 8.6 Hz, 2H), 4.50 (s, 2H), 3.65 (t, J = 5.9 Hz, 2H), 3.01 (t, J = 5.9 Hz, 2H).

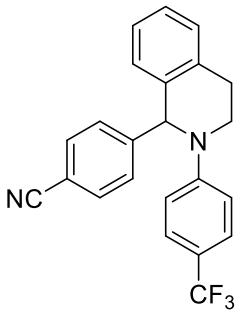

Reaction condition of 3l: CdS gel (2 x 10^{-3} mol %): 5 h, 94 mg, 40% yield. The crude product was purified using flash silica-gel column chromatography (Ethyl acetate : Hexane : NEt_3 = 12:87:1 v/v/v) to afford **3j** as yellow solid. **^{1}H NMR** (400 MHz, $CDCl_3$) δ 7.56 (d, J = 8.5 Hz, 2H), 7.47 (d, J = 8.9 Hz, 2H), 7.38 (d, J = 8.4 Hz, 2H), 7.35 – 7.34 (m, 1H), 7.31 – 7.27 (m, 2H), 7.23 – 7.20 (m, 1H), 6.81 (d, J = 8.9 Hz, 2H), 5.87 (s, 1H), 3.81 (dt, J = 10.4, 4.9 Hz, 1H), 3.54 (td, J = 10.7, 4.5 Hz, 1H), 2.98 (dt, J = 15.5, 4.4 Hz, 1H), 2.89 – 2.84 (m, 1H). **^{13}C NMR** (151 MHz, $CDCl_3$) δ 151.05, 147.73, 136.27, 135.43, 132.76, 132.36, 128.23, 128.06, 127.54, 126.83, 126.65 (q, *J* = 4.0, 3.5 Hz), 112.22, 62.27, 46.19, 44.30, 27.99. **^{19}F NMR** (376 MHz, $CDCl_3$) δ -61.17. **HRMS** (TOF CI$^+$): *m/z* calculated for $C_{23}H_{17}F_3N_2$ $[M+H]^+$: 379.1417, found 379.1409.

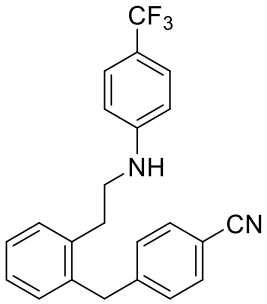

Reaction condition of 4l: CdS gel (2 x 10^{-3} mol %): 5 h, 14 mg, 10% yield. The crude product was purified using flash silica-gel column chromatography (Ethyl acetate : Hexane : NEt_3 = 50:49:1 v/v/v) to afford **3j** as yellow solid. **^{1}H NMR** (400 MHz, $CDCl_3$) δ 7.54 (d, J = 8.3 Hz, 2H), 7.40 (d, J = 8.6 Hz, 2H), 7.31 – 7.22 (m, 4H), 7.19 – 7.11 (m, 3H), 6.53 (d, J = 8.5 Hz, 2H), 4.08 (s, 2H), 3.33 (t, J = 7.1 Hz, 2H), 2.85 (t, J = 7.1 Hz, 2H). **13C NMR** (100 MHz, CDCl3) δ 150.40, 146.48, 137.47, 137.33, 132.53, 131.20, 130.18, 129.47, 127.74, 127.40, 126.90 (q, *J* = 3.8 Hz) 119.03, 112.08, 110.41, 44.09, 39.24, 32.36. **^{19}F NMR** (376 MHz, CDCl3) δ -61.08. **HRMS** (TOF CI$^+$): *m/z* calculated for $C_{23}H_{19}F_3N_2$ $[M+H]^+$: 381.1573, found 381.1564.

References

1. Hewa-Rahinduwage, C. C.; Geng, X.; Silva, K. L.; Niu, X.; Zhang, L.; Brock, S. L.; Luo, L., Reversible Electrochemical Gelation of Metal Chalcogenide Quantum Dots. *J. Am. Chem. Soc.* **2020,** *142* (28), 12207-12215.
2. Zhang, Z.; Miao, C.; Xia, C.; Sun, W., Synergistic acid-catalyzed synthesis of N-aryl-substituted azacycles from anilines and cyclic ethers. *Org. Lett.* **2016,** *18* (7), 1522-1525.
3. Tampio L'Estrade, E.; Shalgunov, V.; Lehel, S.; Nymann Petersen, I.; Poulie, C. B. M.; Edgar, F. G.; Volk, B.; Ohlsson, T.; Erlandsson, M.; Knudsen, G. M., Fragment-based labeling using condensation reactions of six potential 5-HT7R PET tracers. *Journal of Radioanalytical and Nuclear Chemistry* **2020,** *326* (3), 1749-1762.
4. Reilly, S. W.; Mach, R. H., Pd-Catalyzed synthesis of piperazine scaffolds under aerobic and solvent-free conditions. *Org. Lett.* **2016,** *18* (20), 5272-5275.
5. Mudithanapelli, C.; Dhorma, L. P.; Kim, M.-h., PIFA-promoted, solvent-controlled selective functionalization of C (sp2)–H or C (sp3)–H: nitration via C–N bond cleavage of CH3NO2, cyanation, or oxygenation in water. *Org. Lett.* **2019,** *21* (9), 3098-3102.
6. Nguyen, J. D.; D'amato, E. M.; Narayanam, J. M.; Stephenson, C. R., Engaging unactivated alkyl, alkenyl and aryl iodides in visible-light-mediated free radical reactions. *Nature Chem.* **2012,** *4* (10), 854-859.
7. McNally, A.; Prier, C. K.; MacMillan, D. W., Discovery of an α-amino C–H arylation reaction using the strategy of accelerated serendipity. *Science* **2011,** *334* (6059), 1114-1117.
8. Yu, W. W.; Qu, L.; Guo, W.; Peng, X., Experimental determination of the extinction coefficient of CdTe, CdSe, and CdS nanocrystals. *Chem. Mater.* **2003,** *15* (14), 2854-2860.
9. Bullen, C.; Mulvaney, P., The Effects of Chemisorption on the Luminescence of CdSe Quantum Dots. *Langmuir* **2006,** *22* (7), 3007-3013.
10. McNally, A.; Prier, C. K.; MacMillan, D. W. C., Discovery of an α-Amino C–H Arylation Reaction Using the Strategy of Accelerated Serendipity. *Science* **2011,** *334* (6059), 1114-1117.
11. Sheldrick, G. M., SHELXT–Integrated space-group and crystal-structure determination. *Acta Crystallographica Section A: Foundations and Advances* **2015,** *71* (1), 3-8.
12. Sheldrick, G. M., Crystal structure refinement with SHELXL. *Acta Crystallographica Section C: Structural Chemistry* **2015,** *71* (1), 3-8.
13. Dolomanov, O. V.; Bourhis, L. J.; Gildea, R. J.; Howard, J. A.; Puschmann, H., OLEX2: a complete structure solution, refinement and analysis program. *J. Appl. Crystallogr.* **2009,** *42* (2), 339-341.

Copies of NMR Spectra

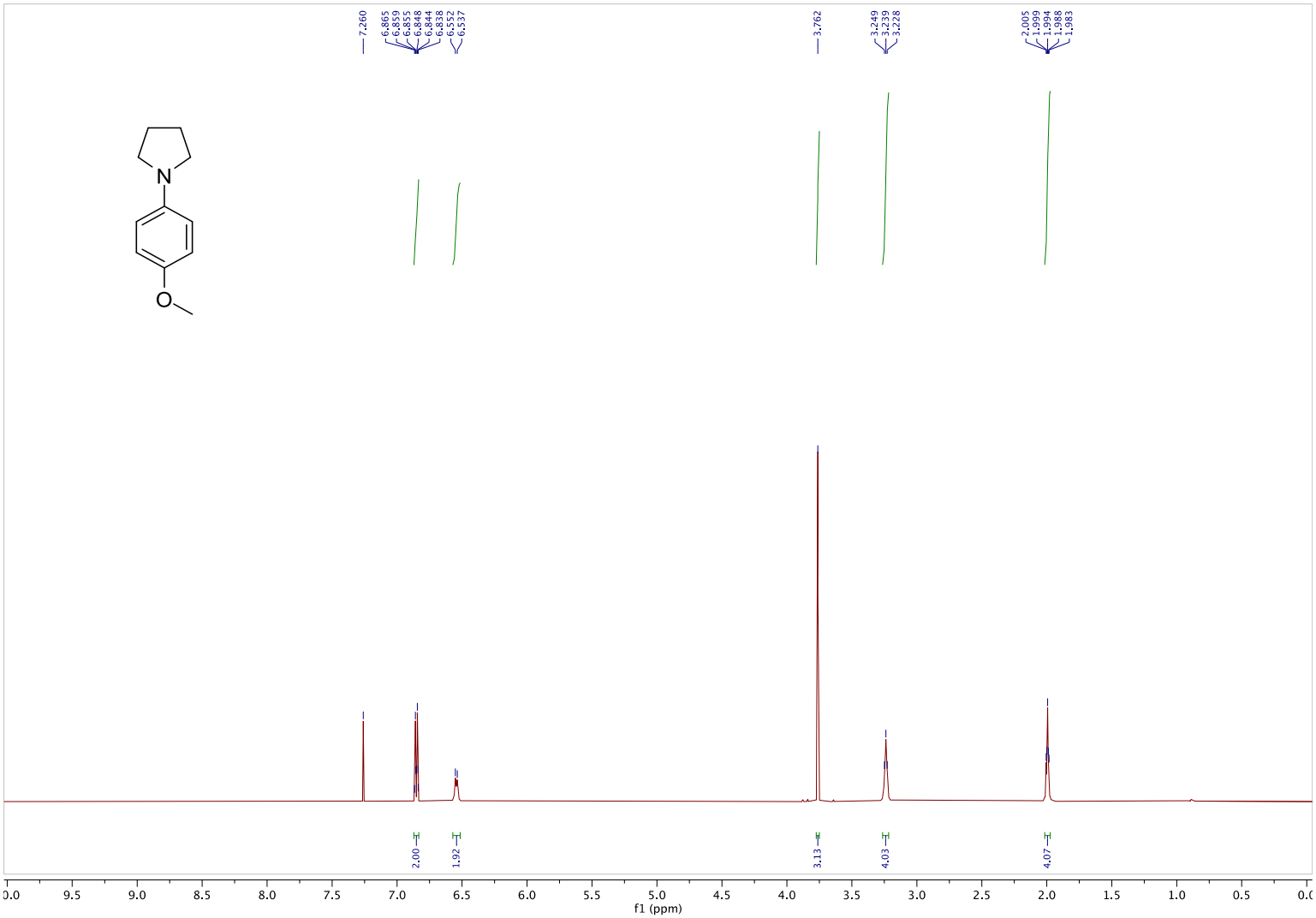

^{1}H NMR spectrum of starting material of **3a** (600 MHz, $CDCl_3$)

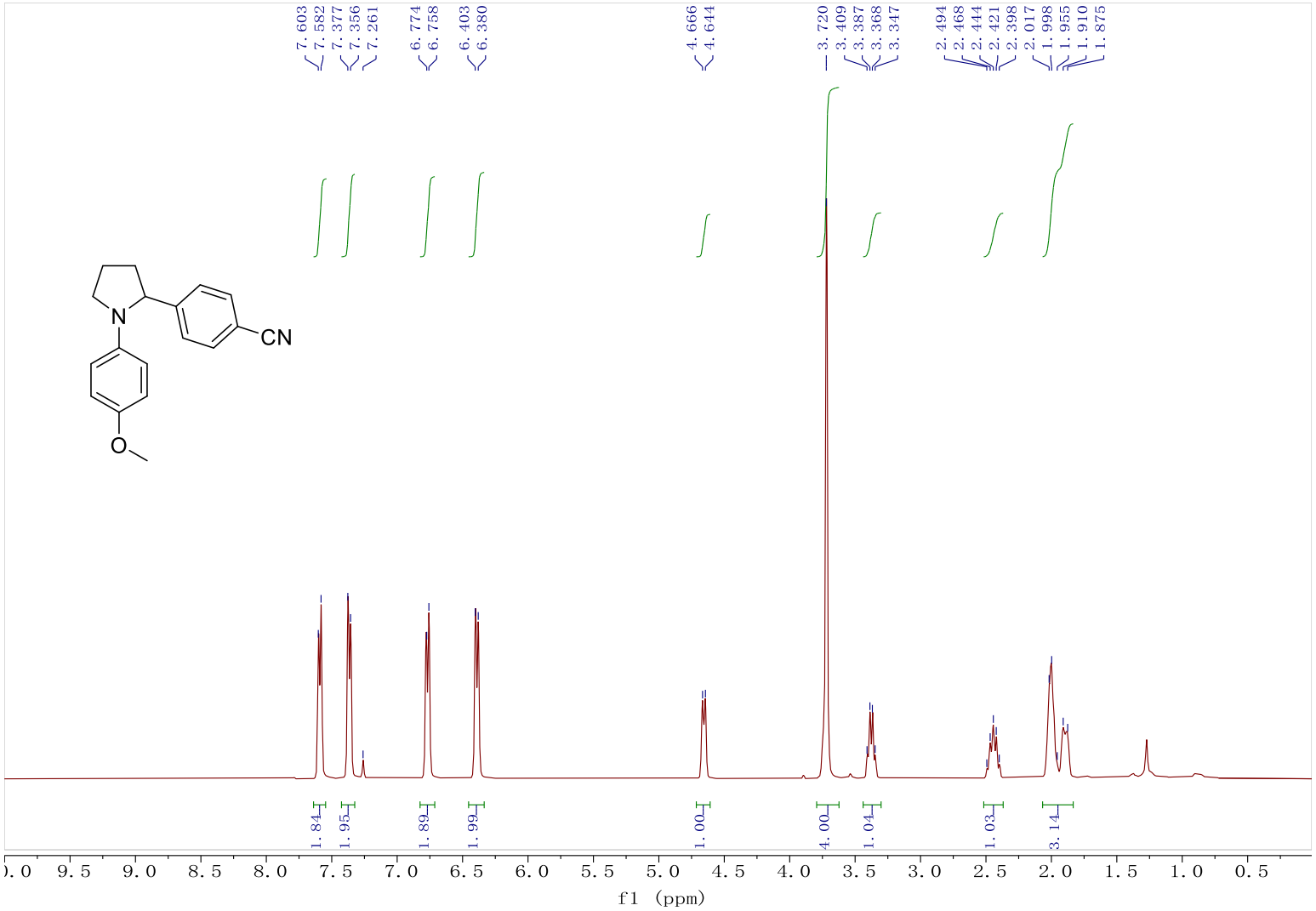

. **^{1}H NMR** spectrum of **3** (400 MHz, $CDCl_3$)

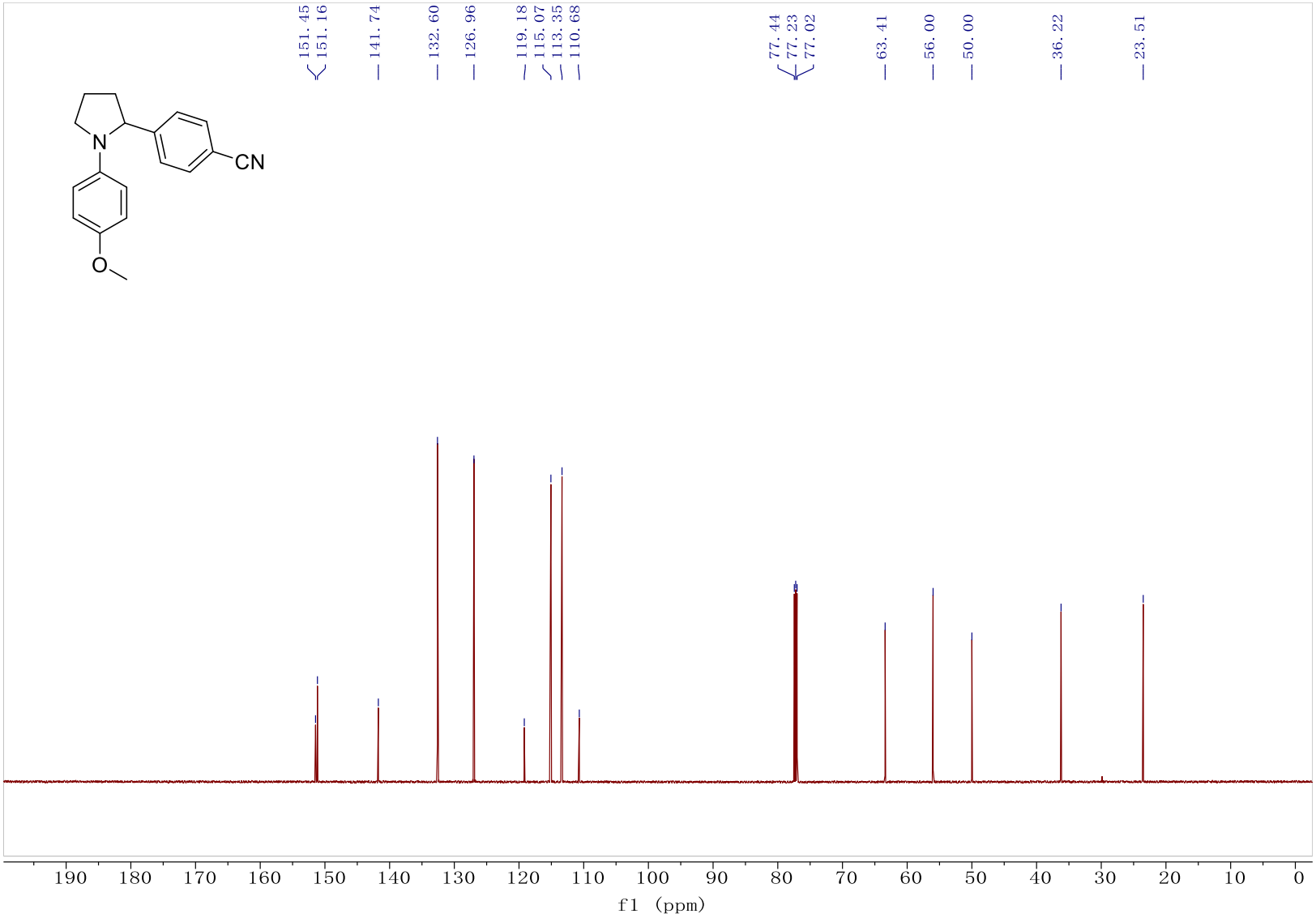

^{13}C NMR spectrum of **3** (151 MHz, $CDCl_3$)

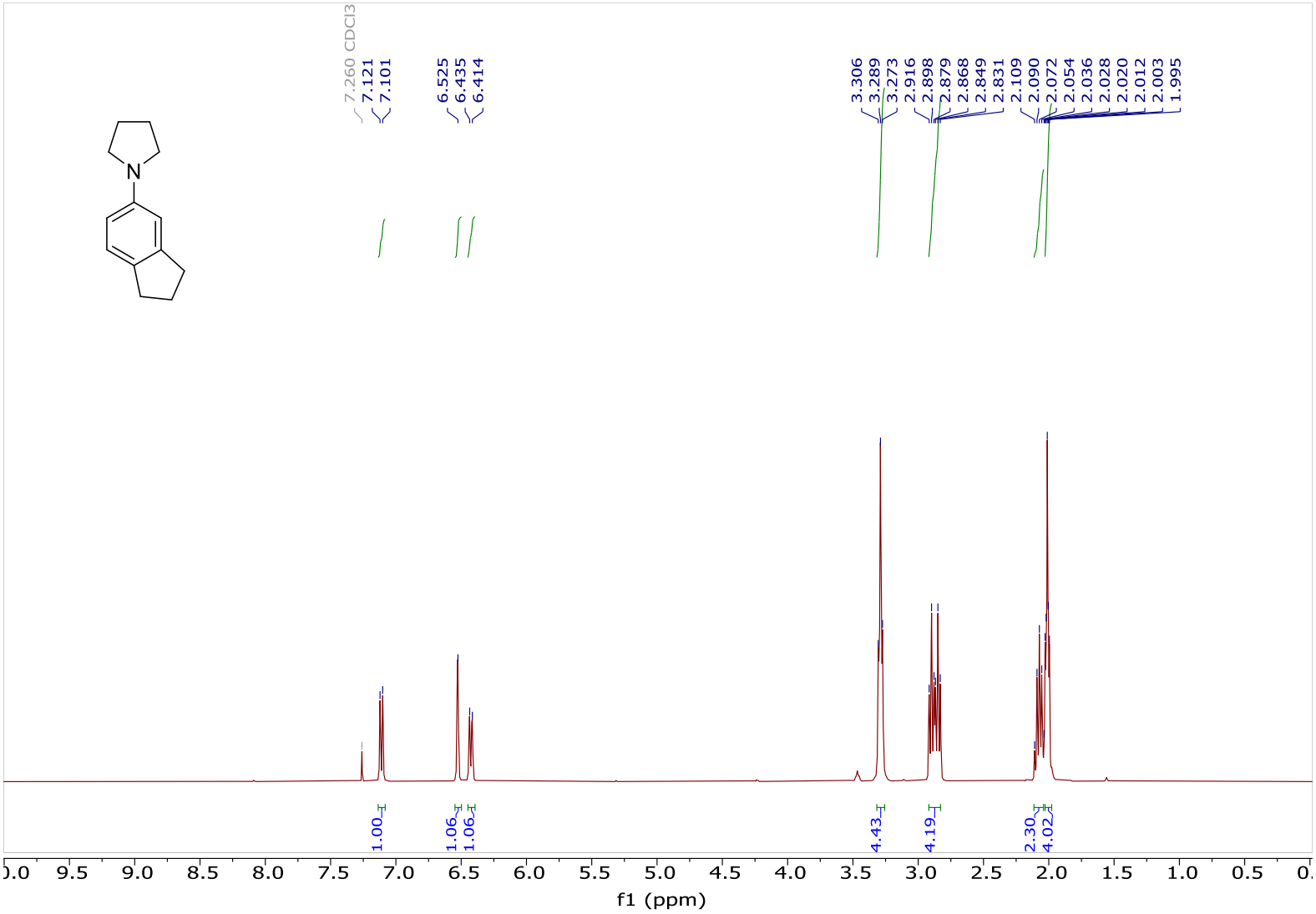

^{1}H NMR spectrum of starting material of **3a** (400 MHz, $CDCl_3$)

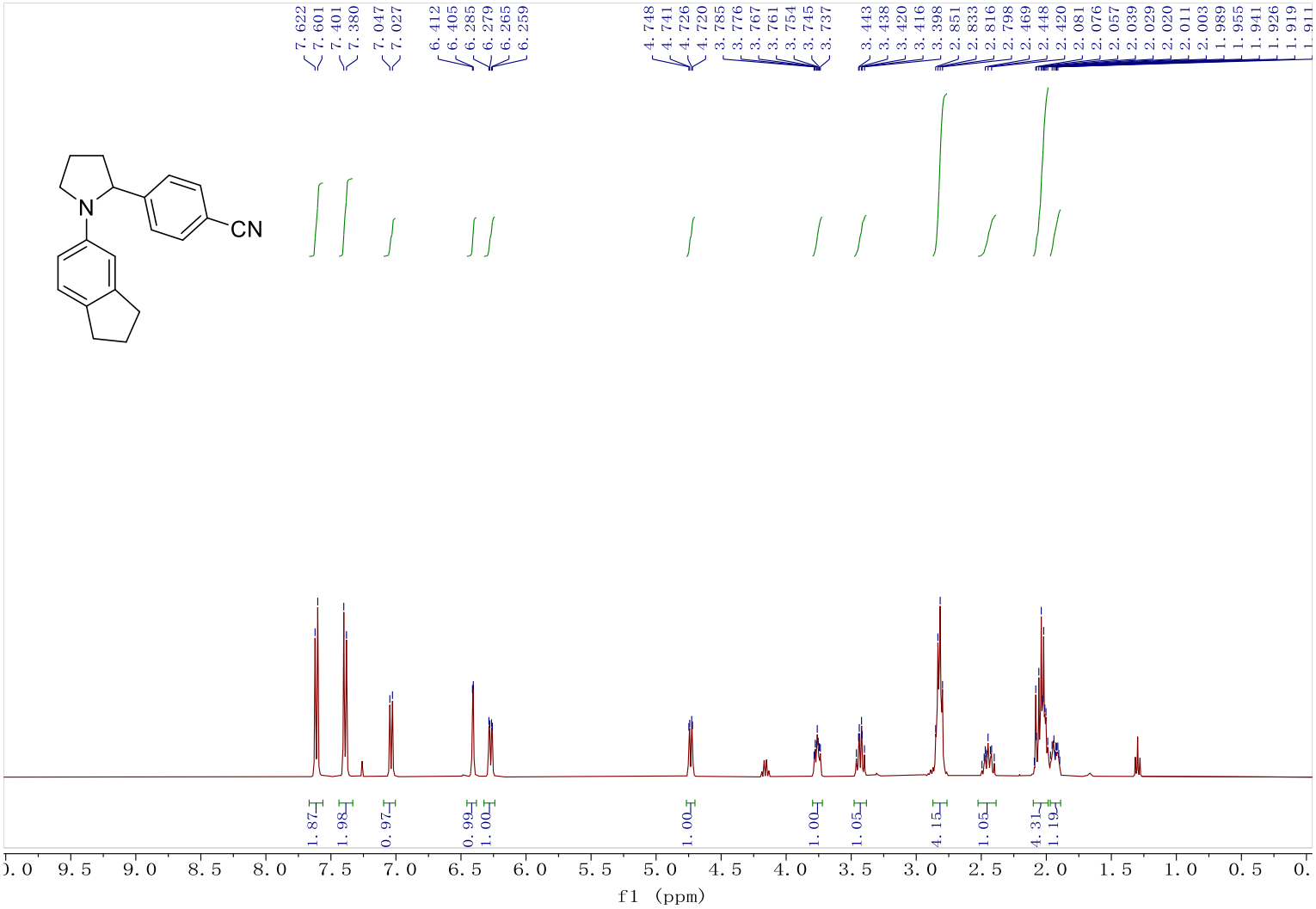

^{1}H NMR spectrum of **3a** (400 MHz, $CDCl_3$)

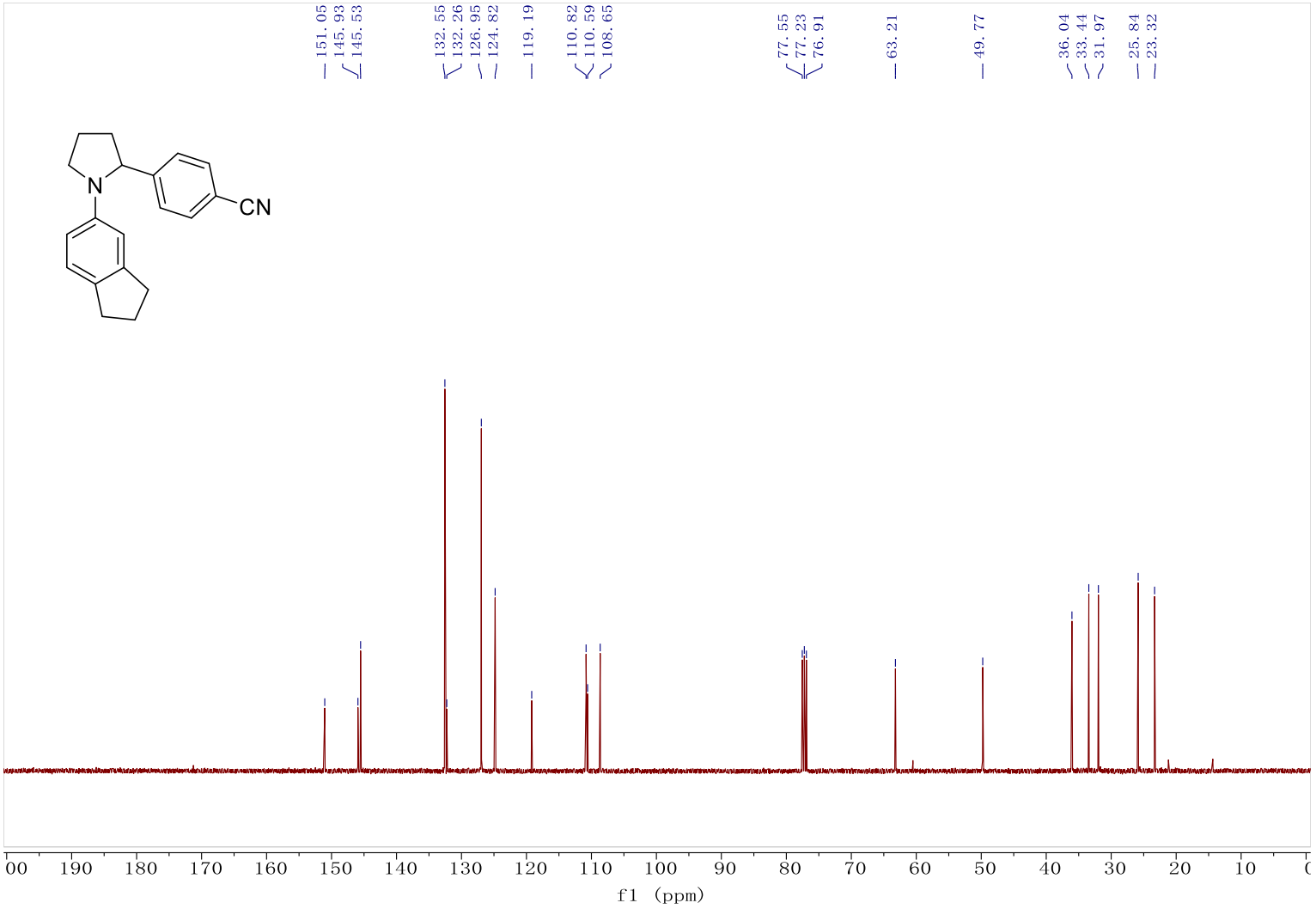

^{13}C NMR spectrum of **3a** (101 MHz, $CDCl_3$)

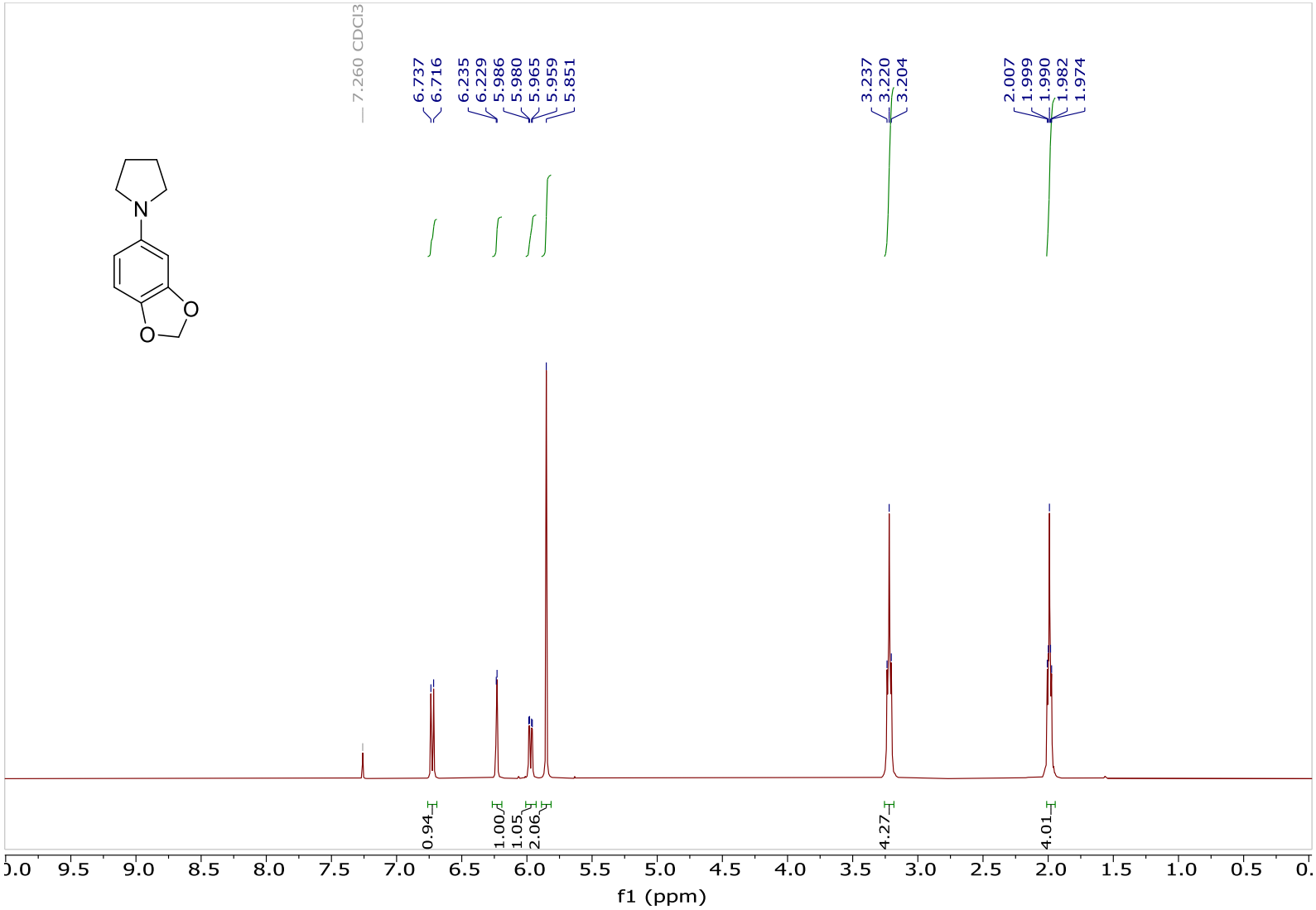

^{1}H NMR spectrum of starting material of **3b** (400 MHz, $CDCl_3$)

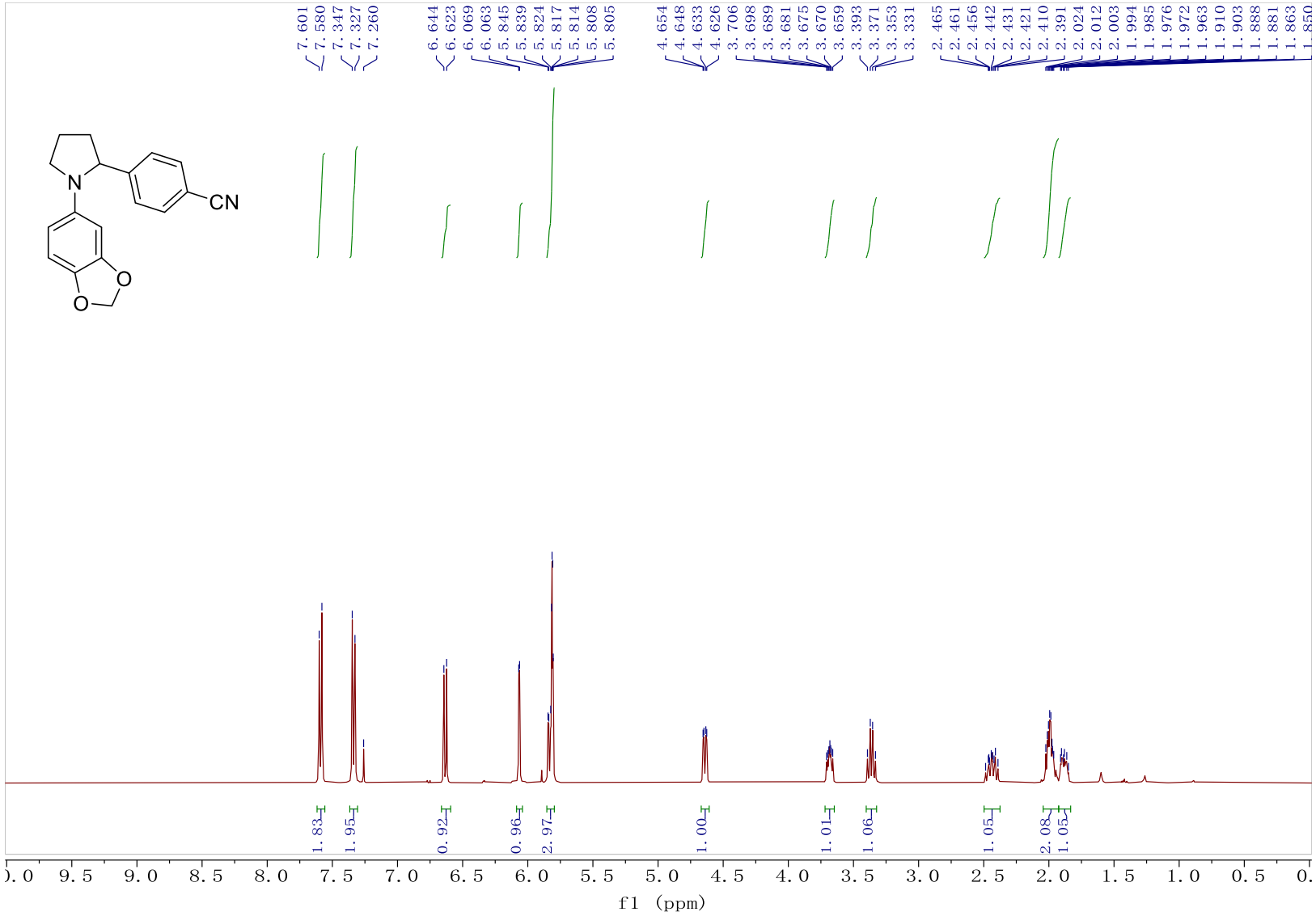

^{1}H NMR spectrum of **3b** (400 MHz, $CDCl_3$)

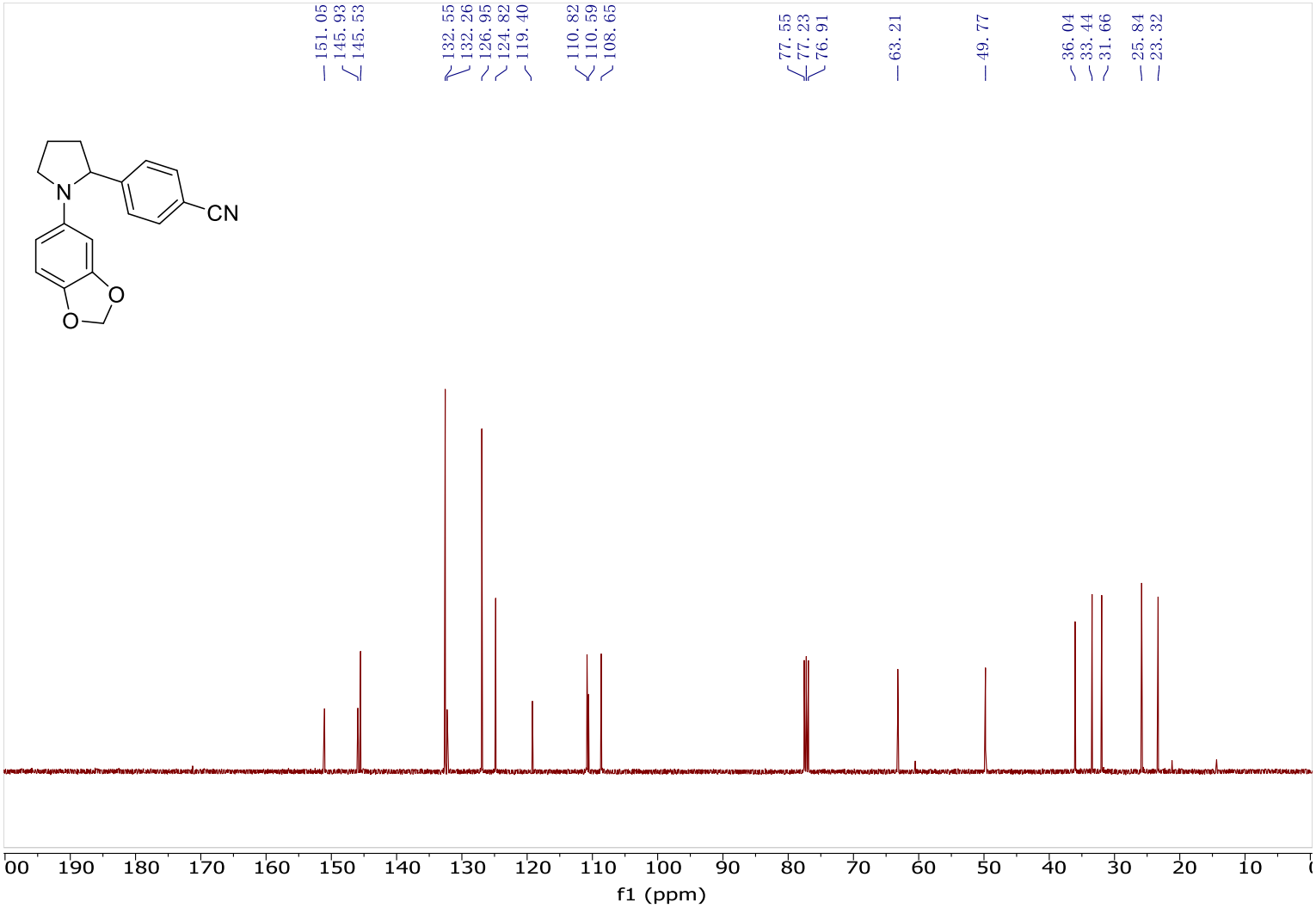

^{13}C NMR spectrum of **3b** (101 MHz, $CDCl_3$)

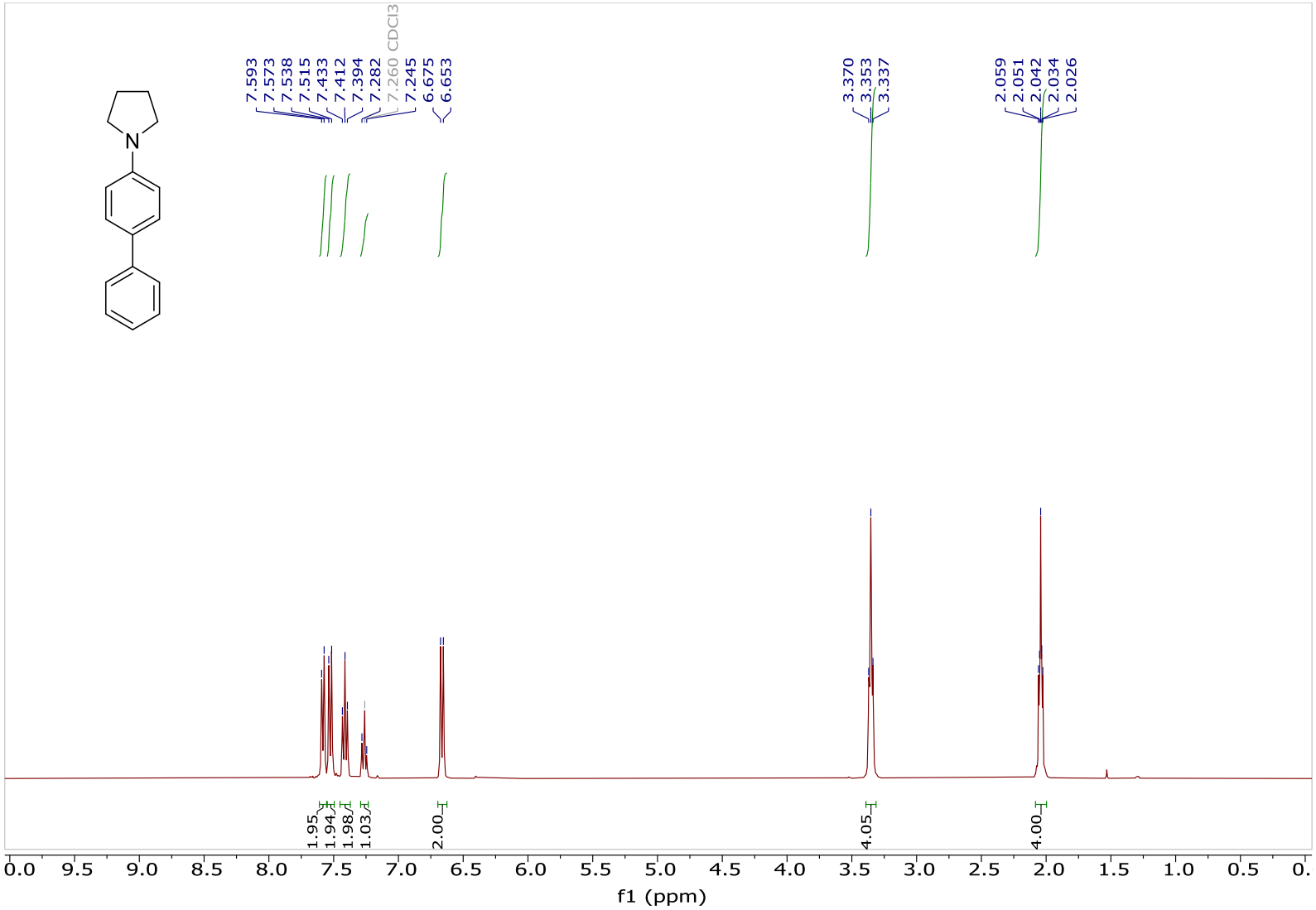

^{1}H NMR spectrum of starting material of **3c** (400 MHz, $CDCl_3$)

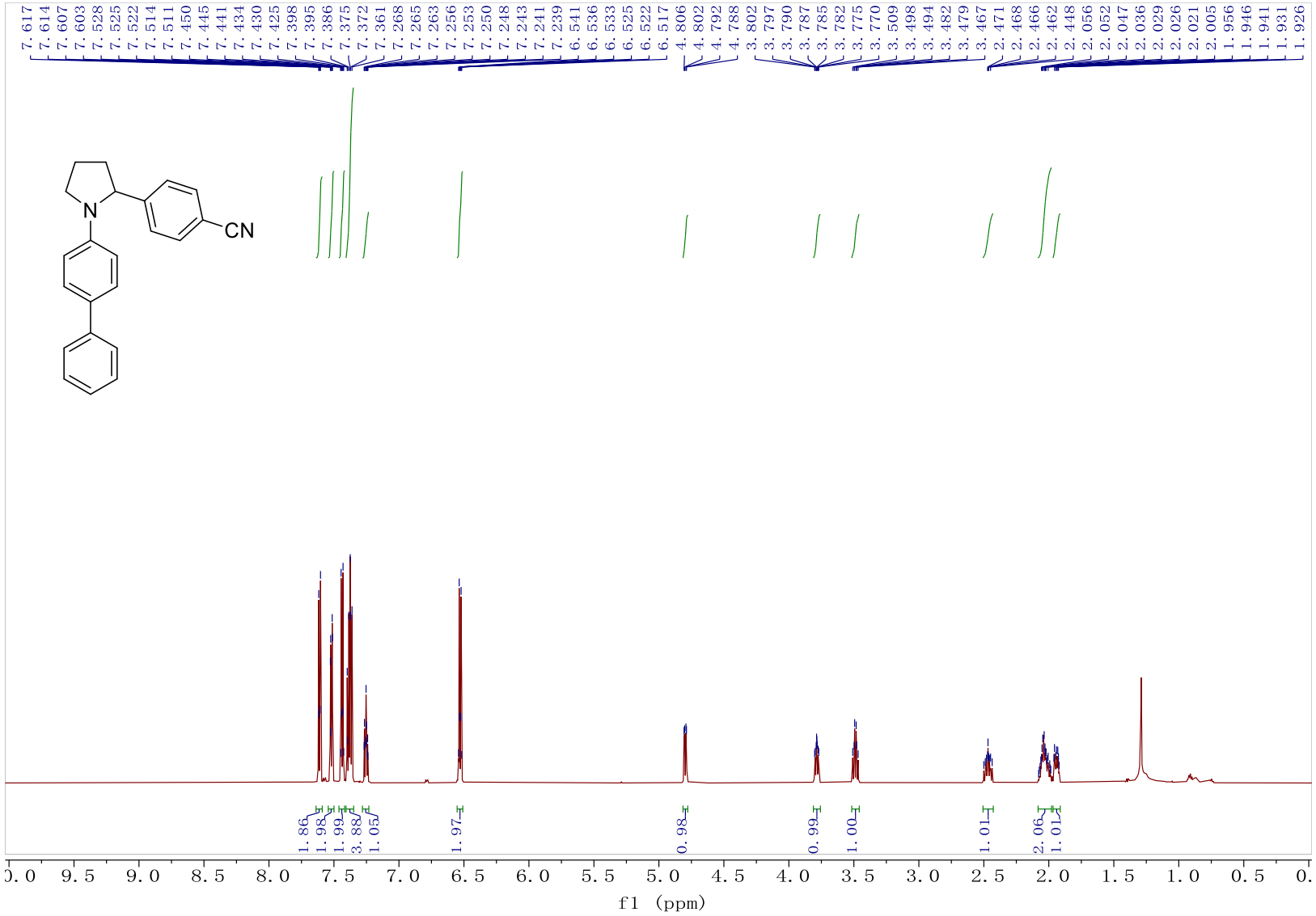

^{1}H NMR spectrum of **3c** (600 MHz, $CDCl_3$)

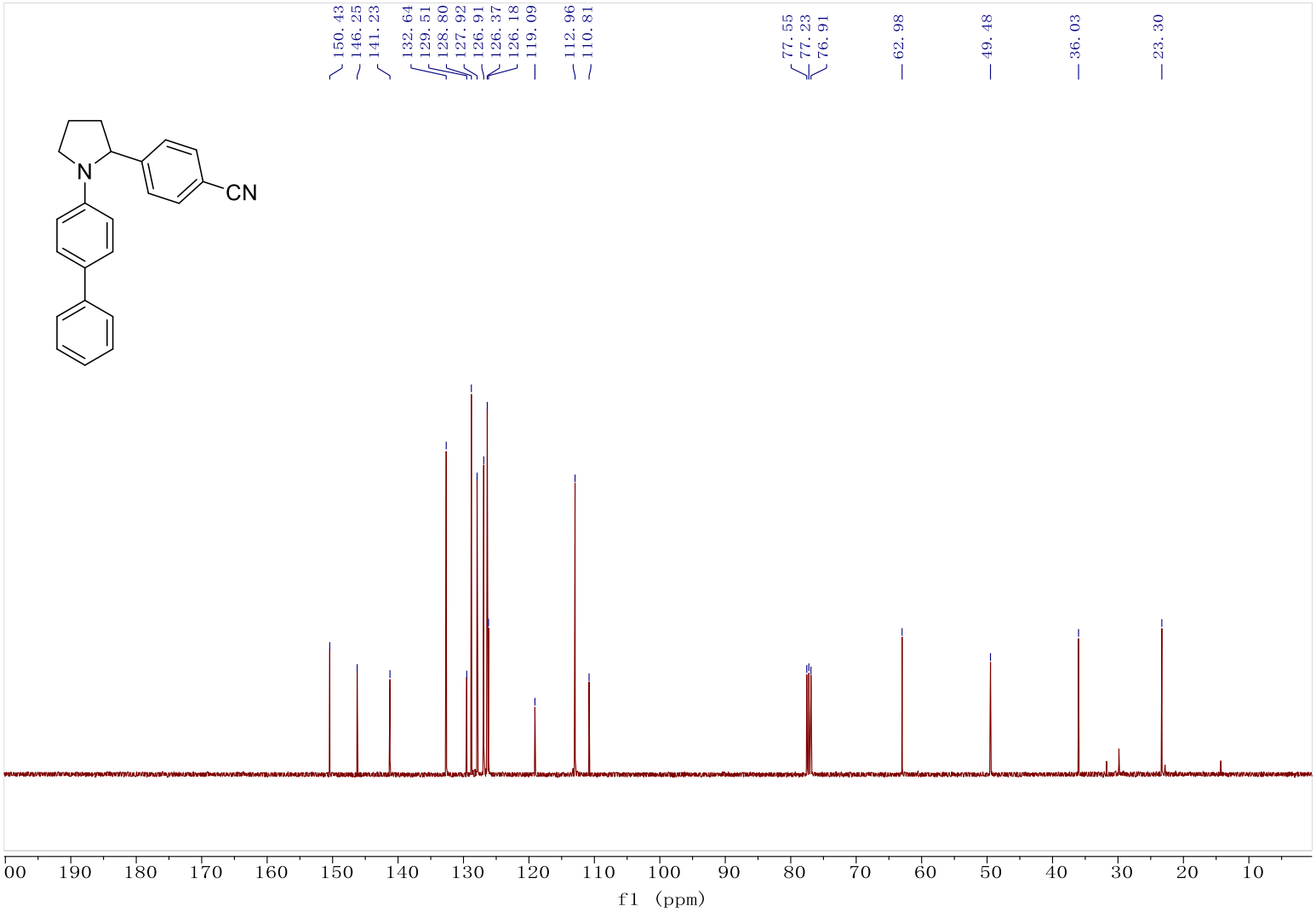

^{13}C NMR spectrum of **3c** (101 MHz, $CDCl_3$)

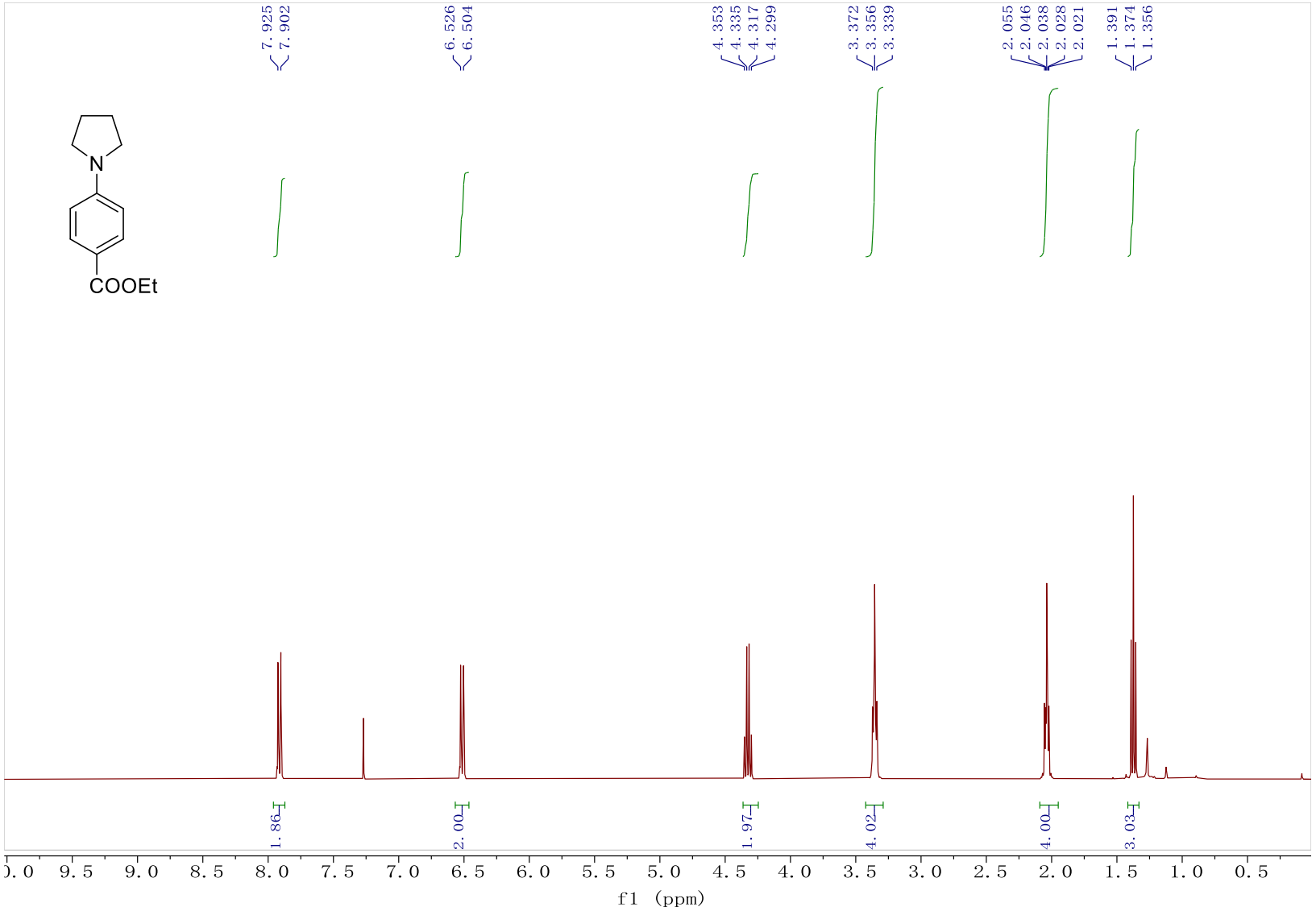

^{1}H NMR spectrum of starting material of **3d** (400 MHz, $CDCl_3$)

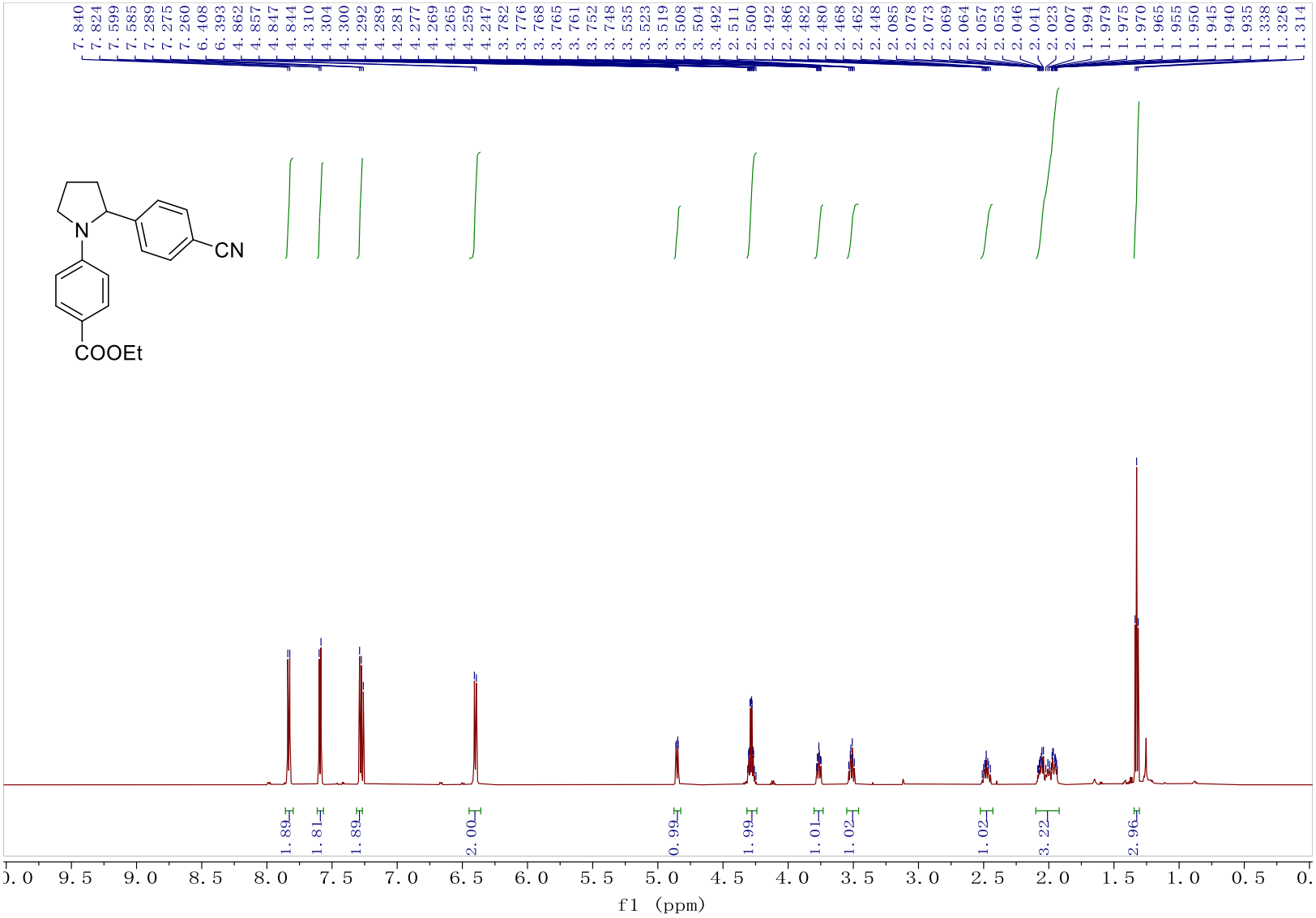

^{1}H NMR spectrum of **3d** (600 MHz, $CDCl_3$)

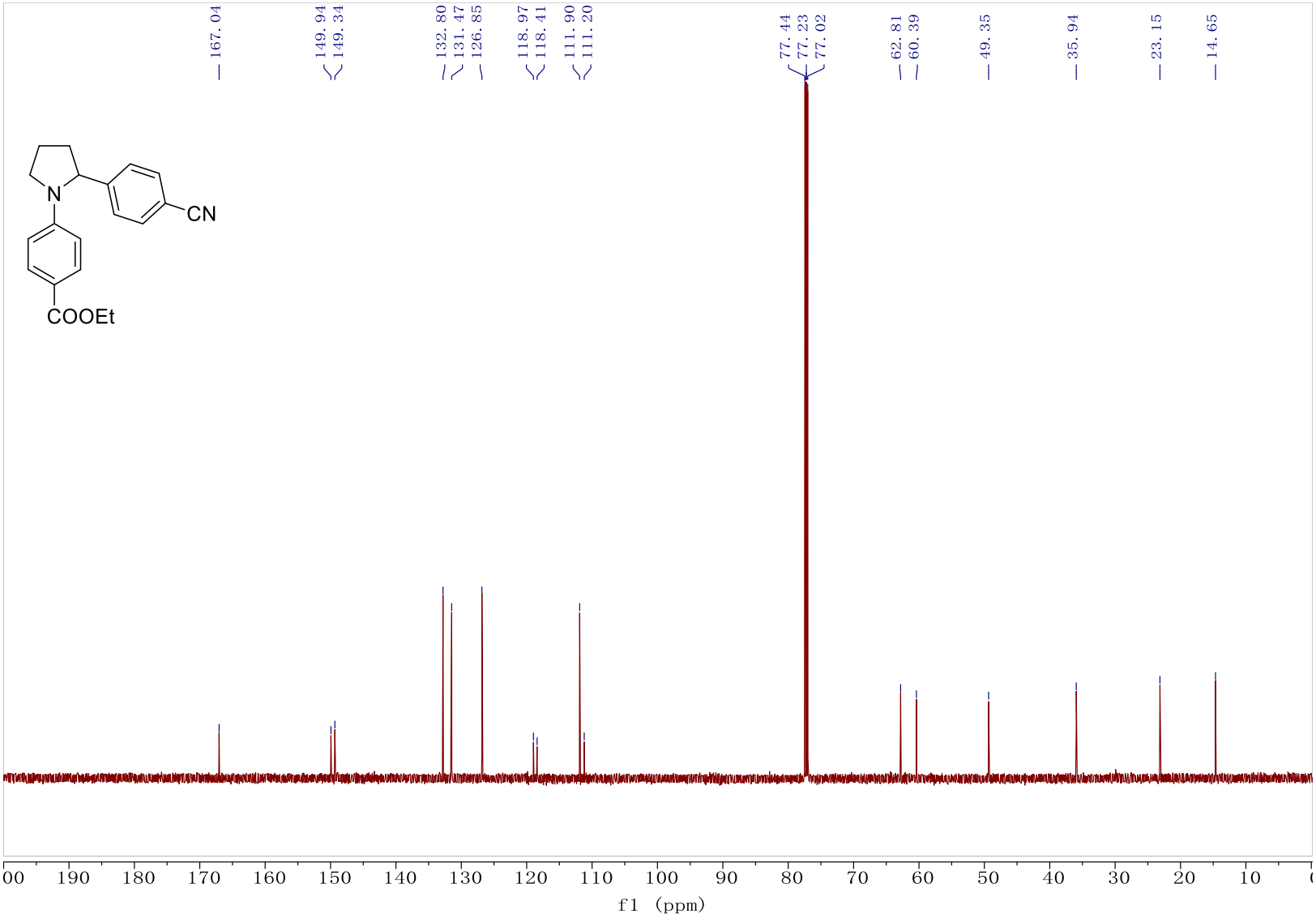

^{13}C NMR spectrum of **3d** (151 MHz, $CDCl_3$)

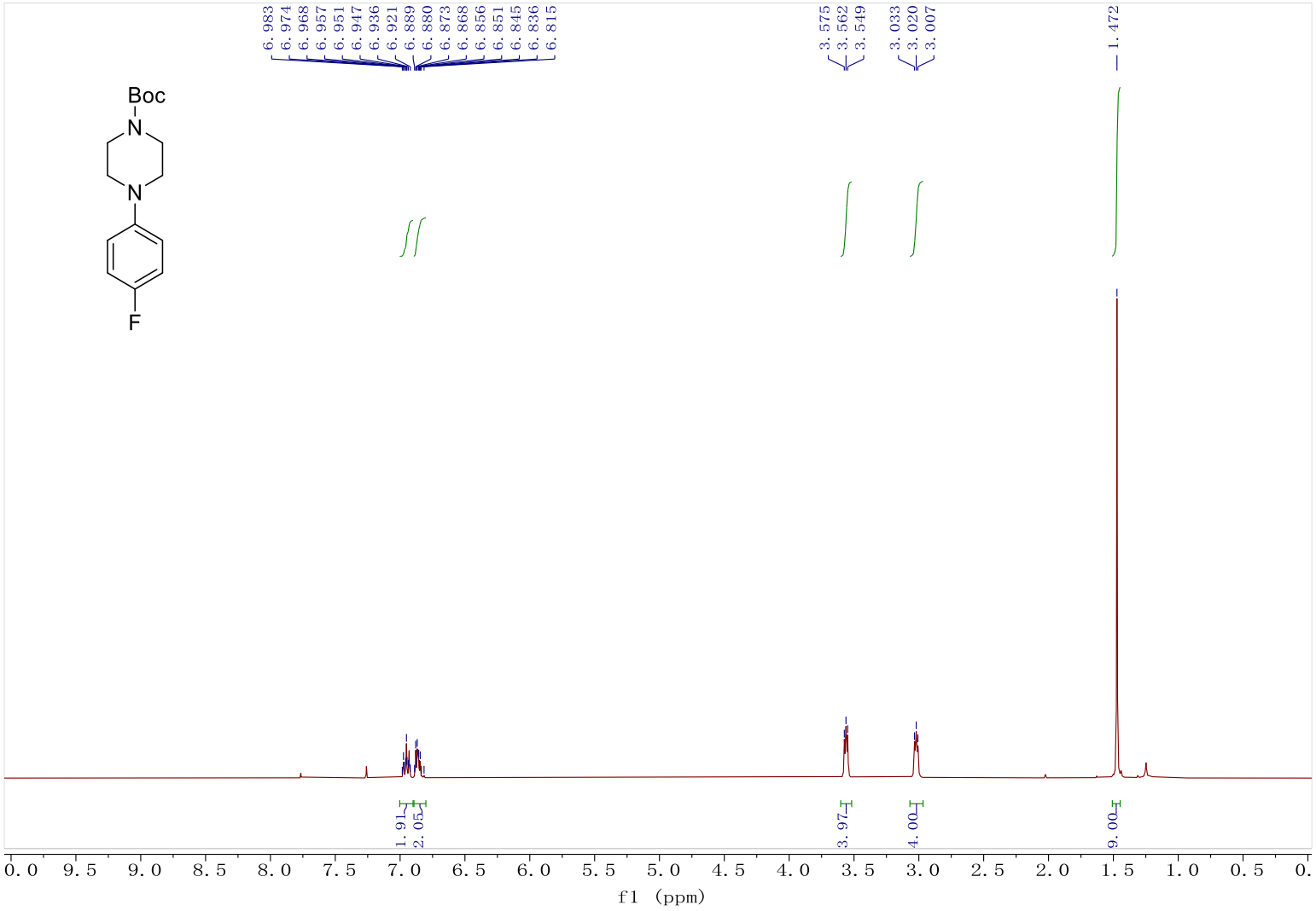

^{1}H NMR spectrum of starting material of **3e** (400 MHz, $CDCl_3$)

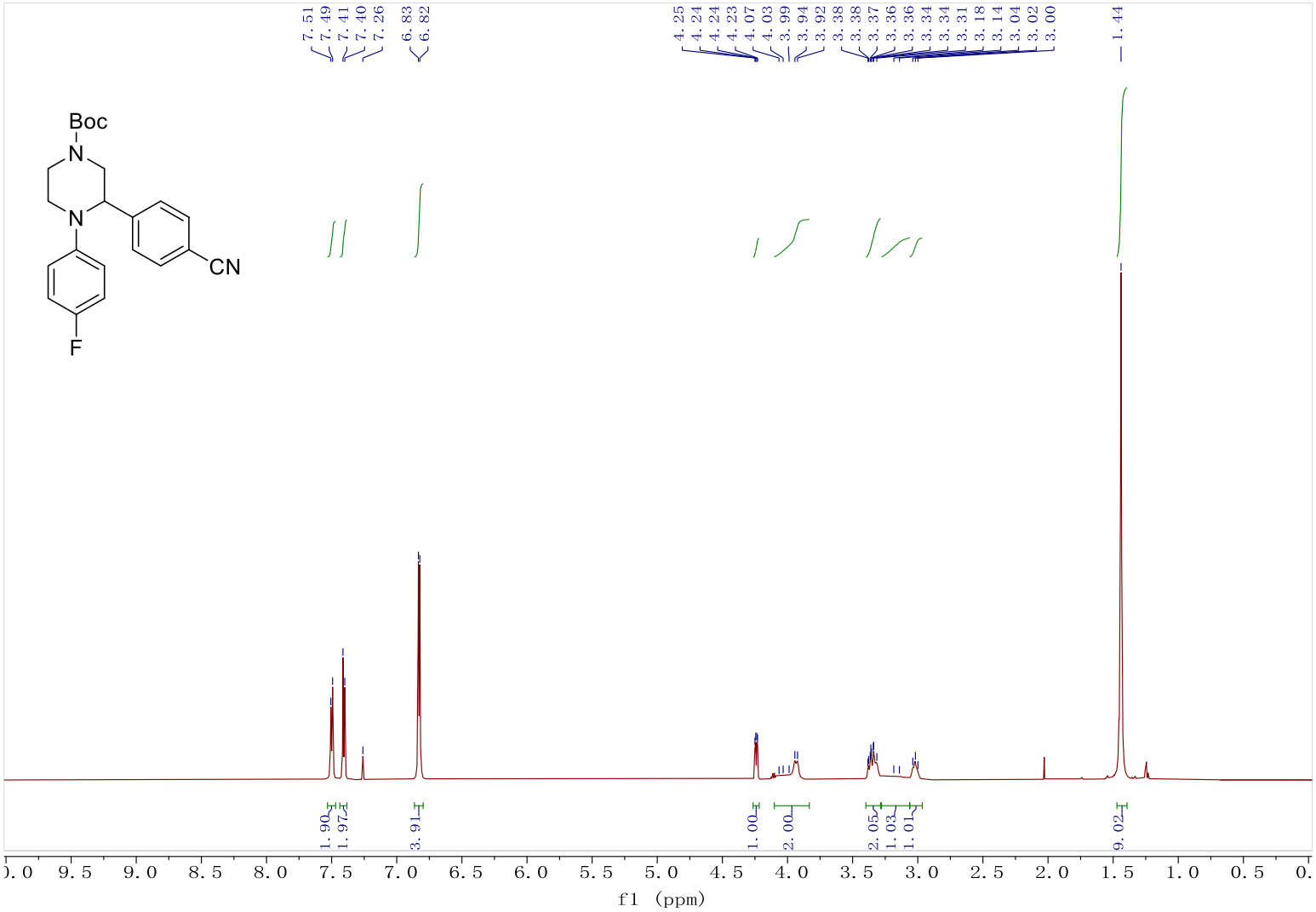

^{1}H NMR spectrum of **3e** (600 MHz, $CDCl_3$)

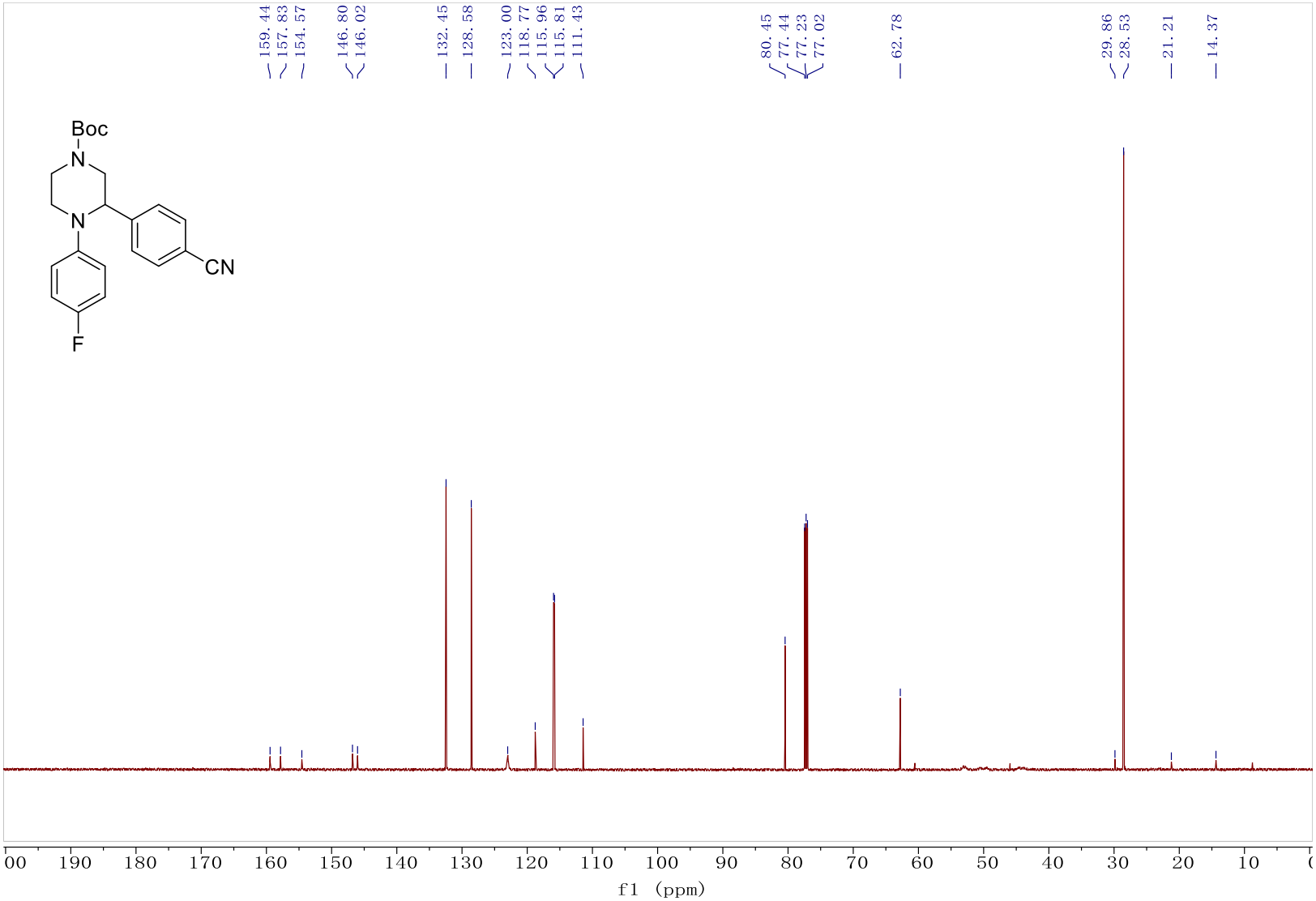

^{13}C NMR spectrum of **3e** (151 MHz, $CDCl_3$)

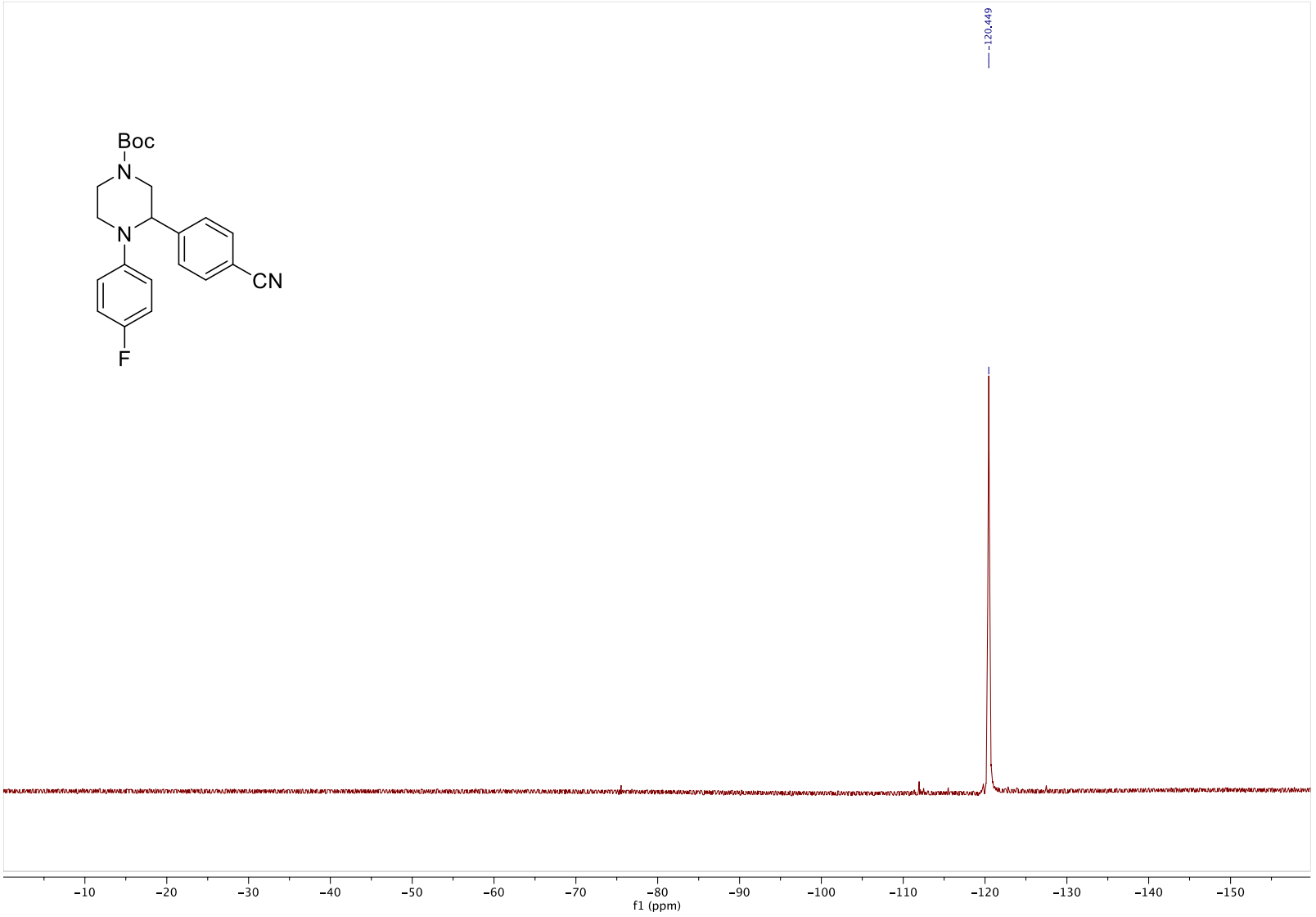

^{19}F NMR spectrum of **3e** (376 MHz, $CDCl_3$)

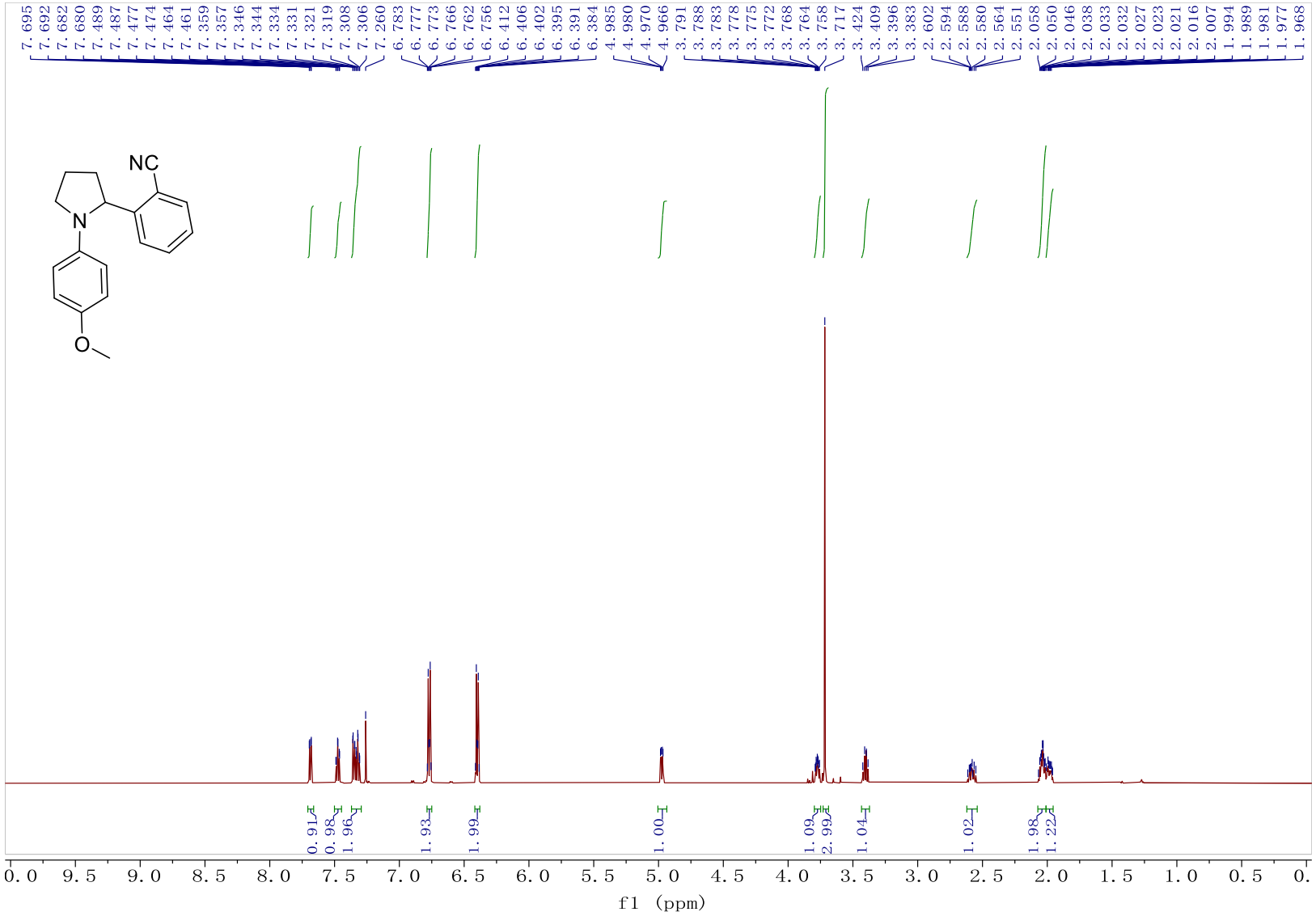

^{1}H NMR spectrum of **3f** (600 MHz, $CDCl_3$)

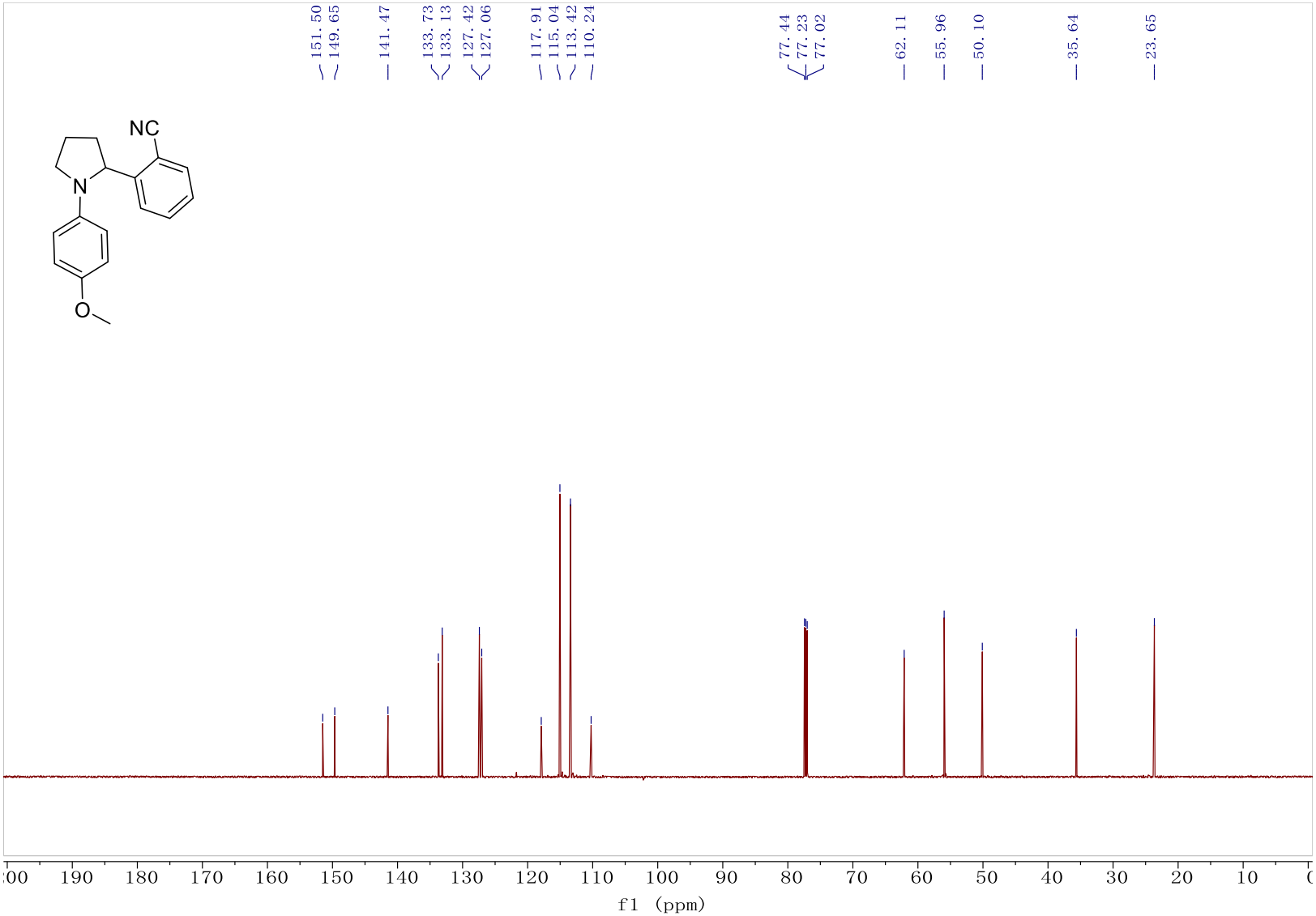

^{13}C NMR spectrum of **3f** (151 MHz, $CDCl_3$)

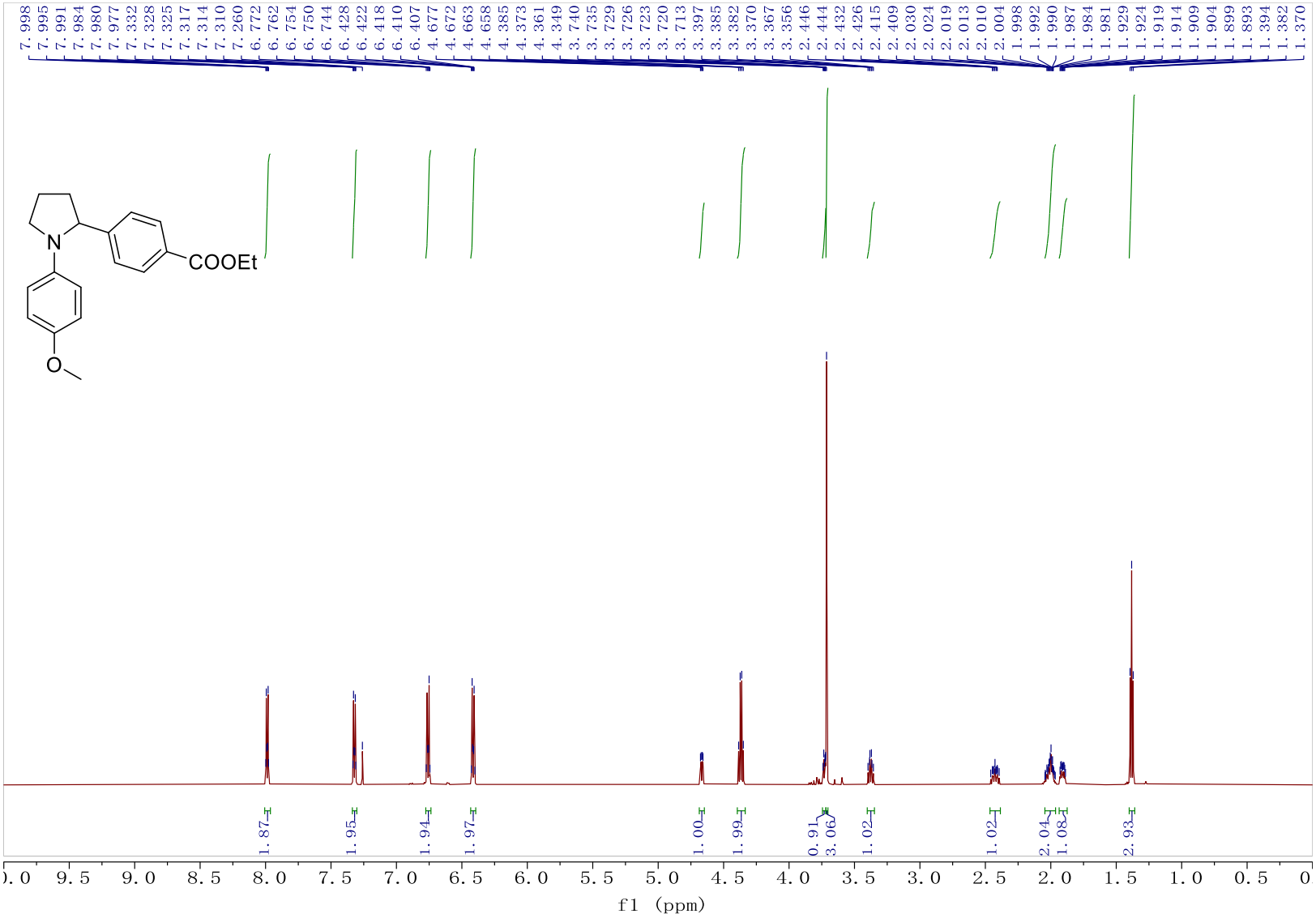

^{1}H NMR spectrum of **3g** (600 MHz, $CDCl_3$)

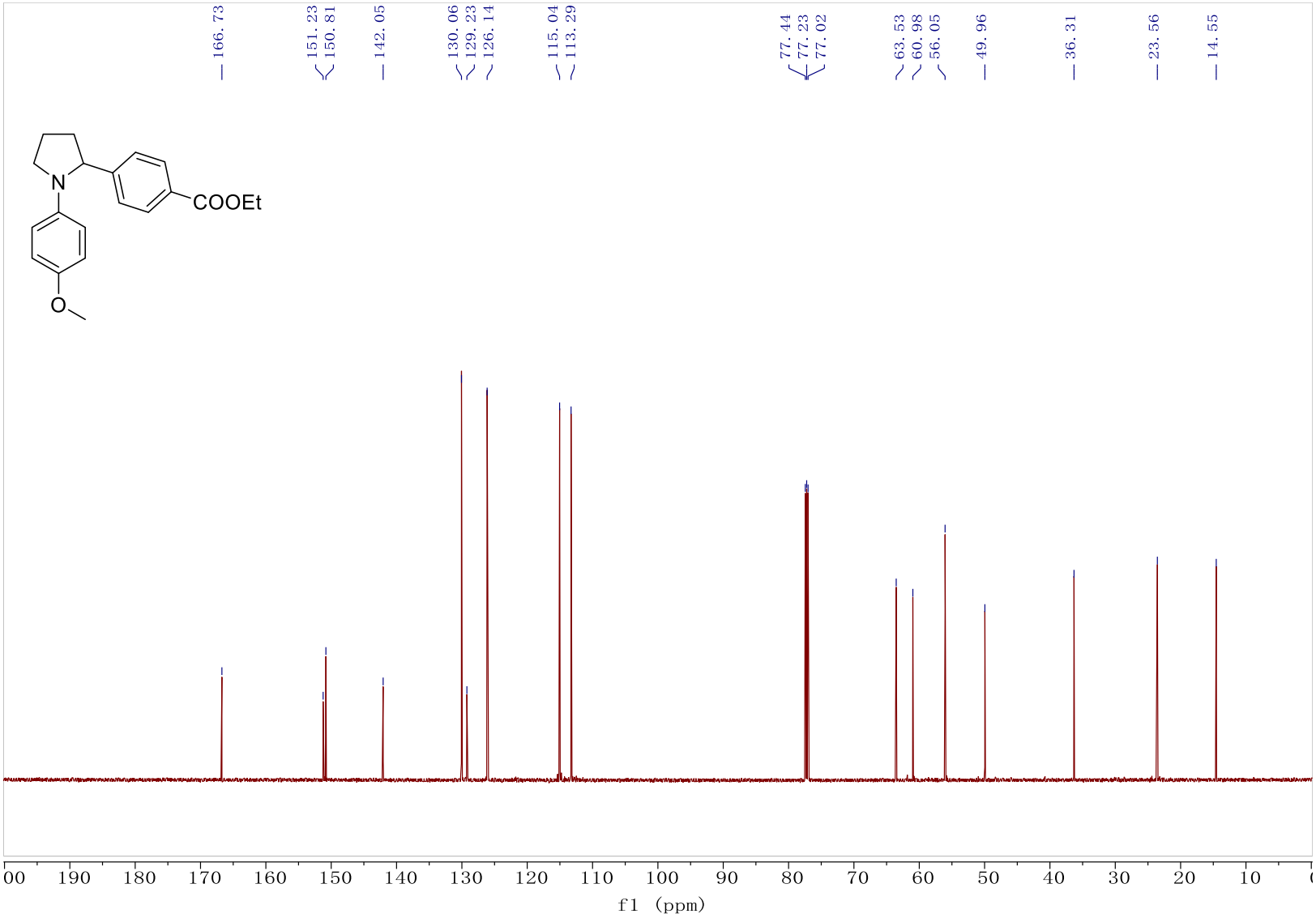

^{13}C NMR spectrum of **3g** (151 MHz, $CDCl_3$)

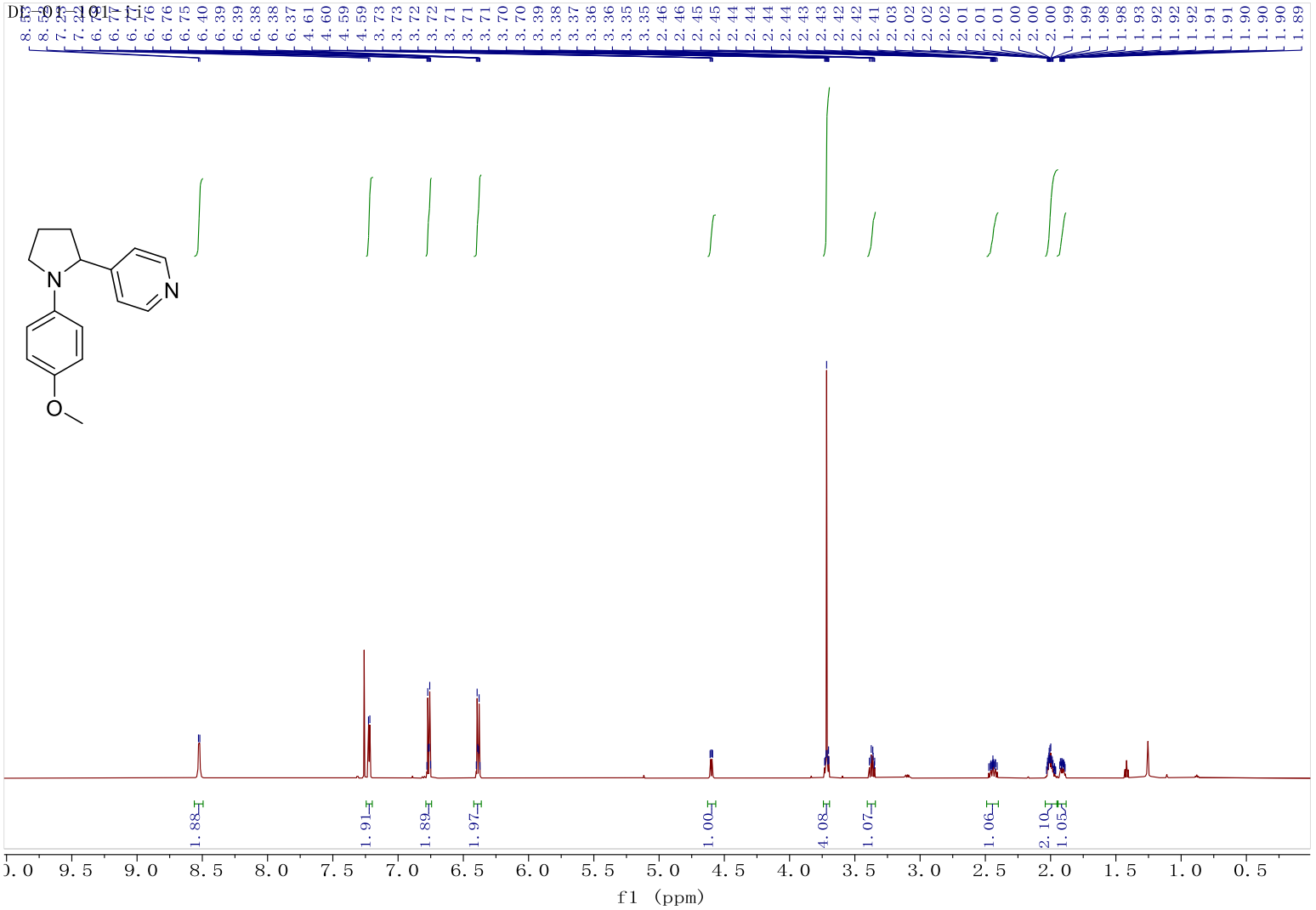

^{1}H NMR spectrum of **3h** (600 MHz, $CDCl_3$)

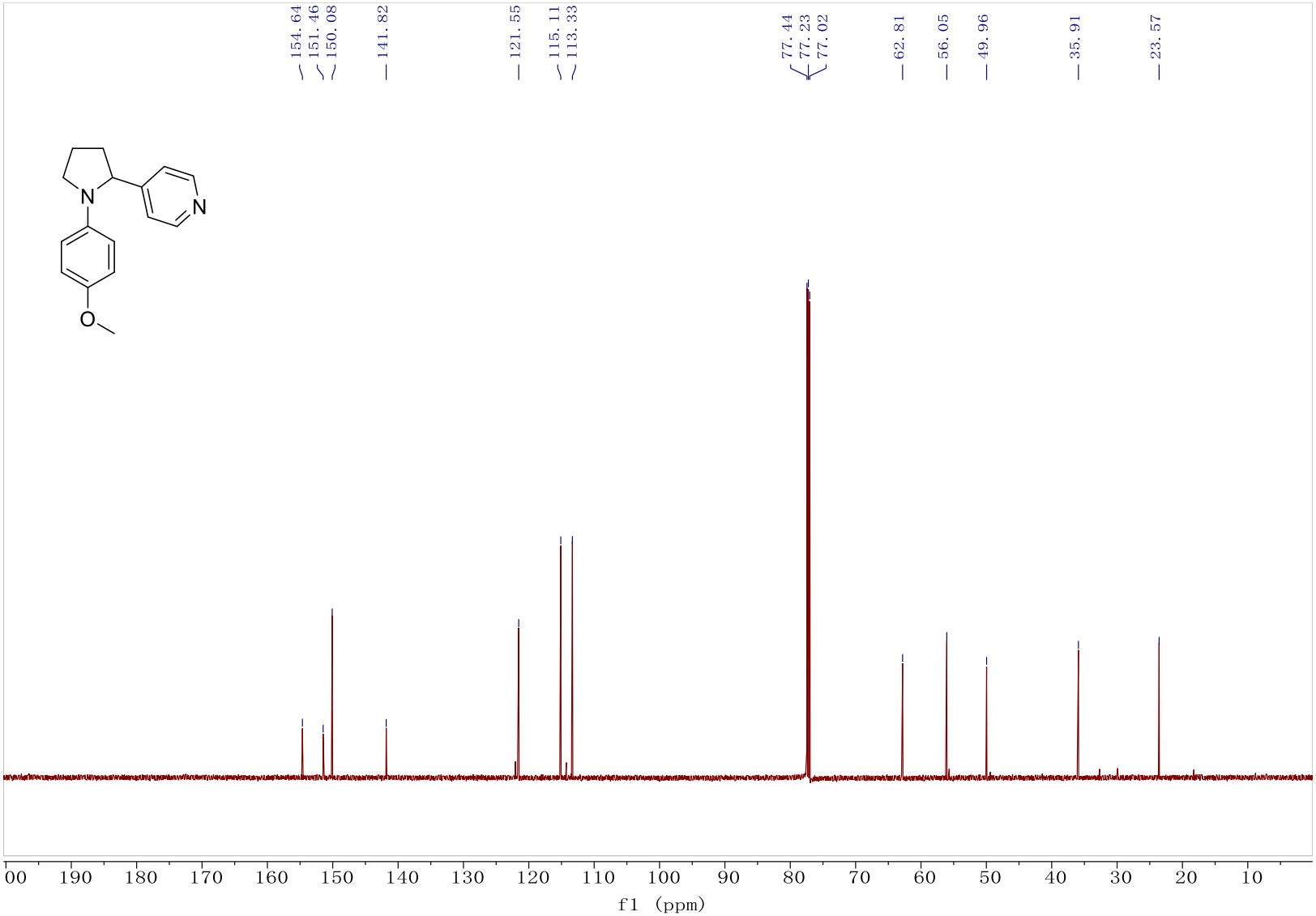

^{13}C NMR spectrum of **3h** (151 MHz, $CDCl_3$)

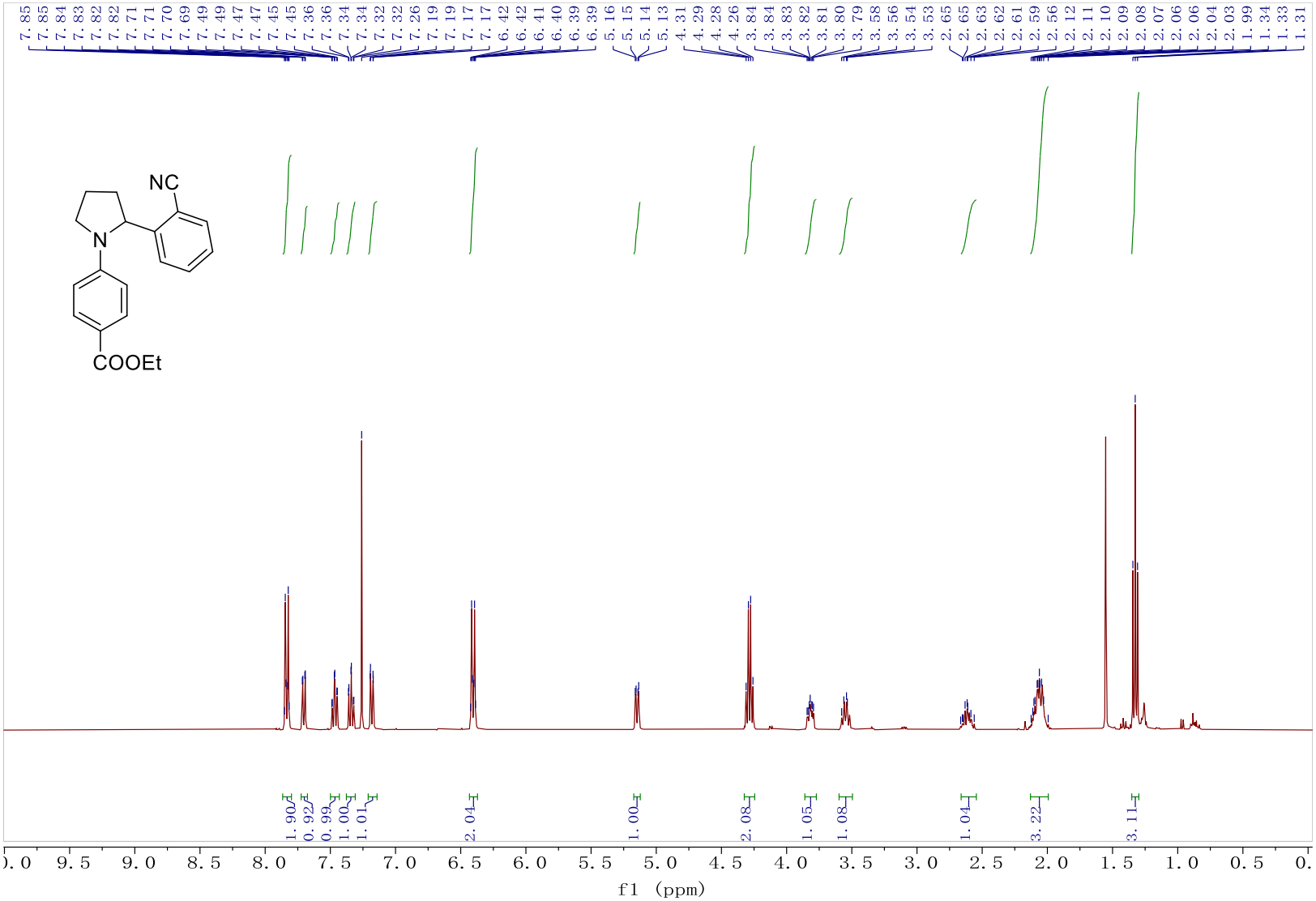

^{1}H NMR spectrum of **4d** (600 MHz, $CDCl_3$)

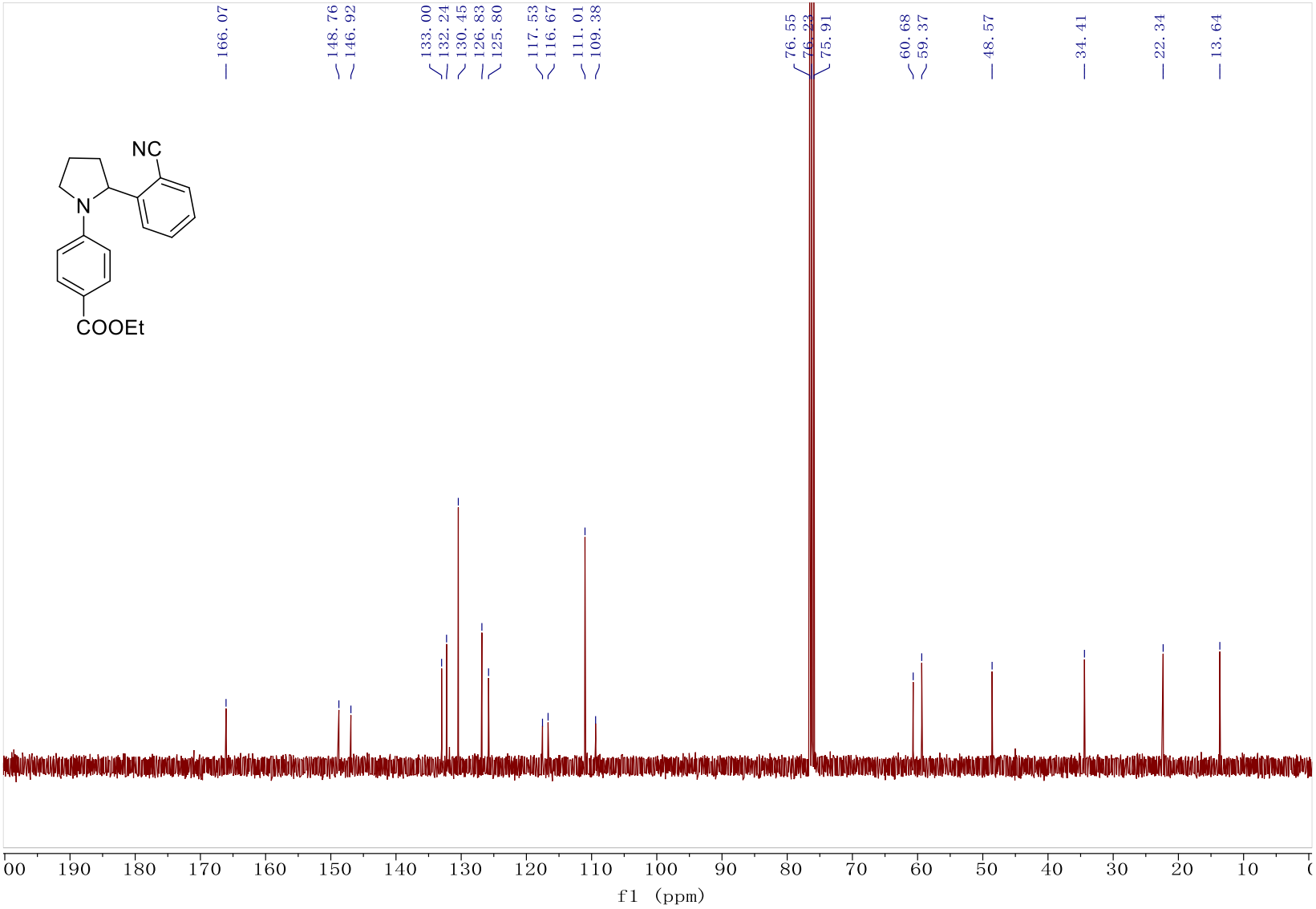

^{13}C NMR spectrum of **4d** (101 MHz, $CDCl_3$)

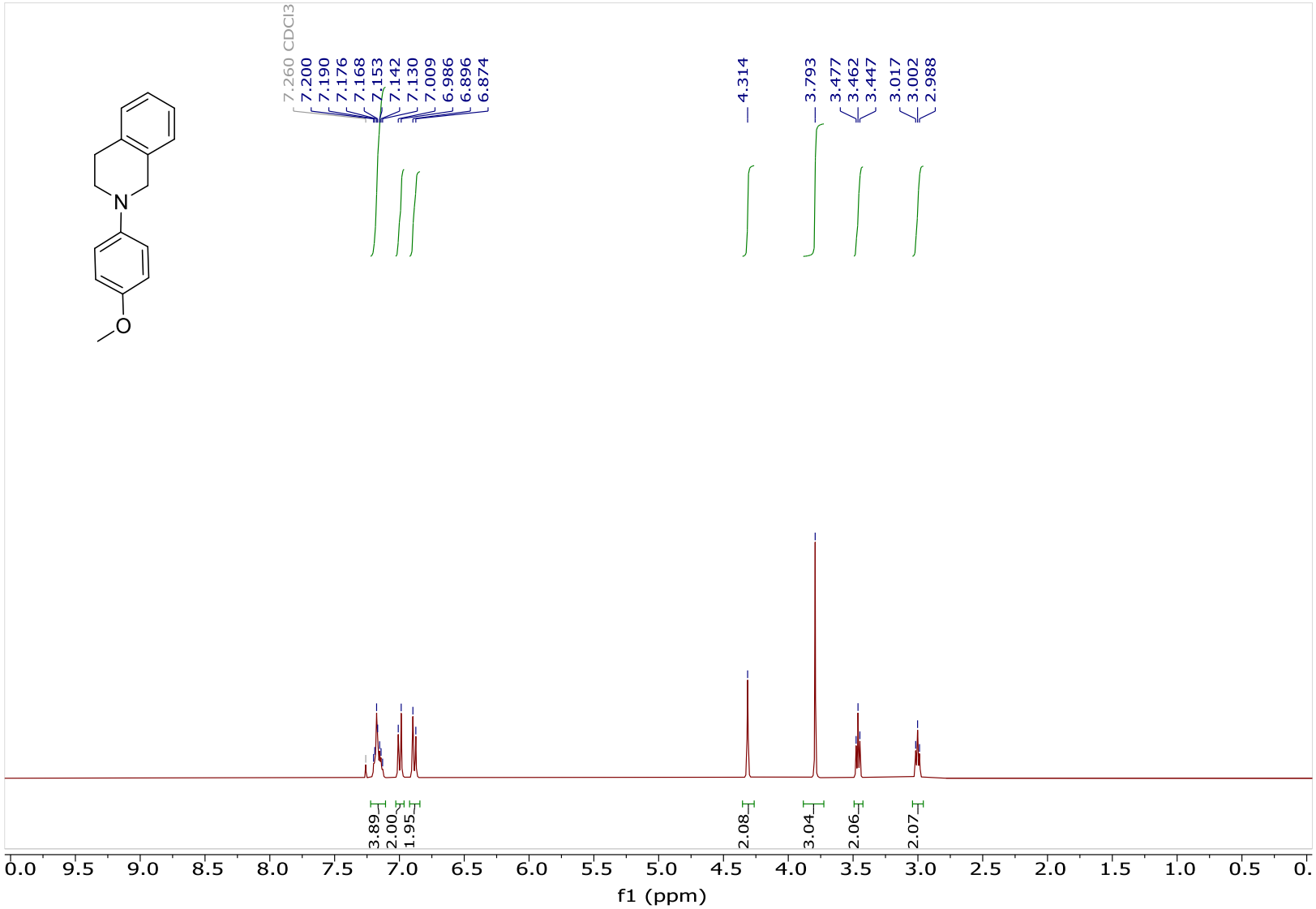

^{1}H NMR spectrum of starting material of **3i** (400 MHz, $CDCl_3$)

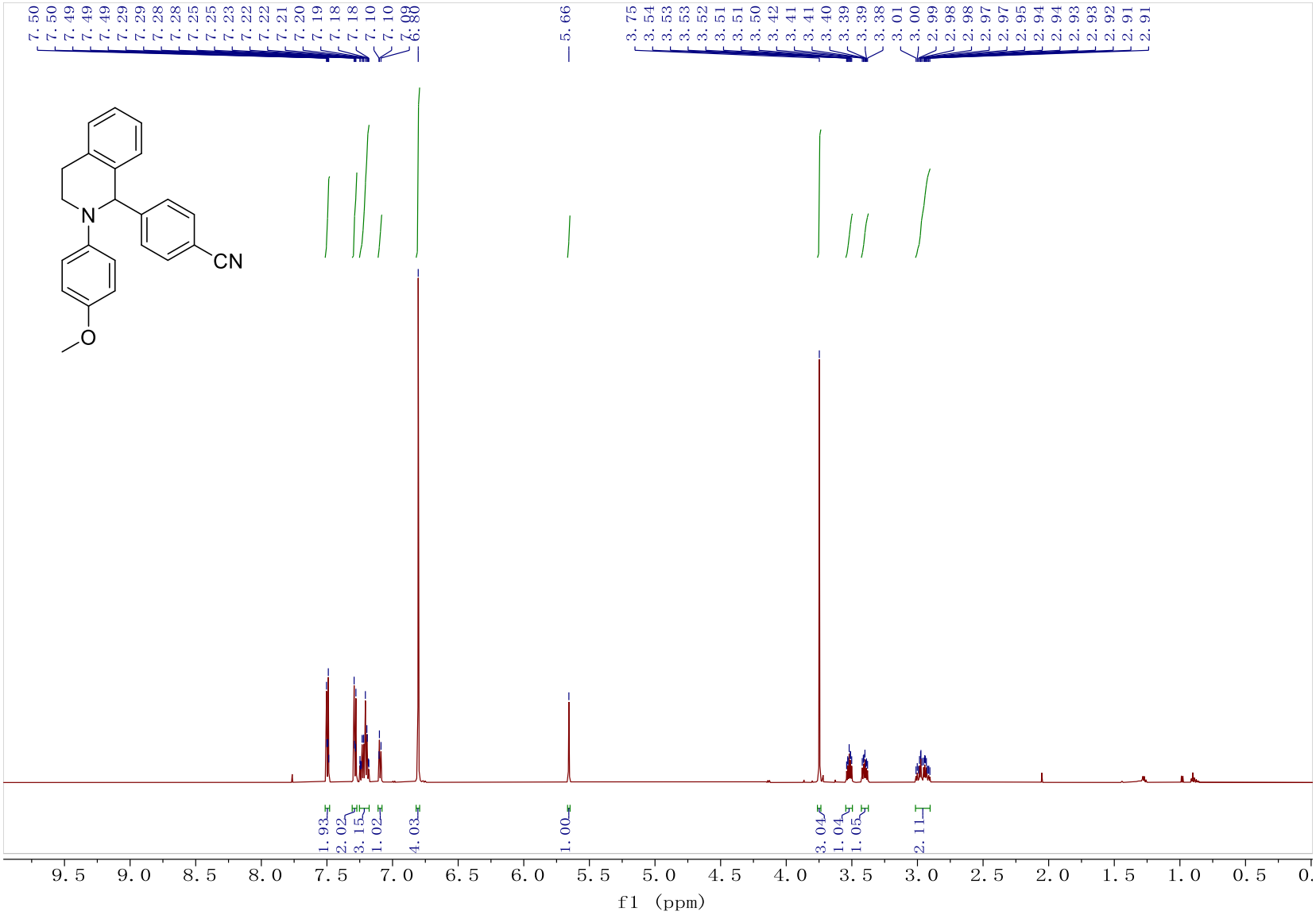

^{1}H NMR spectrum of **3i** (400 MHz, $CDCl_3$)

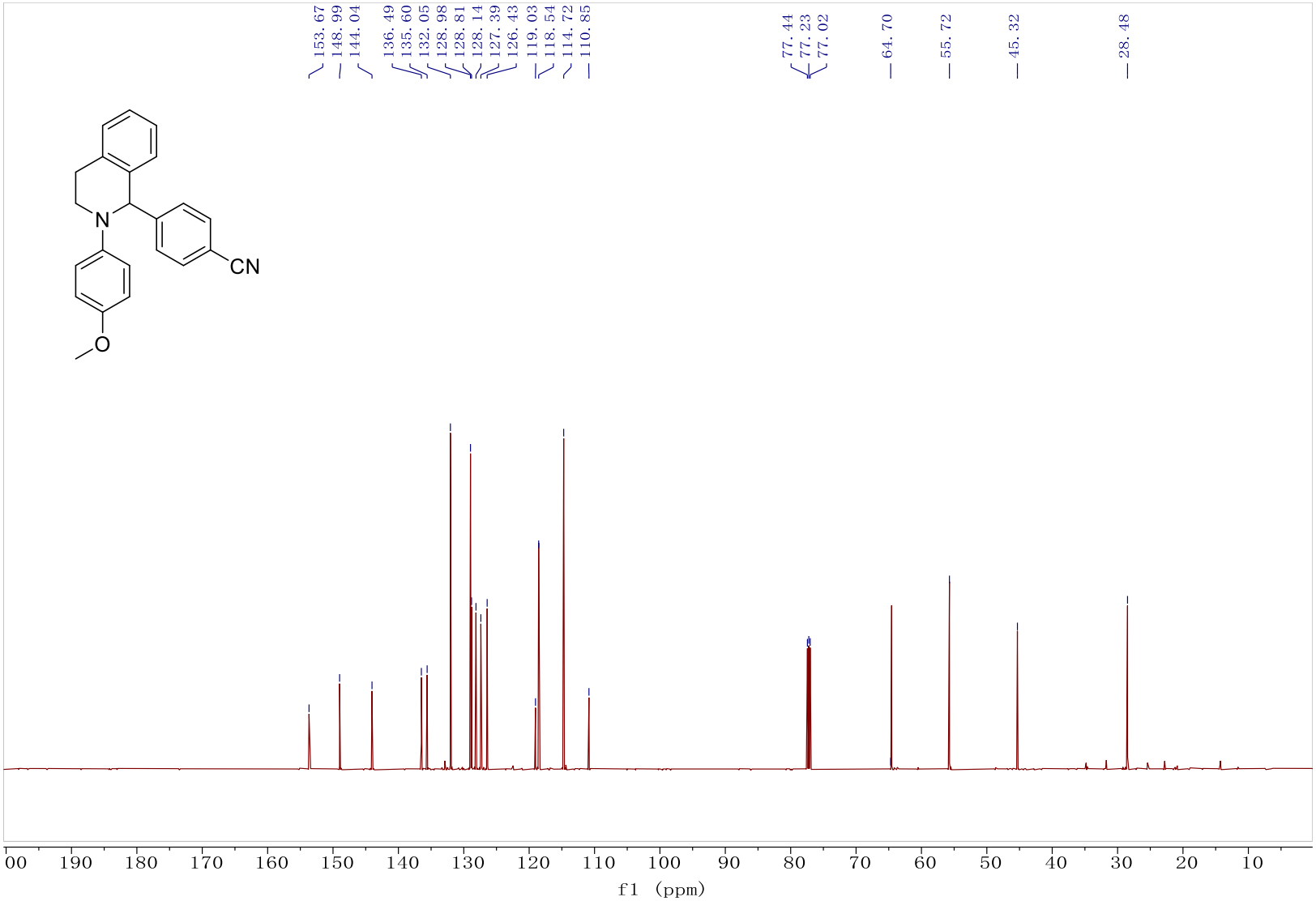

^{13}C NMR spectrum of **3i** (151 MHz, $CDCl_3$)

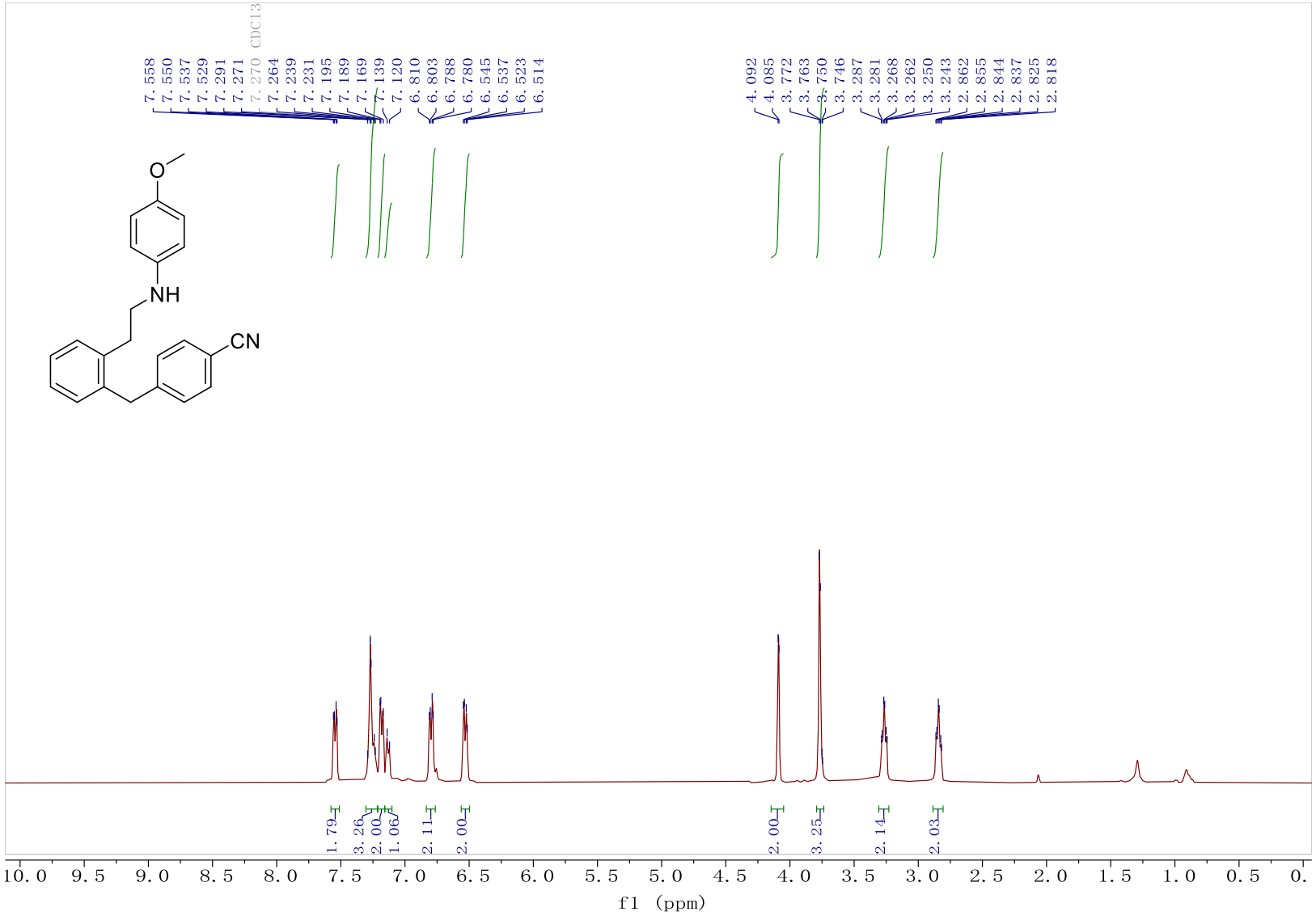

^{1}H NMR spectrum of **4i** (400 MHz, $CDCl_3$)

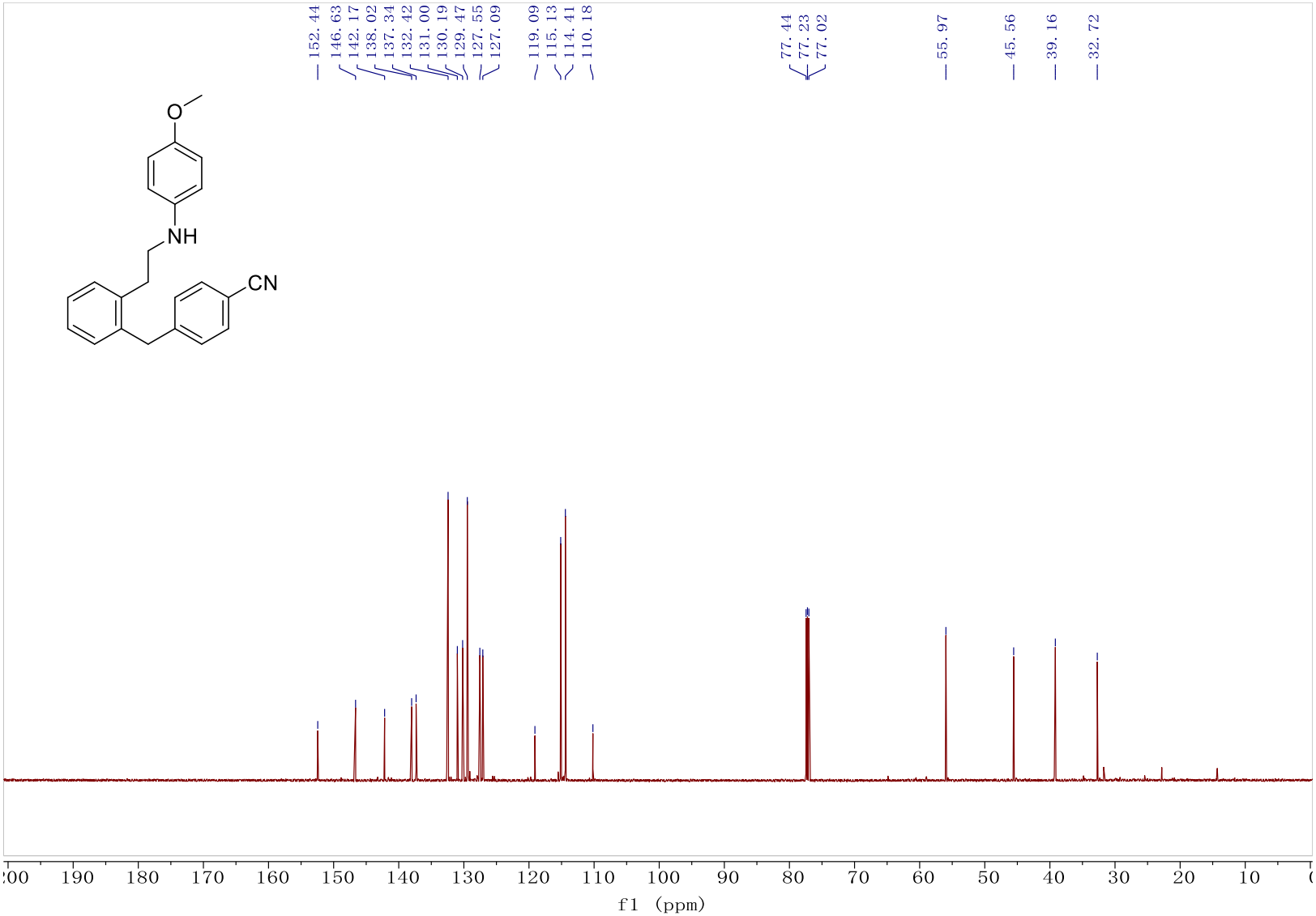

^{13}C NMR spectrum of **4i** (151 MHz, $CDCl_3$)

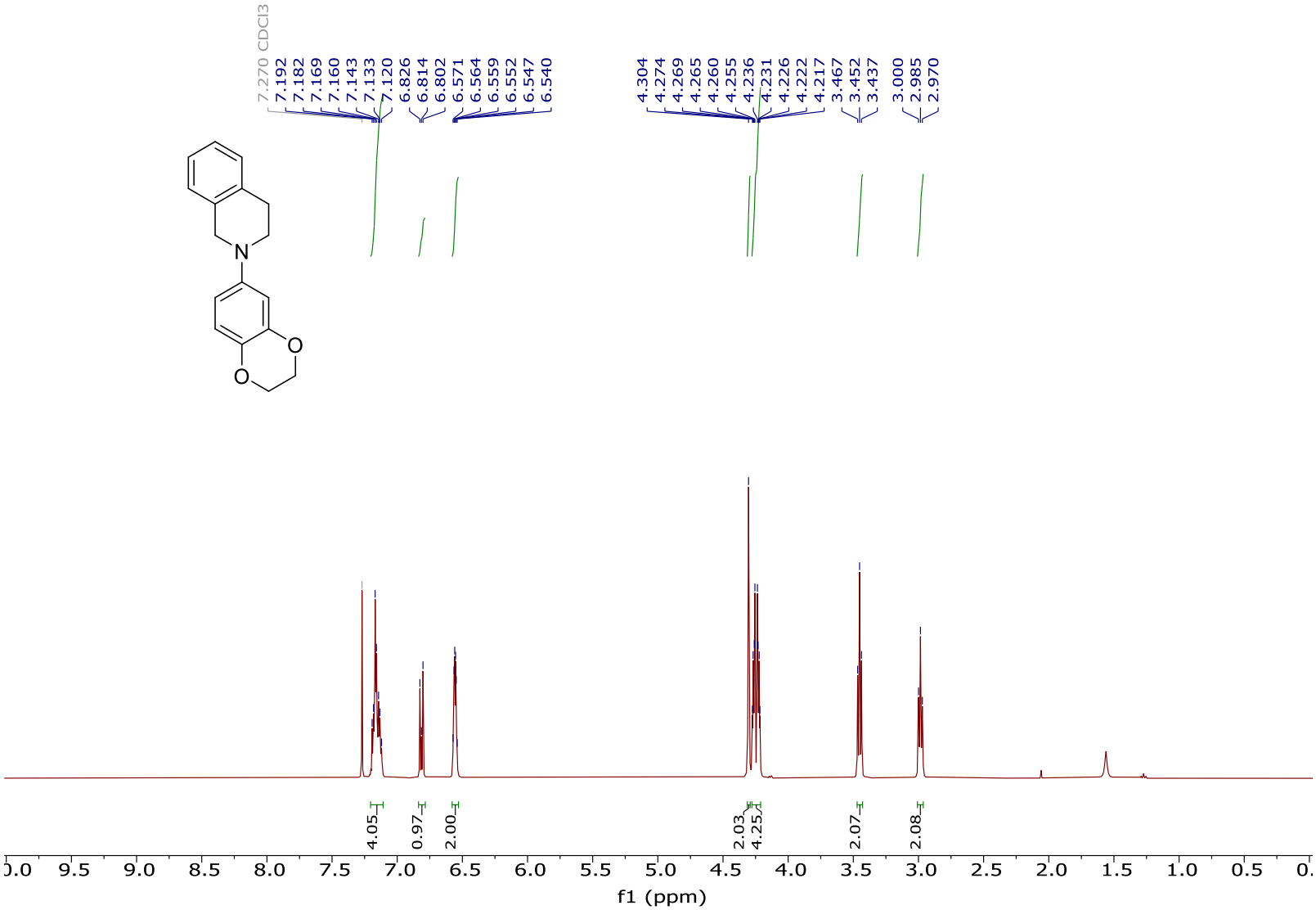

^{1}H NMR spectrum of starting material of **3j** (400 MHz, $CDCl_3$)

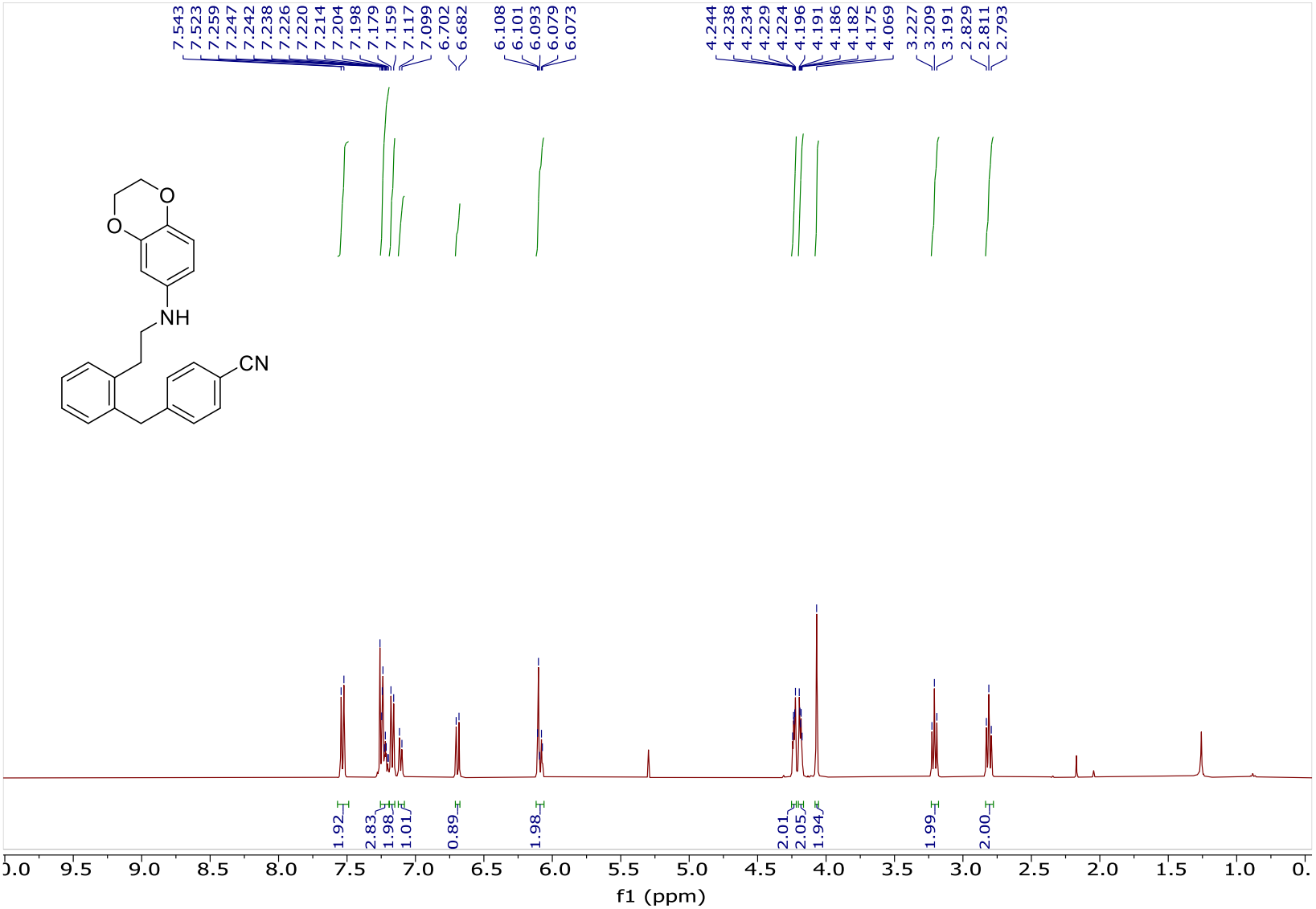

^{1}H NMR spectrum of **4j** (400 MHz, $CDCl_3$)

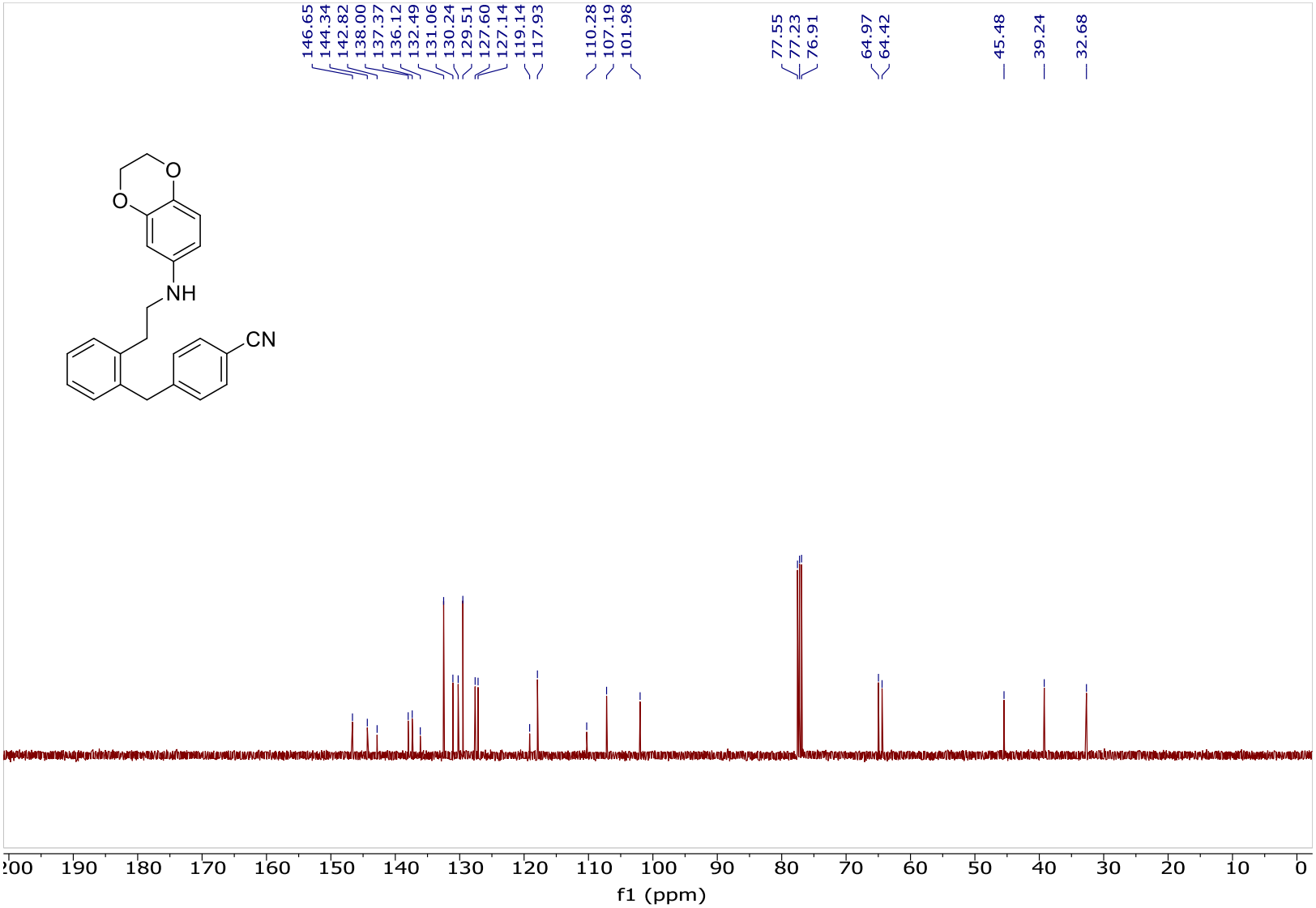

^{13}C NMR spectrum of **4j** (151 MHz, $CDCl_3$)

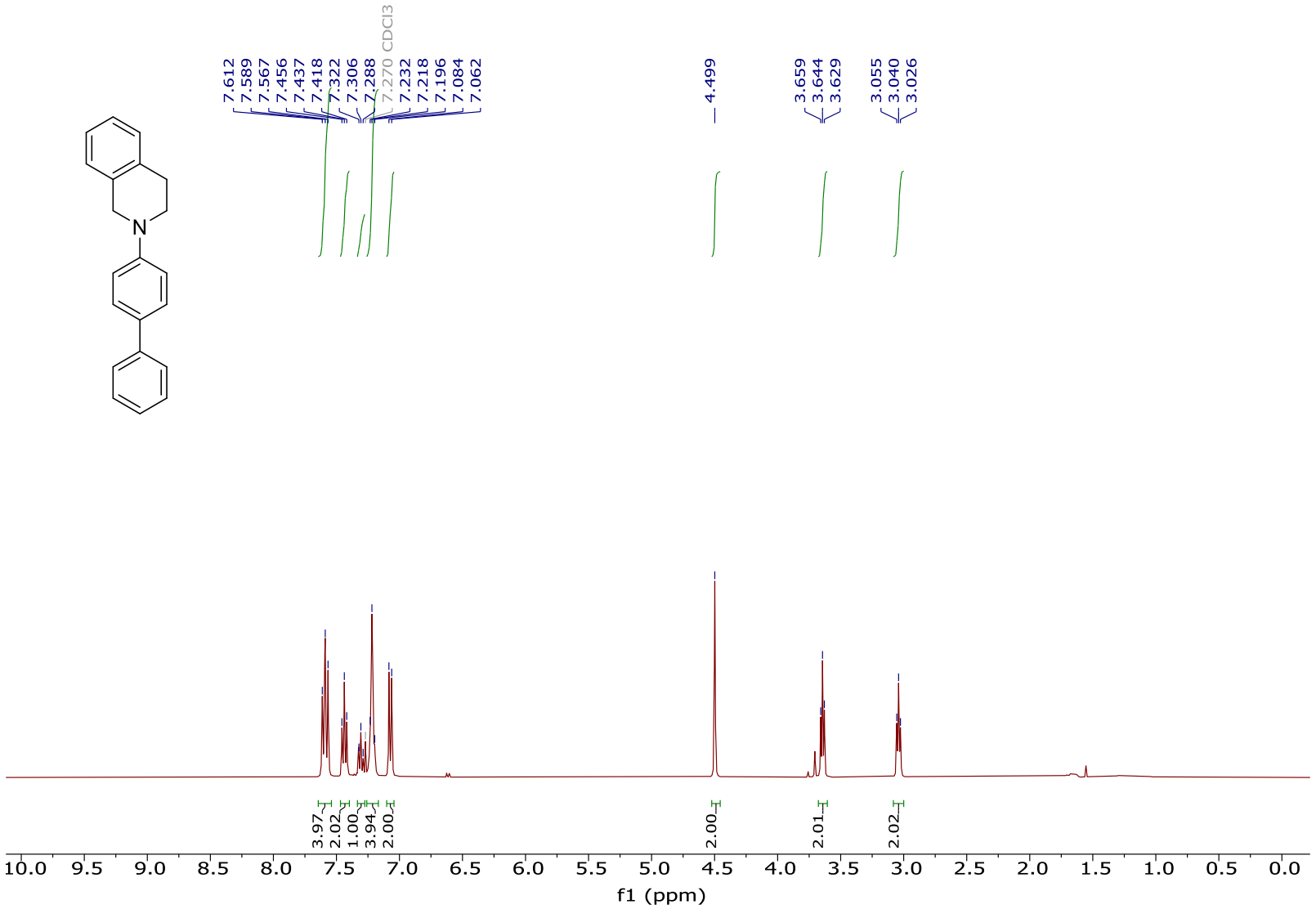

^{1}H NMR spectrum of starting material of **3k** (400 MHz, $CDCl_3$)

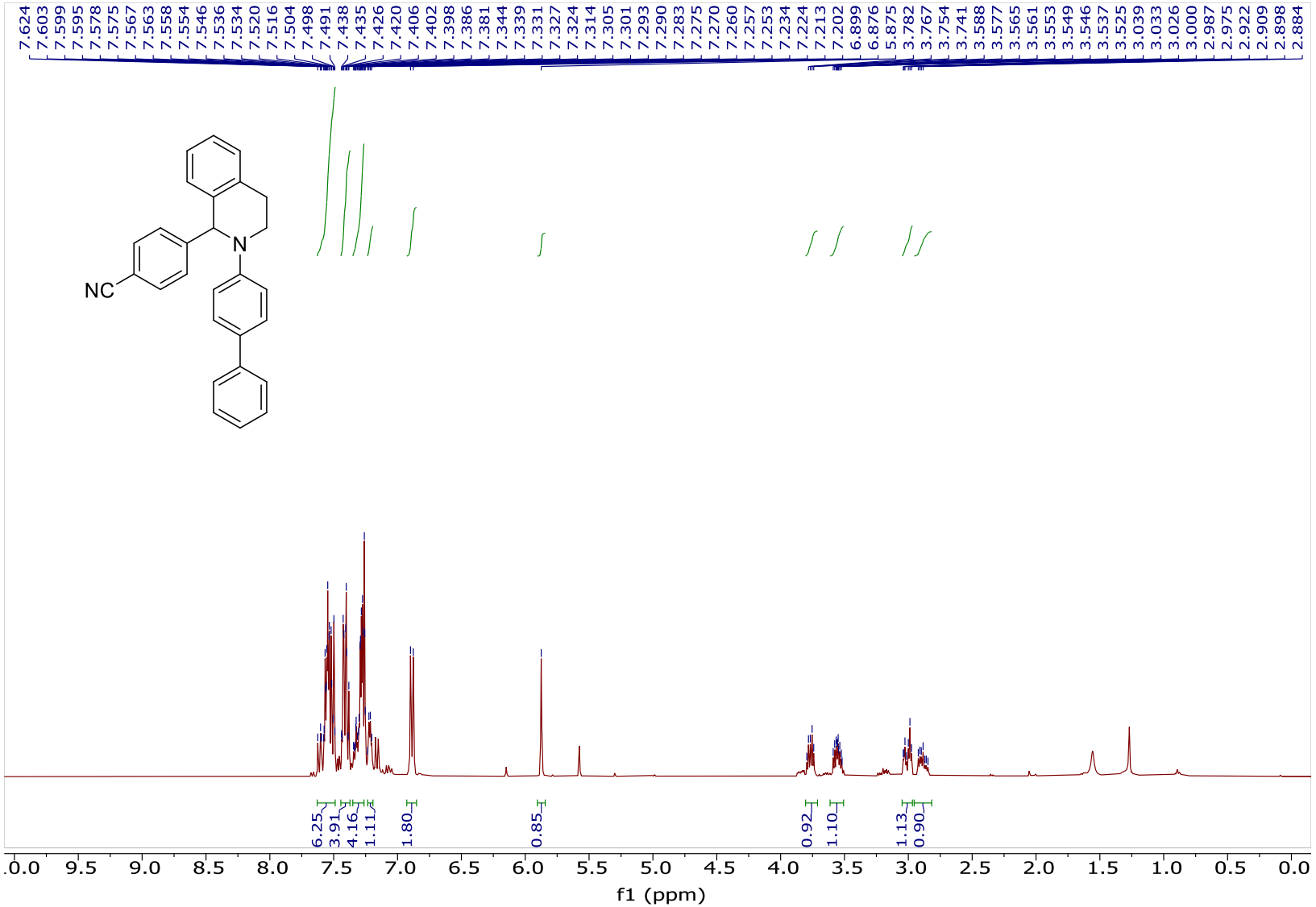

^{1}H NMR spectrum of **3k** (400 MHz, $CDCl_3$)

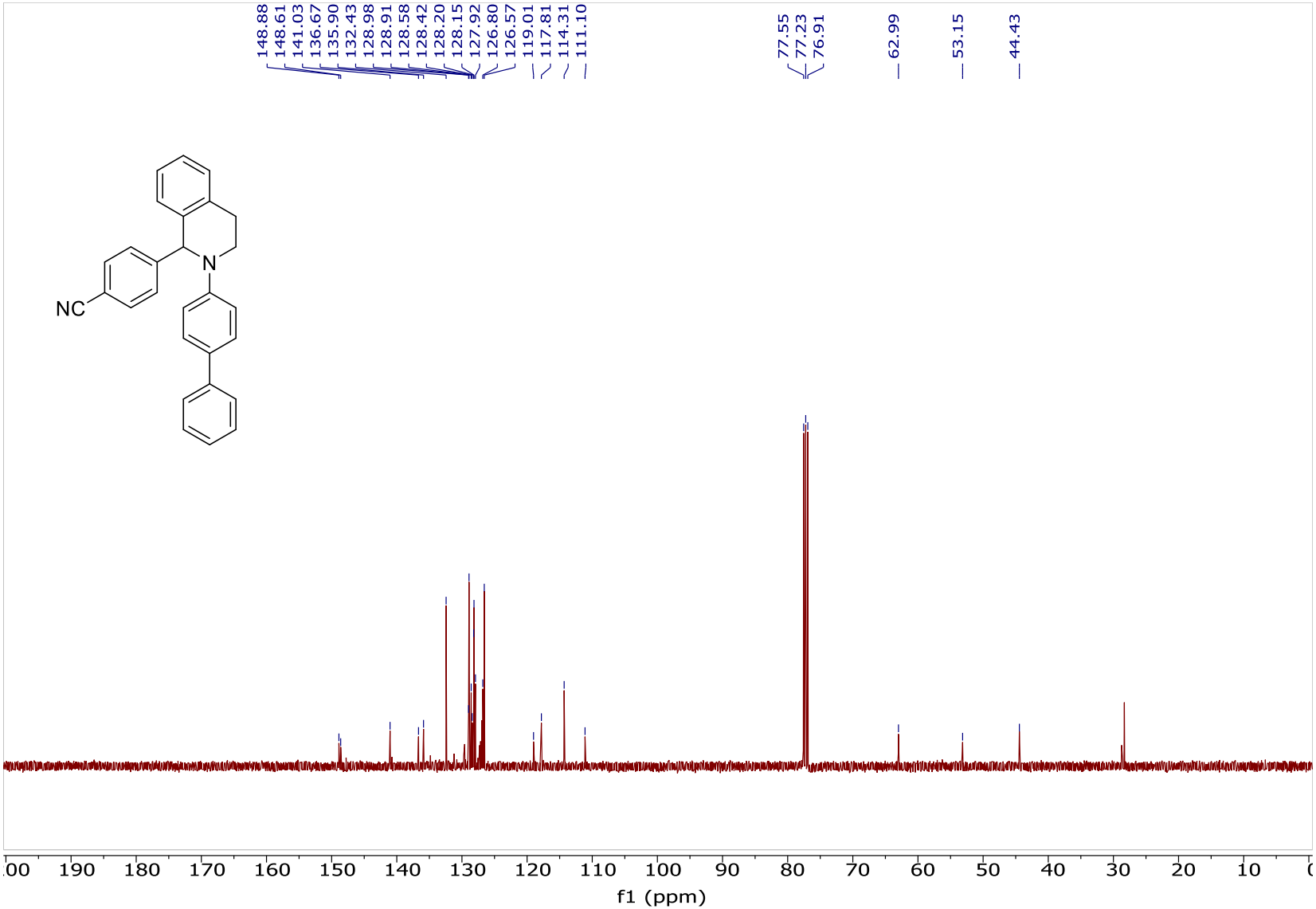

^{13}C NMR spectrum of **4k** (151 MHz, $CDCl_3$)

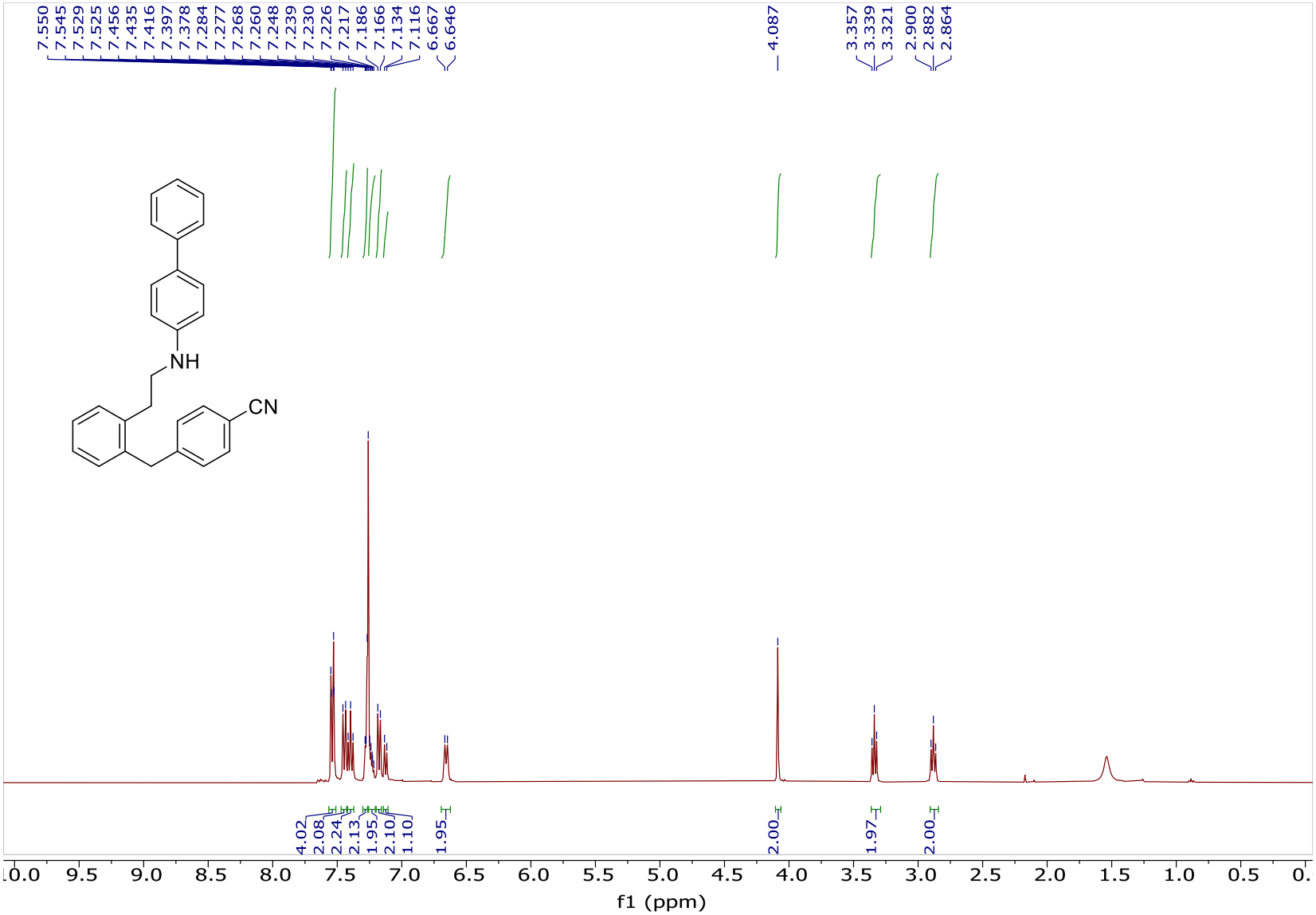

^{1}H NMR spectrum of **4k** (400 MHz, $CDCl_3$)

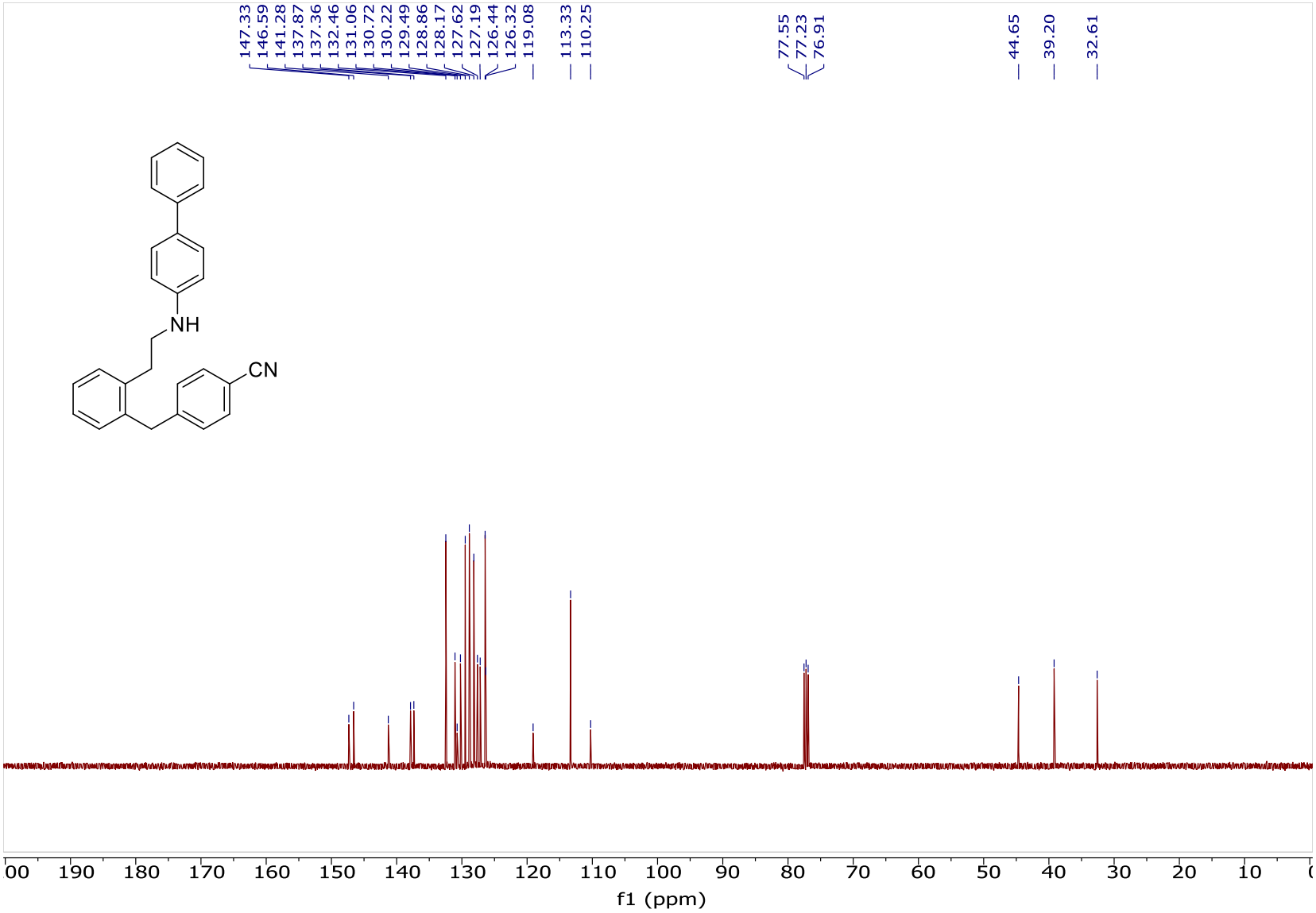

^{13}C NMR spectrum of **4k** (151 MHz, $CDCl_3$)

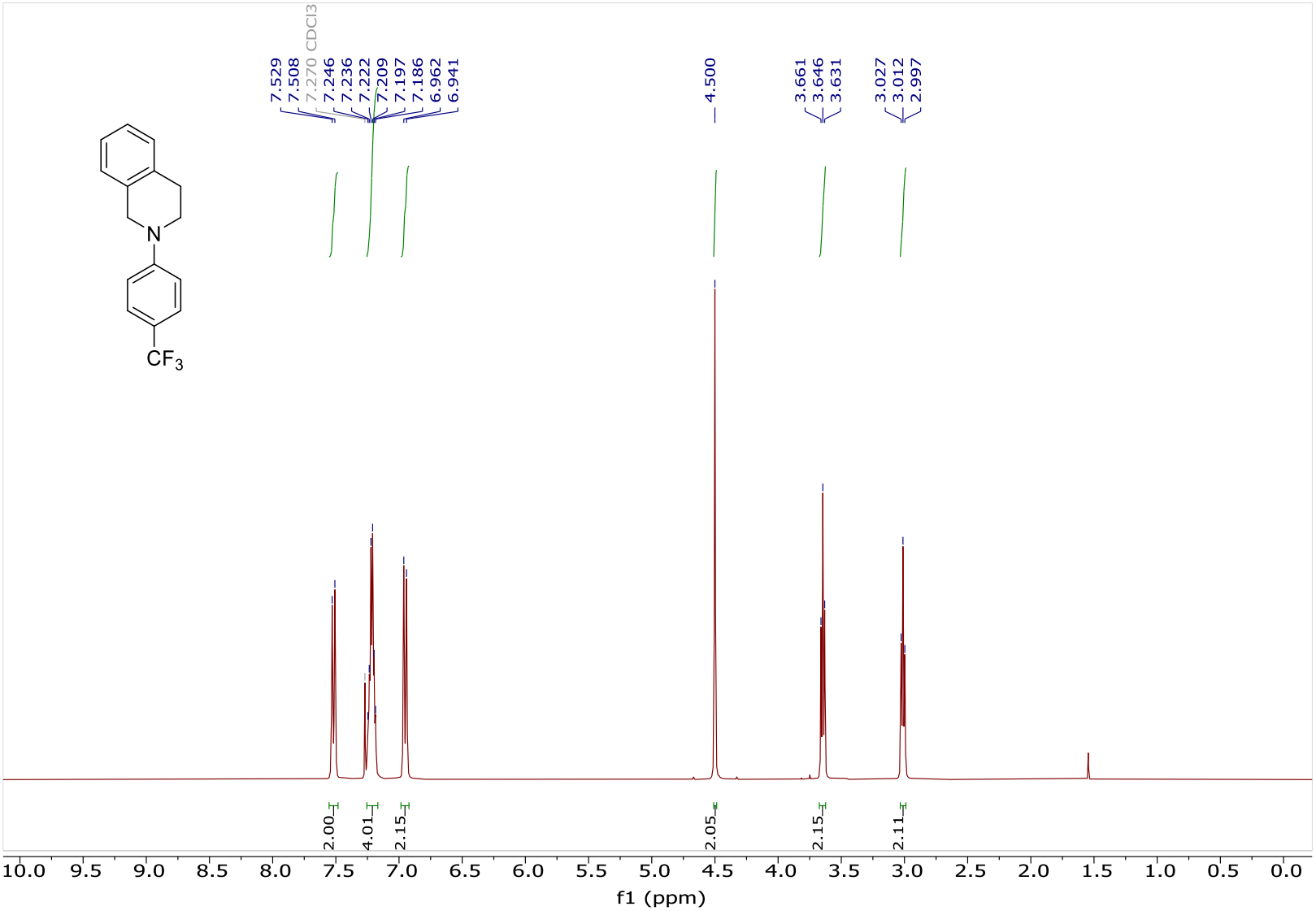

^{1}H NMR spectrum of starting material of **3l** (400 MHz, $CDCl_3$)

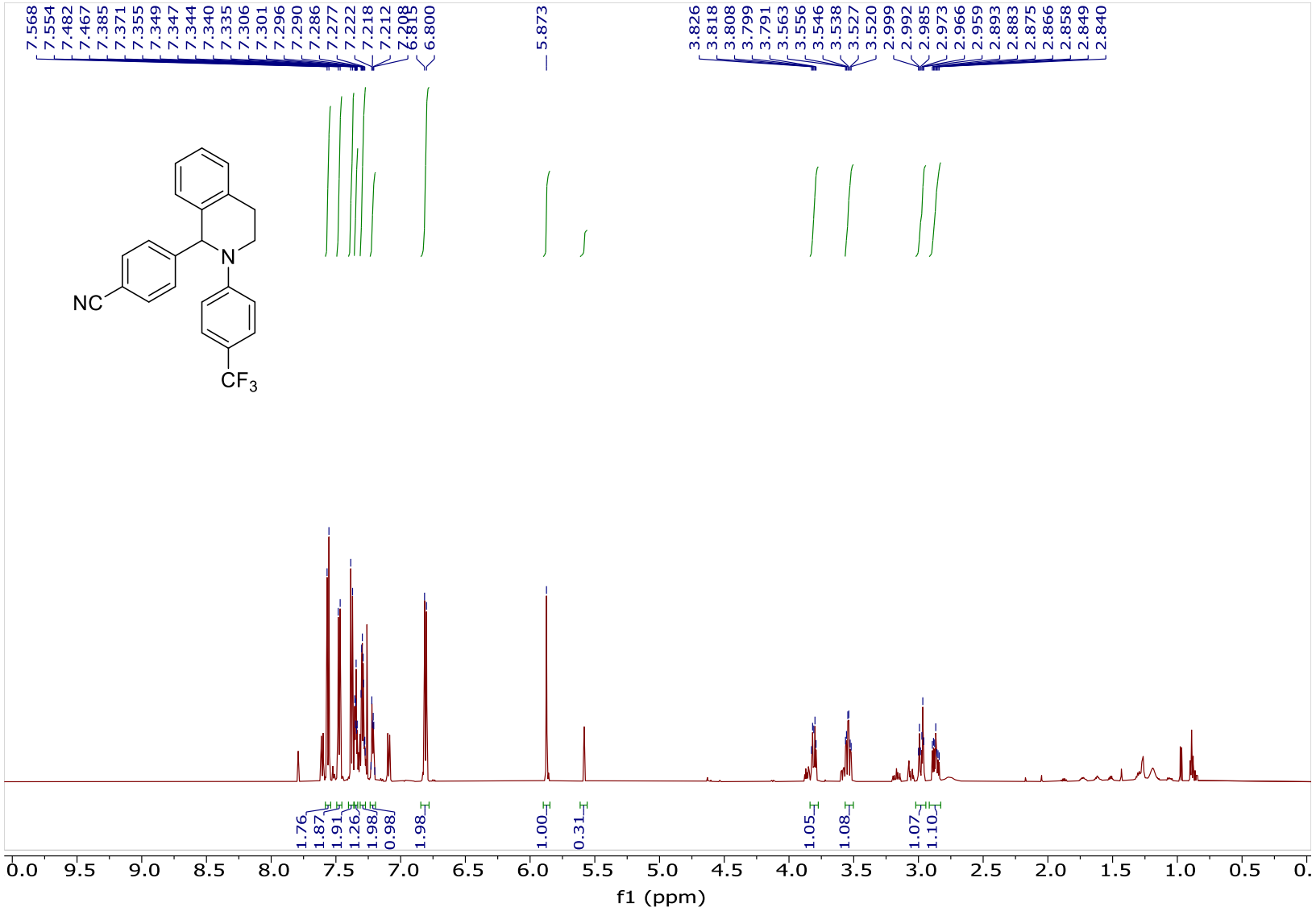

^{1}H NMR spectrum of **3l** (400 MHz, $CDCl_3$)

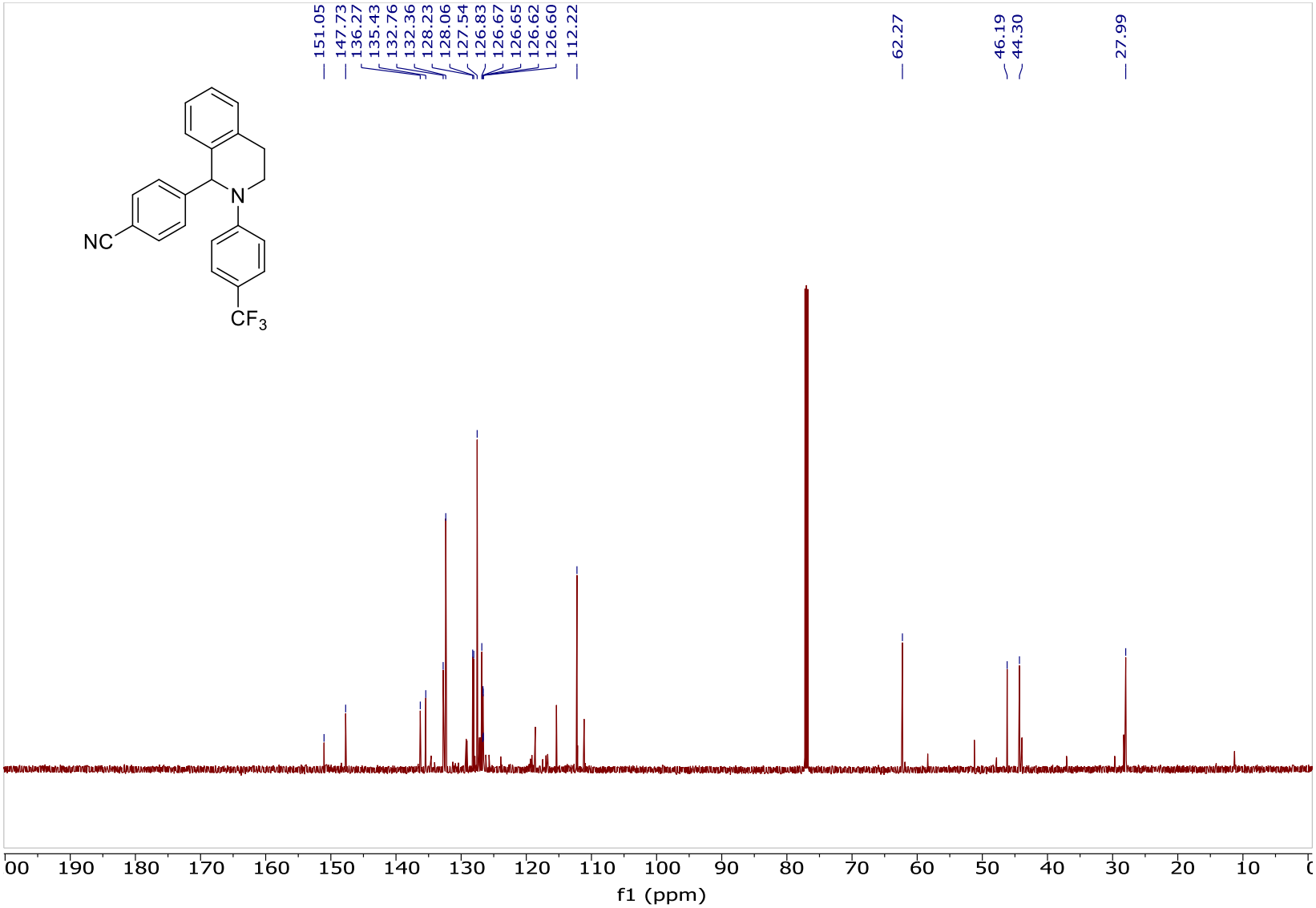

^{13}C NMR spectrum of **3l** (151 MHz, $CDCl_3$)

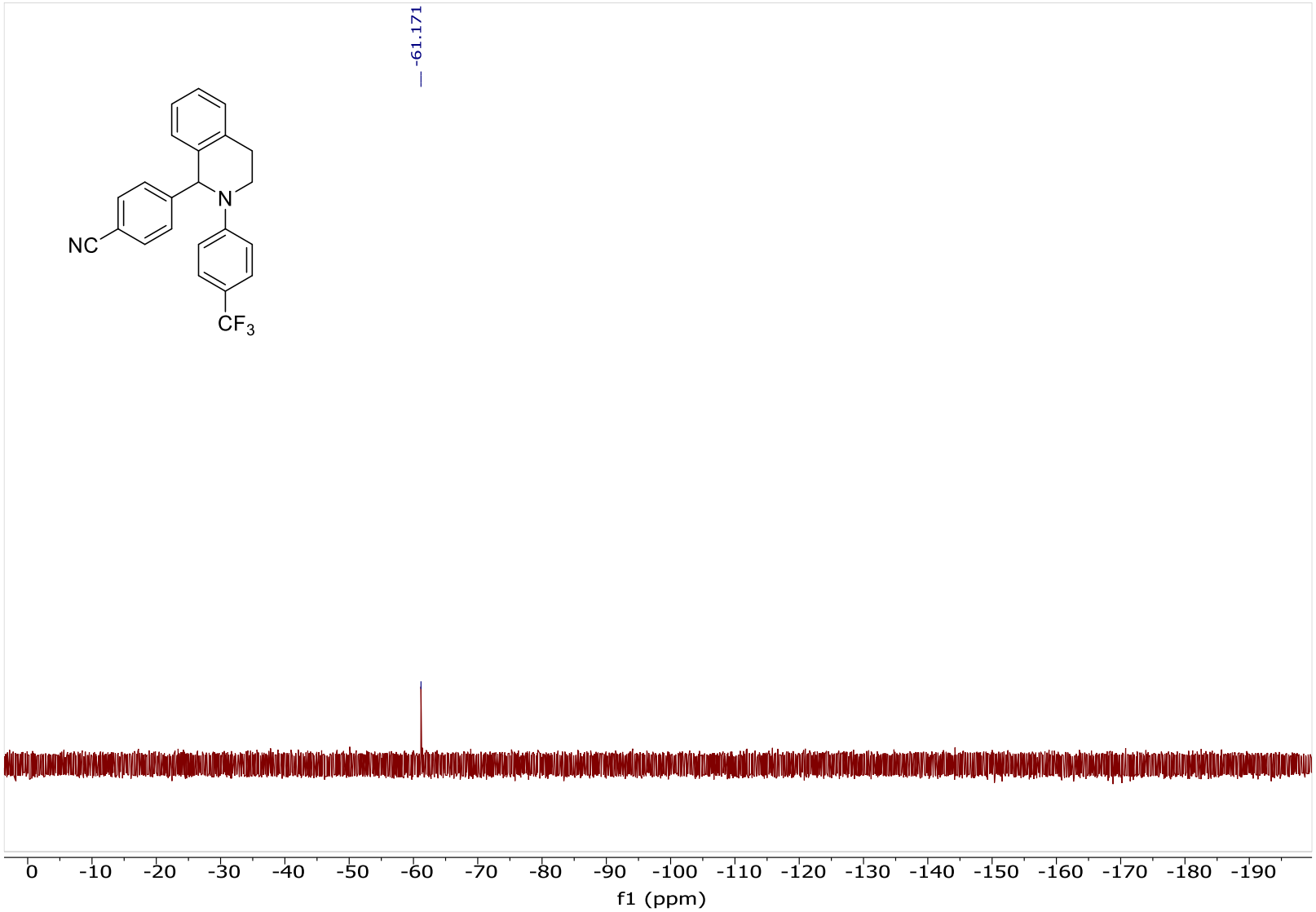

^{19}F NMR spectrum of **3l** (376 MHz, $CDCl_3$)

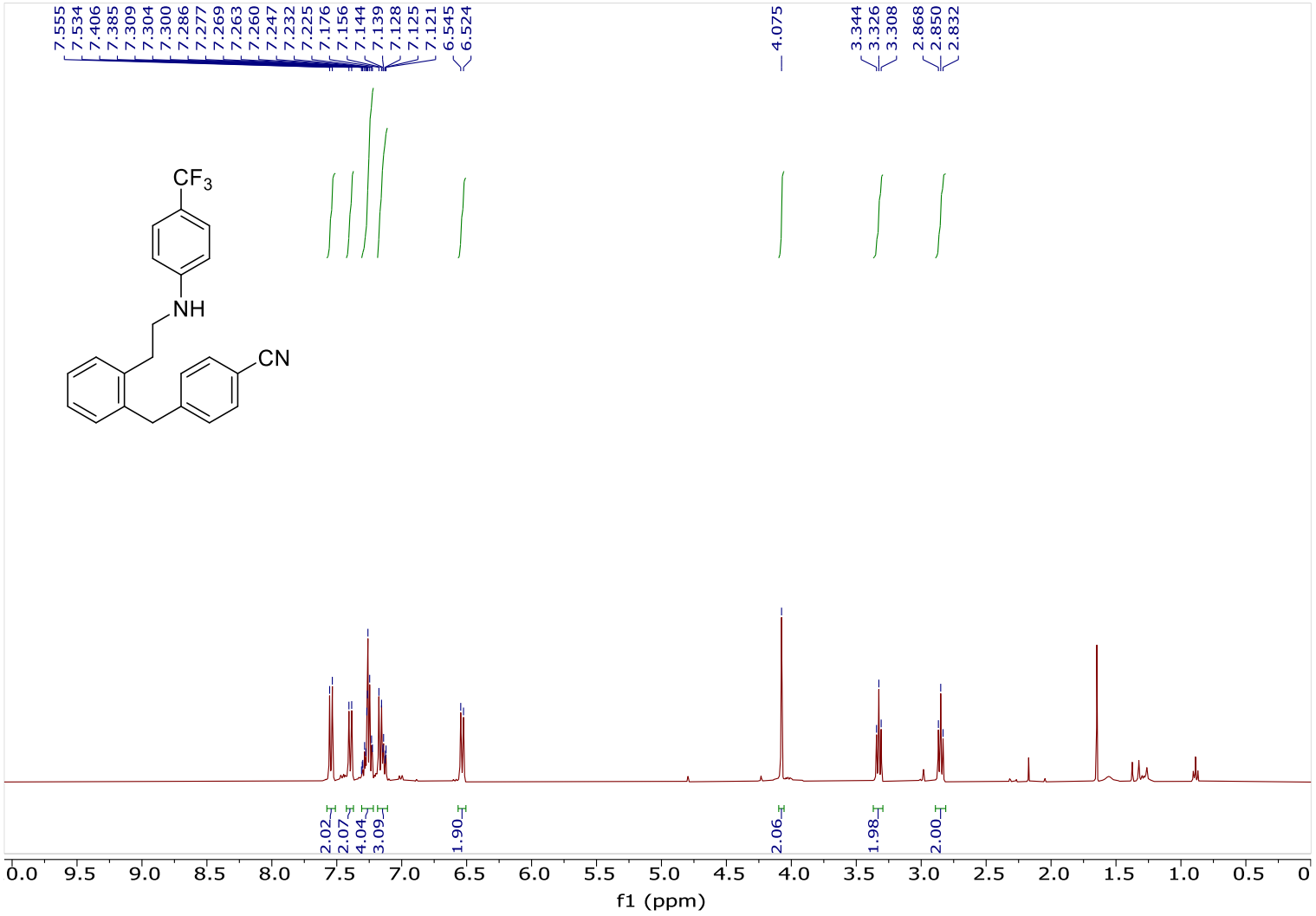

^{1}H NMR spectrum of **4l** (400 MHz, $CDCl_3$)

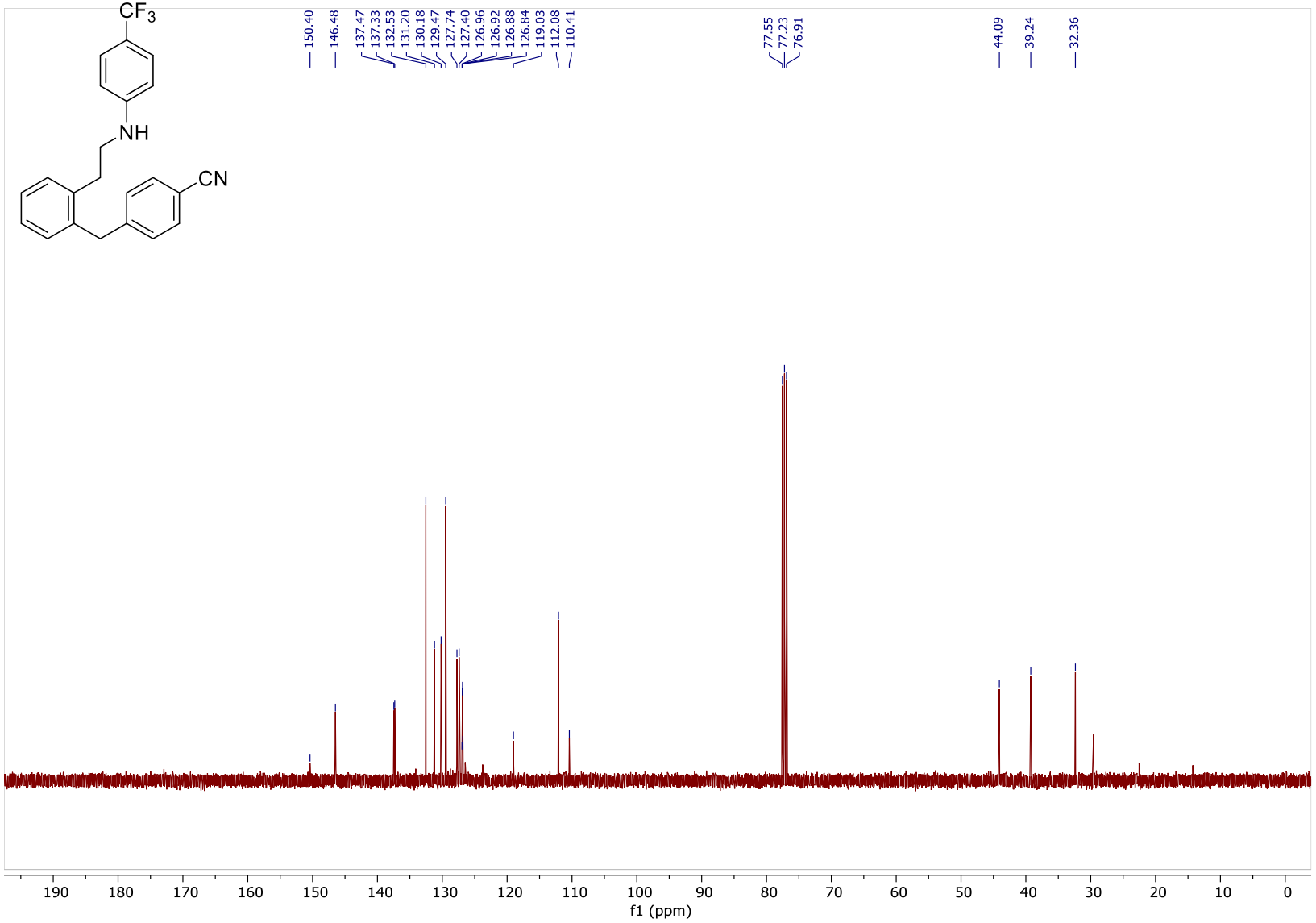

^{13}C NMR spectrum of **4l** (151 MHz, $CDCl_3$)

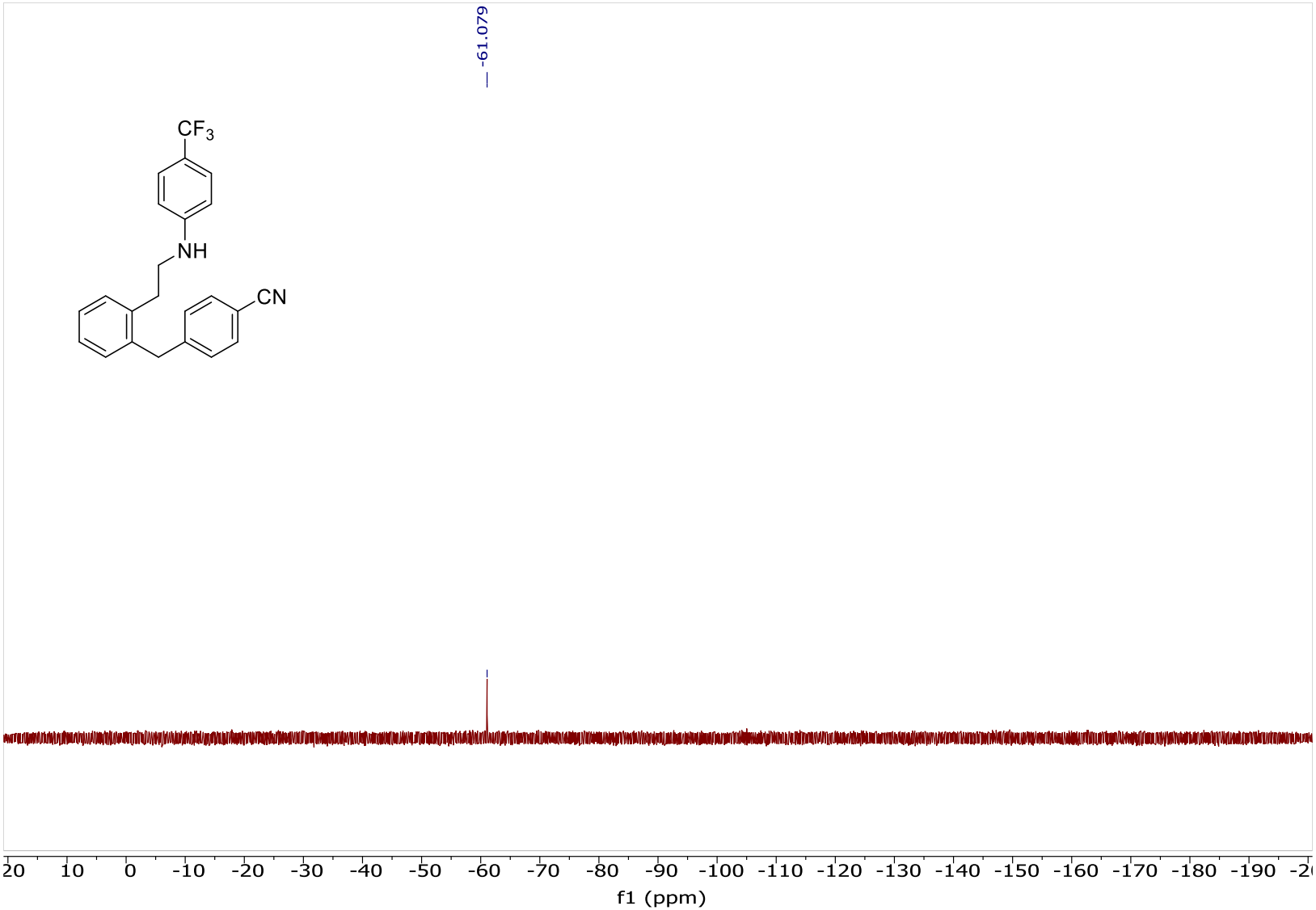

^{19}F NMR spectrum of **4l** (376 MHz, $CDCl_3$)